FORENSIC EVALUATION

LTPP SPS-5 Project (040500)

I-8 Eastbound
Casa Grande, Arizona

DRAFT REPORT

June 30, 2009

Western Regional Support Contractor

Nichols Consulting Engineers, Chtd.
1885 S Arlington Ave., Suite 111
Reno, NV 89509
(775) 329-4955

EXECUTIVE SUMMARY

In 2008, utilizing Focus Area Leadership and Coordination (FALCON) funds, the Federal Highway Administration (FHWA) initiated forensic evaluations at one Specific Pavement Studies (SPS) project in each of the four LTPP regions. In the Western Region, four sections (0502, 0505, 0506, and 0509) from the Arizona SPS-5 were selected based on the pavement condition and the Arizona Department of Transportation (ADOT) support. The test site begins at milepost 159.01 near Casa Grande on Interstate-8 in the Eastbound direction. The roadway was originally opened to traffic in 1968 and was rehabilitated per LTPP SPS-5 guidelines in 1990.

The main objectives of this forensic investigation were to:

- identify the causes of pavement failures and investigate the associated distress mechanism
- examine pavement structural and functional performances
- measure within-section layer thicknesses and material properties
- test end-state physical properties.

Destructive and non-destructive tests utilizing LTPP protocols were conducted in September 2008. The destructive testing included coring, Dynamic Cone Penetration (DCP) tests, Standard Penetration Tests (SPT), and trenching. Laboratory testing on base and subgrade materials and AC cores were also performed. The non-destructive testing included performing distress surveys, transverse profiles, longitudinal profiles, and Falling Weight Deflectometer (FWD) measurements.

From this forensic investigation, the following conclusions can be drawn:

- Base thicknesses were measured in the trench and on the split spoon samples taken along the section at core locations. They were uniform throughout the sections.
- Most of the cracks were top-down cracks (high severity at top and low severity at the bottom of the layer). A significant number of the cracks were full-depth.
- A couple of non-vertical cracks were observed at the trench edges, possibly the effect of the top-down cracking mechanism.
- Rutting was observed in the overlay layer only.
- The original asphalt layer was deteriorated and lost its viscous properties.
- The asphalt layers in the trench slabs were intact and no separation/slippage of layers were observed. No voids were observed at the edges of the slabs or trenches.

Table of Contents

List of Tables

List of Figures

INTRODUCTION

Specific Pavement Studies (SPS) experiments were developed under the Long-Term Pavement Performance (LTPP) program primarily to assess the effect of various structural parameters on pavement performance. There is widespread agreement that forensic investigations of LTPP test sections should be pursued, especially for those SPS test sections going out of study or scheduled for rehabilitation, but funding limitations precluded pursuing these as part of normal LTPP operations.

In 2008, utilizing Focus Area Leadership and Coordination (FALCON) funds, Federal Highway Administration (FHWA) initiated forensic evaluations at one LTPP SPS project in each of the four regions. In the Western Region, four sections from the Arizona SPS-5 were selected. This selection was based on the distress mechanisms and Arizona's outstanding agency support to perform the forensic activities. The Arizona SPS-5 test site (Figure 1) begins at milepost 159.01 near Casa Grande on Interstate-8 in the Eastbound direction. The roadway was originally opened to traffic in 1968 and rehabilitation per LTPP guidelines was performed in 1990. Eight sections were constructed as part of the standard LTPP experiment. These sections have the same design characteristics as the standard eight sections on SPS-5 projects throughout the LTPP study, as well as the same guidelines for pre-construction maintenance and subsequent rehabilitation activities. This SPS-5 site also included a control section and two supplemental test sections designed by the Arizona Department of Transportation (ADOT).

This forensic investigation follows the guidelines in the "Framework for LTPP Forensic Investigations - Final" developed in April 2004 to promote consistency and uniformity and to maximize benefits. Key elements of the guidelines include distress mechanism investigations and surveys, the collection of missing or desirable data, measurements of material properties, within-section layer thicknesses, end-state physical properties, deflection, and profile. Planning for the FALCON funded forensic investigations was discussed at the Transportation Research Board (TRB) LTPP Special Activities Expert Task Group (ETG) Meeting on April 2 to 3, 2008 in Woods Hole, Massachusetts.

The Arizona SPS-5 test site was originally constructed with 14 inches of granular base, 4.5 inches of Asphalt Concrete (AC), and 0.9 inches of Open Graded Asphalt Concrete Friction Course (OGACFC). Test sections 0504, 0505, 0506, and 0507 were overlaid with virgin asphalt, whereas sections 0502, 0503, 0508, 0509, and 0559 were overlaid with recycled asphalt. Section 0560 was overlaid with asphalt rubber AC.

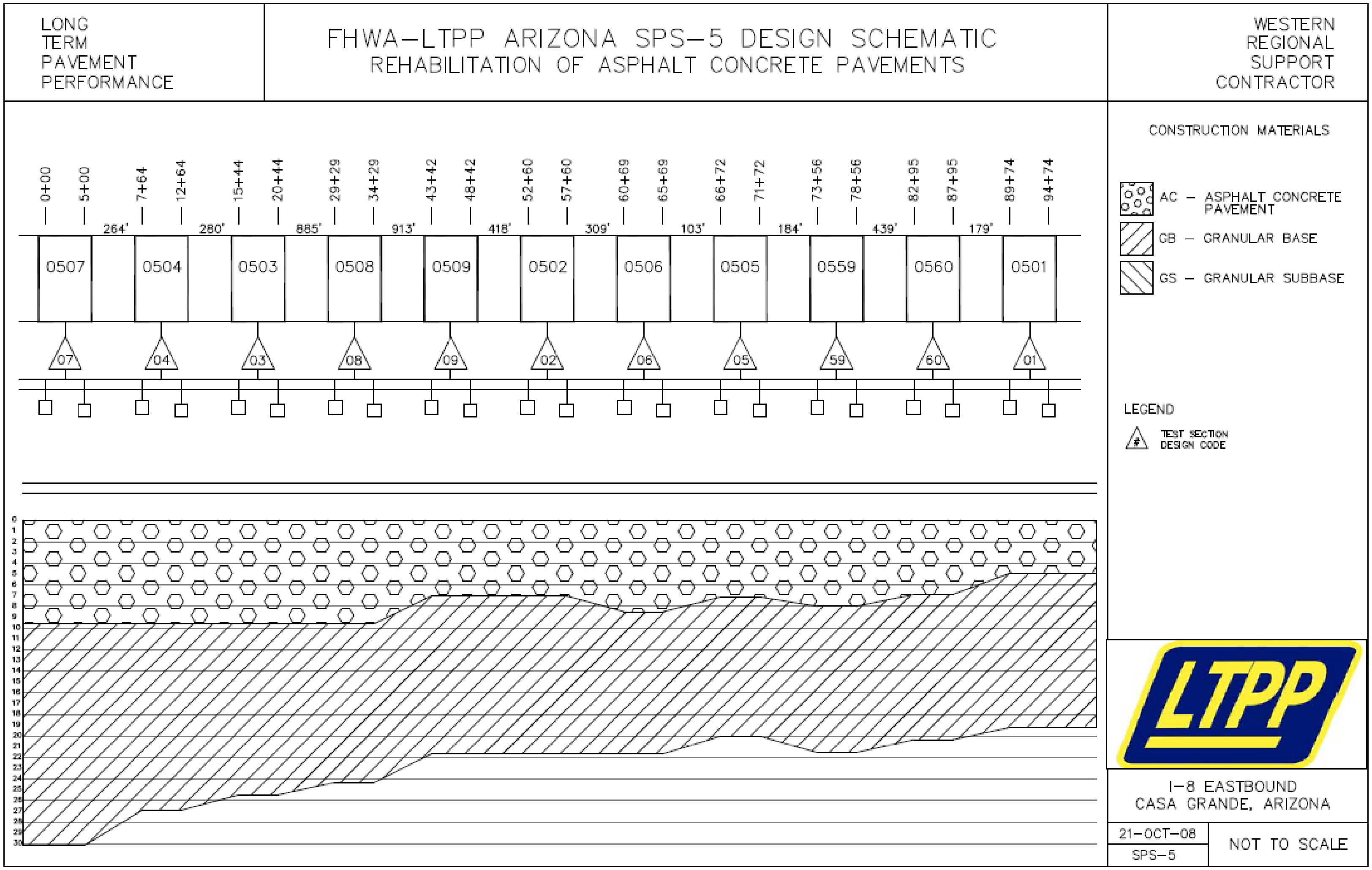

Figure 1. Arizona SPS-5 Test Sections.

Table 1 summarizes the rehabilitation designs for each test section. SPS-5 test sites were established for the study of asphalt pavement rehabilitation strategies, including the level of surface preparation, the overlay material, and overlay thickness. Test sections 0502 through 0509 make up a standard set of test sections for an SPS-5 site. Minimum surface preparation refers to, among other activities, about 0.5 inch of milling depth. Intensive surface preparation refers to about 2.5 inches of milling depth and “filling” the milled depth with AC. Section 0501 was a control section, which only received routine maintenance. Section 0560 used asphalt rubber asphalt concrete as an overlay material, and section 0559 “inverted” the design of section 0509 by placing the recycled layer over the virgin AC layer. The milling depth for section 0559 was about 4 inches. The AZ SPS-5 construction report provides more detail on the layout and structural properties of the site **[1]**.

Table 1.Arizona SPS-5 Rehabilitation Alternatives.

Section	**Surface Preparation**	**Overlay Material**	**Design Overlay Thickness**	
			(in)	**(mm)**
0501	Routine maintenance		-	
0502	Minimum	Recycled	2.0	50.8
0503	Minimum	Recycled	5.0	127.0
0504	Minimum	Virgin	5.0	127.0
0505	Minimum	Virgin	2.0	50.8
0506	Intensive	Virgin	2.0	50.8
0507	Intensive	Virgin	5.0	127.0
0508	Intensive	Recycled	5.0	127.0
0509	Intensive	Recycled	2.0	50.8
0559	Intensive	Recycled	2.0	50.8
0560	Minimum	ARAC	2.5	63.5

ARAC: Asphalt Rubber Asphalt Concrete

The existing pavement structure of the four forensic SPS-5 test sections are presented in Table 2. For sections 0502 and 0505, the open graded friction course and existing AC layers were milled off and an overlay layer of 2.7 inches and 2.8 inches, respectively were placed during the SPS-5 rehabilitation in 1990. For section 0506, the open graded friction course and existing AC layer were milled off and two overlay layers of 2.8 and 2.4 inches were placed. For section 0509, the open graded friction course and existing asphalt pavement were milled off and two overlay layers of 2.6 and 1.3 inches were placed. Each of the sections received crack sealing in May 2002 and fog seal coats in May 1998, August 2001, and April 2003. The subgrade material in these test sections is predominantly silty gravel with sand.

Table 2. Pavement Structure at Selected SPS-5 Test Sections.

Section	Layer	Thickness (in)	Thickness (mm)	Year	Construction Activity
0502	Granular Base	14.7	373.4	1968	New Pavement
	Recycled AC	3.7	94.0	1968	
	Recycled AC	2.7	68.6	1990	Rehabilitation
	Fog Seal	0.1	2.5	1998	Maintenance
	Fog Seal	0.1	2.5	2001	
	Fog Seal	0.1	2.5	2003	
0505	Granular Base	12.8	325.1	1968	New Pavement
	Virgin AC	4.1	104.1	1968	
	Virgin AC	2.8	71.1	1990	Rehabilitation
	Fog Seal	0.1	2.5	1998	Maintenance
	Fog Seal	0.1	2.5	2001	
	Fog Seal	0.1	2.5	2003	
0506	Granular Base	12.8	325.1	1968	New Pavement
	Virgin AC	3.0	76.2	1968	
	Virgin AC	2.8	71.1	1990	Rehabilitation
	Virgin AC	2.4	61.0	1990	
	Fog Seal	0.1	2.5	1998	Maintenance
	Fog Seal	0.1	2.5	2001	
	Fog Seal	0.1	2.5	2003	
0509	Granular Base	14.8	375.9	1968	New Pavement
	Virgin AC	2.6	66.0	1968	
	Recycled AC	2.6	66.0	1990	Rehabilitation
	Recycled AC	1.3	33.0	1990	
	Fog Seal	0.1	2.5	1998	Maintenance
	Fog Seal	0.1	2.5	2001	
	Fog Seal	0.1	2.5	2003	

Over time, these test sections have exhibited significant pavement distress primarily in the form of rutting, fatigue cracking, transverse cracking, and pumping. Looking at LTPP performance data, sections 0502 and 0505 show moderate to high severity fatigue cracking, rutting and pumping. Section 0506 shows high severity transverse cracking with loss of materials. Low severity fatigue cracking and rutting were also observed at this section. Section 0509 shows moderate to high severity transverse cracking throughout the section with significant rutting along the outer wheel path.

PURPOSE AND SCOPE

The primary objectives of this forensic investigation were developed in consultation between ADOT, FHWA, and the LTP Western Region Support Contractor (WRSC). These are discussed in Appendix A and included:

- Identifying the causes of pavement failures and investigating the distress mechanism.
- Examining the pavement structural and functional performances.
- Measuring within-section layer thicknesses and material properties.
- Testing end-state physical properties.

To achieve the above-stated objectives, forensic investigations consisting of destructive and non-destructive tests were conducted in September 2008. The destructive testing included coring, Dynamic Cone Penetration (DCP) tests, Standard Penetration Tests (SPT), and trenching. Moreover, laboratory testing on base and subgrade materials and AC cores were performed. The non-destructive testing included performing distress surveys, transverse profiles using a Dipstick™, longitudinal profiles using an inertial profiler, and Falling Weight Deflectometer (FWD) measurements – all per LTPP protocols. The as sampled field sampling and testing plans are presented in Appendix A.

TRAFFIC LOADING

The SPS-5 test sections were opened to traffic on June 13, 1990. Since 1993, Weigh-in-Motion (WIM) traffic data has been collected on these sections. The LTPP LTAS software version 1.7.2 was used to process the traffic weight data and to compute the 18-kip Equivalent Single Axle Loads (ESALs). The Sheet 10 (LTPP Traffic Data - Traffic Volume and Load Estimate Update - No Site Count) estimated ESALs were utilized for the years1994, 1995, 1996, and 2000. The traffic loading at SPS-5 is shown in Figure 2. A constant increase in traffic volume is observed.

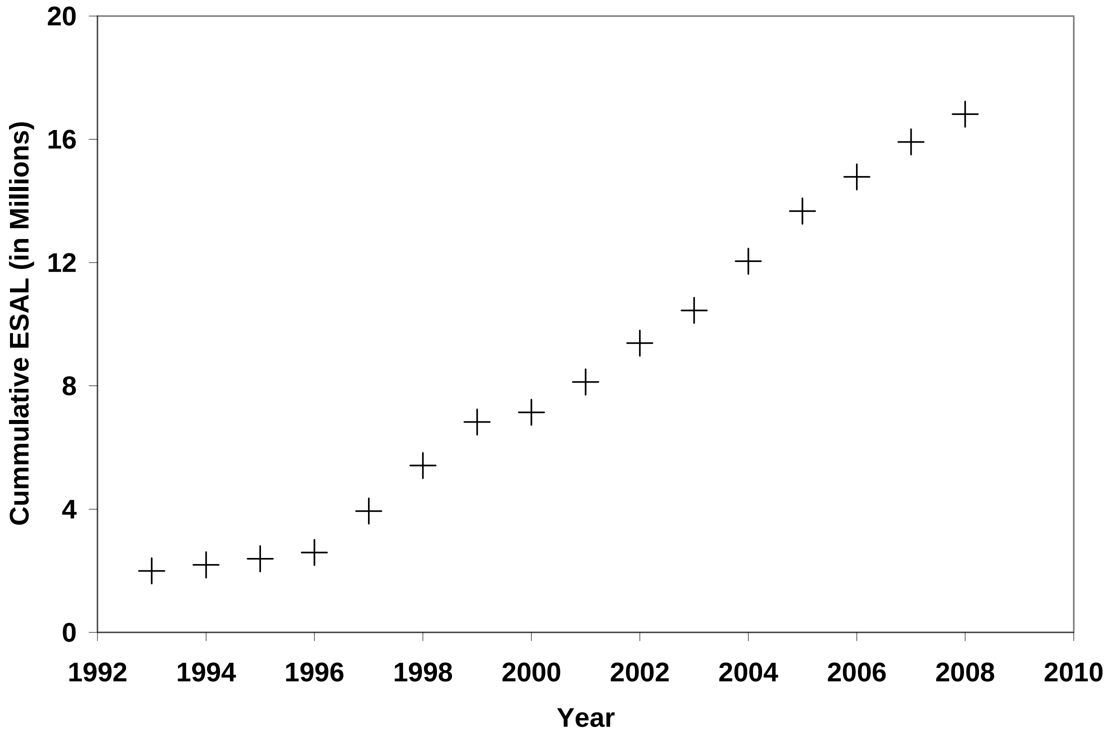

Figure 2. Traffic Loading at SPS-5.

DESTRUCTIVE TESTING

CORING

As per LTPP recommendations, 4 inch diameter cores at FWD locations and 6 inch diameter cores over selected cracks and within 0.5 m of the cracked area were drilled. An ADOT coring rig equipped with a diamond barrel tip was used to extract core samples (Figure 3). Most of the cores were taken along the wheel paths. Core samples along Inner Wheel Path (IWP) and Outer Wheel Path (OWP) are located at offsets 0.9 m (3 ft) and 2.75 m (9 ft), respectively. The core log information for each test section is presented in Tables 3 through 6.

Core thickness measurements were performed to assess construction variability (Figure 4). The AC overlay thicknesses measured from the cores are shown in Figures 5 through 8. The average AC overlay thickness for test sections 0502, 0505, 0506, and 0509 are 1.8, 1.8, 2.4, and 2 inches (44, 44, 60, and 50 mm), respectively. Reduction in AC overlay thickness, i.e., layer densification, is anticipated during the pavement service life due to traffic axle loading.

In addition, the core samples were used to determine the location of the crack starting point and to check whether the crack extended completely through the bound surface layer. This was also performed to determine whether the crack mechanism was primarily top-down or bottom-up cracking. The AC core samples were visually inspected before destructive testing was conducted. Photographs were taken for each core sample (Appendix B). Most of the recovered core samples were intact, while some of the cores extracted over the cracks were fragmented. In general, the core samples exhibited medium to high severity cracks initiated at the pavement surface and extending to the inlay layer, showing a top-down cracking pattern. A typical top-down crack is shown in Figure 9 for a core sample recovered from test section 0509. Similar crack patterns were generally observed for other test section core samples.

Figure 3. ADOT Core Rig.

Table 3. Core Log; Section 0502.

Core Hole No.	Core Sample No.	Station (m)	Offset (m)	Overlay Thickness		Remark
				(in)	(mm)	
A61	CA111	2.7	0.8	2.0	50.8	6 in diameter cores.
A62	CA112	2.7	1.2	1.9	48.3	
A63	CA113	12.3	1.2	1.4	35.6	
A64	CA114	12.3	0.9	2.2	55.9	
A65	CA115	23.8	0.9	1.3	33.0	
A66	CA116	35.0	0.9	1.5	38.1	
A67	CA117	35.4	1.0	2.4	61.0	
A68	CA118	51.5	0.8	1.5	38.1	
A69	CA119	66.1	0.9	2.1	53.3	
A70	CA120	66.1	0.5	1.5	38.1	
A71	CA121	84.1	1.1	1.5	38.1	
A73	CA123	103.1	0.9	2.0	50.8	
A76	CA126	129.8	0.7	2.3	58.4	
A80	CA130	147.9	1.0	1.6	40.6	

Table 4. Core Log; Section 0505.

Core Hole No.	Core Sample No.	Station (m)	Offset (m)	Overlay Thickness		Remark
				(in)	(mm)	
A42	CA92	10.2	1.1	1.9	48.3	6 in diameter cores.
A43	CA93	35.8	1.4	1.9	48.3	
A44	CA94	55.6	1.8	1.9	48.3	
A45	CA95	85.6	0.8	1.9	48.3	
A47	CA97	108.8	1.5	2.0	50.8	
A48	CA98	135.8	1.6	1.1	27.9	

Table 5. Core Log; Section 0506.

Core Hole No.	Core Sample No.	Station (m)	Offset (m)	Overlay Thickness		Remark
				(in)	(mm)	
A21	CA71	4.1	1.0	2	50.8	6 in diameter cores.
A22	CA72	6.7	1.6	2	50.8	
A23	CA73	11.9	0.7	2	50.8	
A24	CA74	20.9	0.9	2.5	63.5	
A25	CA75	27.8	1.2	2.3	58.4	
A26	CA76	36.9	0.5	2.5	63.5	
A27	CA77	42.0	0.8	2	50.8	
A28	CA78	42.0	0.5	2.4	61.0	
A29	CA79	60.4	1.3	2.6	66.0	
A30	CA80	60.4	0.5	2.8	71.1	
A31	CA81	96.3	1.2	2.5	63.5	
A32	CA82	107.0	1.2	2.4	61.0	
A33	CA83	107.0	0.8	2.5	63.5	
A34	CA84	114.9	0.4	1.8	45.7	
A35	CA85	115.5	0.4	2.1	53.3	
A36	CA86	125.7	0.8	2.5	63.5	
A37	CA87	131.2	0.8	2.5	63.5	
A38	CA88	131.2	0.4	2.4	61.0	
A39	CA89	152.3	0.6	2.3	58.4	
A40	CA90	153.4	0.5	2.4	61.0	

Table 5. Core Log; Section 0506 (Continued).

Core Hole No.	Core Sample No.	Station (m)	Offset (m)	Overlay Thickness		Remark
				(in)	(mm)	
C11	CA11	0.0	1.8	2.5	63.5	4 in diameter cores.
C12	CA12	30.5	1.8	2.5	63.5	
C13	CA13	61.0	1.8	2.5	63.5	
C14	CA14	91.4	1.8	2.5	63.5	
C15	CA15	121.9	1.8	2.6	66.0	
C16	CA16	152.4	1.8	2.9	73.7	
C17	CA17	15.2	0.8	2.5	63.5	
C18	CA18	45.7	0.8	2.2	55.9	
C19	CA19	106.7	0.8	2.5	63.5	
C20	CA20	137.2	0.8	2.6	66.0	

Table 6. Core Log; Section 0509.

Core Hole No.	Core Sample No.	Station (m)	Offset (m)	Overlay Thickness		Remark
				(in)	(mm)	
A01	CA51	6.2	0.8	1.9	48.3	6 in diameter cores.
A02	CA52	20.3	0.8	1.9	48.3	
A03	CA53	25.9	1.0	1.9	48.3	
A04	CA54	23.3	1.7	2.0	50.8	
A05	CA55	20.1	1.1	2.0	50.8	
A06	CA56	32.7	1.3	1.9	48.3	
A07	CA57	47.3	1.7	1.9	48.3	
A08	CA58	53.4	0.9	1.8	45.7	
A10	CA60	60.0	0.7	2.5	63.5	
A11	CA61	96.1	1.2	2.0	50.8	
A12	CA62	102.0	0.6	2.0	50.8	
A14	CA64	117.6	0.9	2.0	50.8	
A15	CA65	117.9	0.9	1.8	45.7	
A16	CA66	132.2	0.8	1.8	45.7	
A17	CA67	132.2	0.5	1.9	48.3	
A18	CA68	137.8	1.5	1.9	48.3	
A19	CA69	144.8	1.0	1.9	48.3	
A20	CA70	145.2	0.9	2.1	53.3	

Table 6. Core Log; Section 0509 (Continued).

Core Hole No.	Core Sample No.	Station (m)	Offset (m)	Overlay Thickness		Remark
				(in)	(mm)	
C01	CA01	0.0	1.8	2.0	50.8	4 in diameter cores.
C02	CA02	30.5	1.8	2.0	50.8	
C03	CA03	61.0	1.8	2.0	50.8	
C04	CA04	91.4	1.8	2.0	50.8	
C05	CA05	121.9	1.8	2.0	50.8	
C06	CA06	152.4	1.8	2.0	50.8	
C07	CA07	15.2	0.8	1.9	48.3	
C08	CA08	45.7	0.8	1.8	45.7	
C09	CA09	106.7	0.8	1.8	45.7	
C10	CA10	137.2	0.8	1.9	48.3	
C1A	CA02	30.5	1.7	2.0	50.8	

Figure 4. Core Sample; Section 0502, Core No. A69.

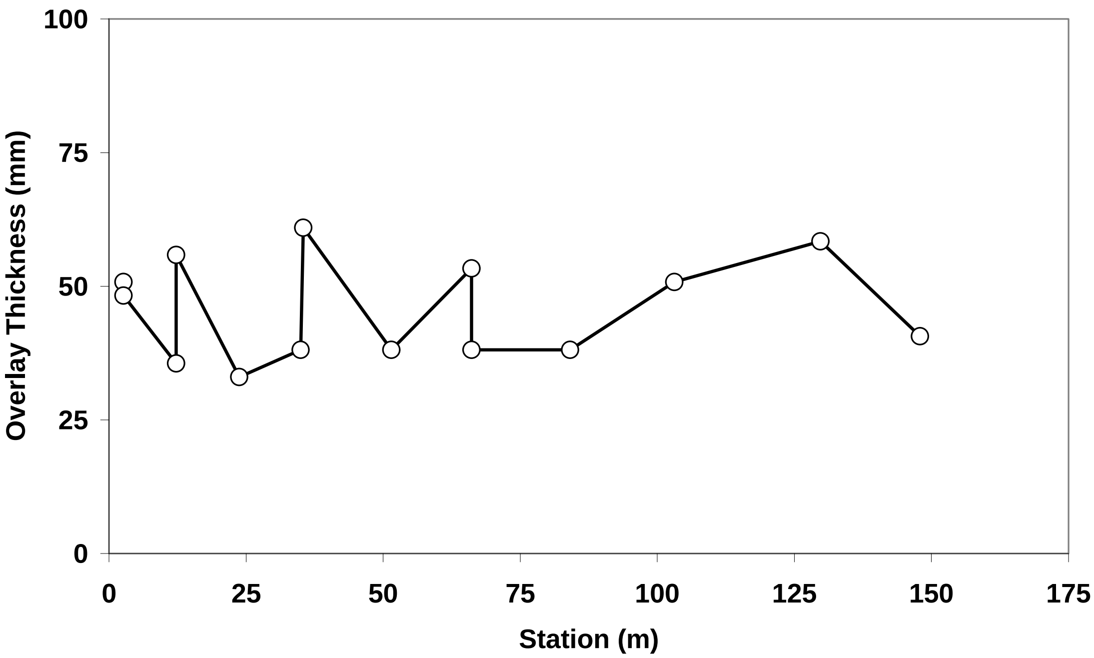

Figure 5. AC Overlay Thickness; Section 0502.

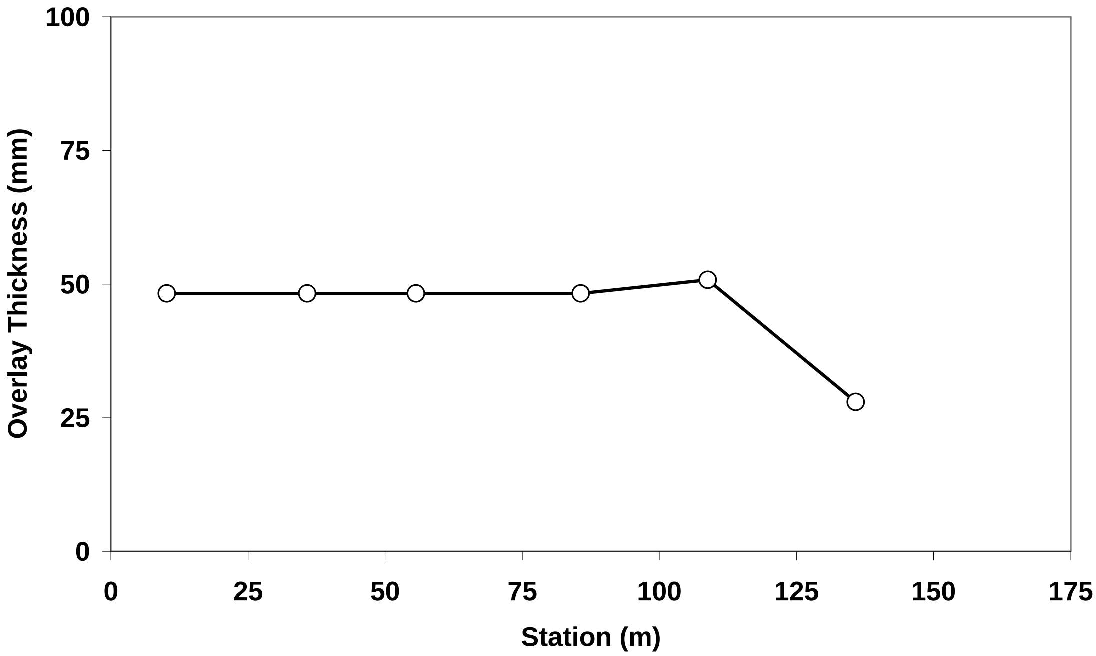

Figure 6. AC Overlay Thickness; Section 0505.

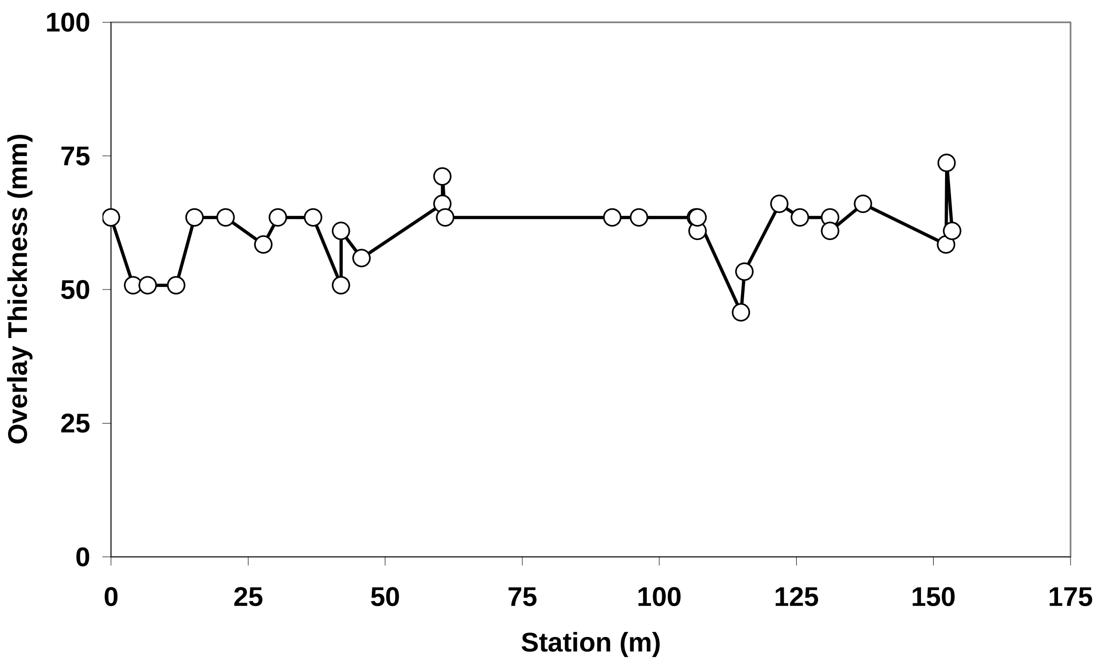

Figure 7. AC Overlay Thickness; Section 0506.

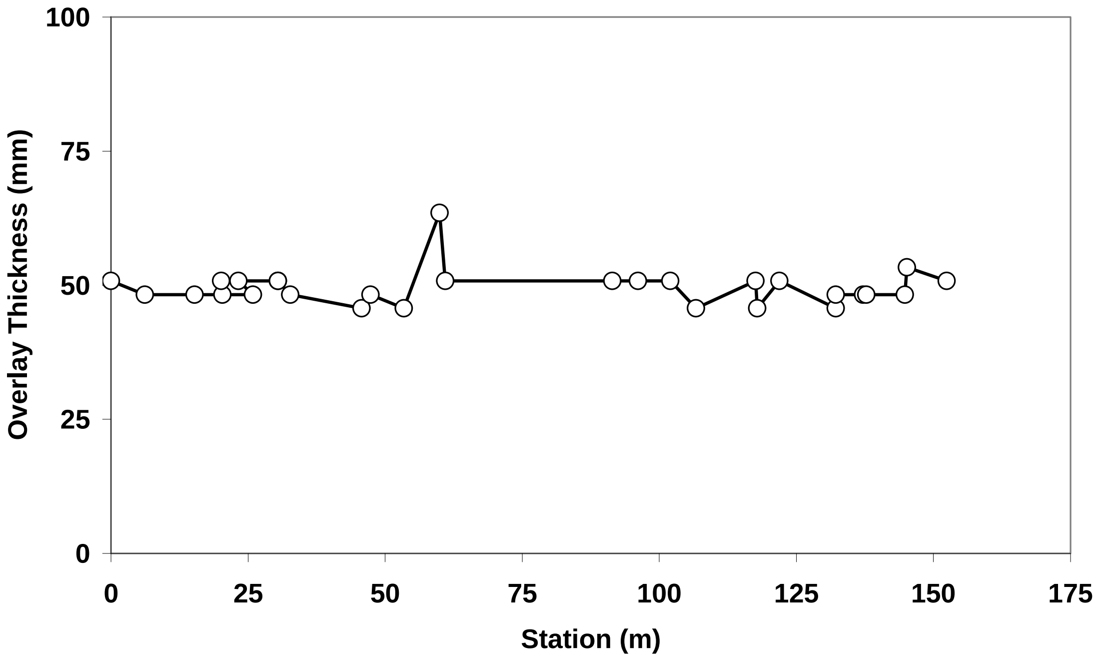

Figure 8. AC Overlay Thickness; Section 0509.

Figure 9. Top-Down Cracking; Section 0509, Core No. A12.

DYNAMIC CONE PENETRATION (DCP)

The Dynamic Cone Penetrometer (DCP) is a testing device used to measure the in-situ mechanical response of the granular layers in the pavement structure. As part of the forensic investigation, DCP tests were conducted to characterize the relative stiffness of base and subgrade materials. The DCP device consisted of two 16 mm diameter rods with the lower rod serving to measure the penetration of the device and the upper rod containing an 8 kg sliding drop hammer used to provide the driving force (Figure 10).

The DCP test locations are shown in Table 7. Six inch diameter cores were used for DCP tests. At least two DCP tests were performed for each of the test sections. Additional DCP tests were conducted prior to trench excavation at test sections 0506 and 0509. A typical DCP plot is presented in Figure 11. The slope of the graph expressed in millimeters per blow yields the DCP Penetration Index (PI) which represents the resistance offered by the material. DCP is also an important tool in determining changes in a material's response with depth. As illustrated in this figure, a change in material response (i.e., from base to subgrade) occurred at about 240 mm in depth. A consistent slope for base and subgrade layers is shown indicating uniform material response. Similar findings were obtained from the other DCP test locations.

Figure 10. DCP Testing.

Table 7. DCP Test Locations.

Section	Core No.	Offset (m)	Station (m)
0502	A69	0.9	66.2
	A76	0.7	129.8
0505	A43	1.4	35.8
	A47	1.5	108.9
0506	A27	0.8	42.0
	A36	0.8	125.8
	TP2_IWP	2.7	76.9
	TP2_C	1.8	76.9
	TP2_OWP	0.8	76.9
0509	A17	0.5	132.3
	TP1_IWP	2.7	76.9
	TP1_C	1.8	76.9
	TP1_OWP	0.8	76.9

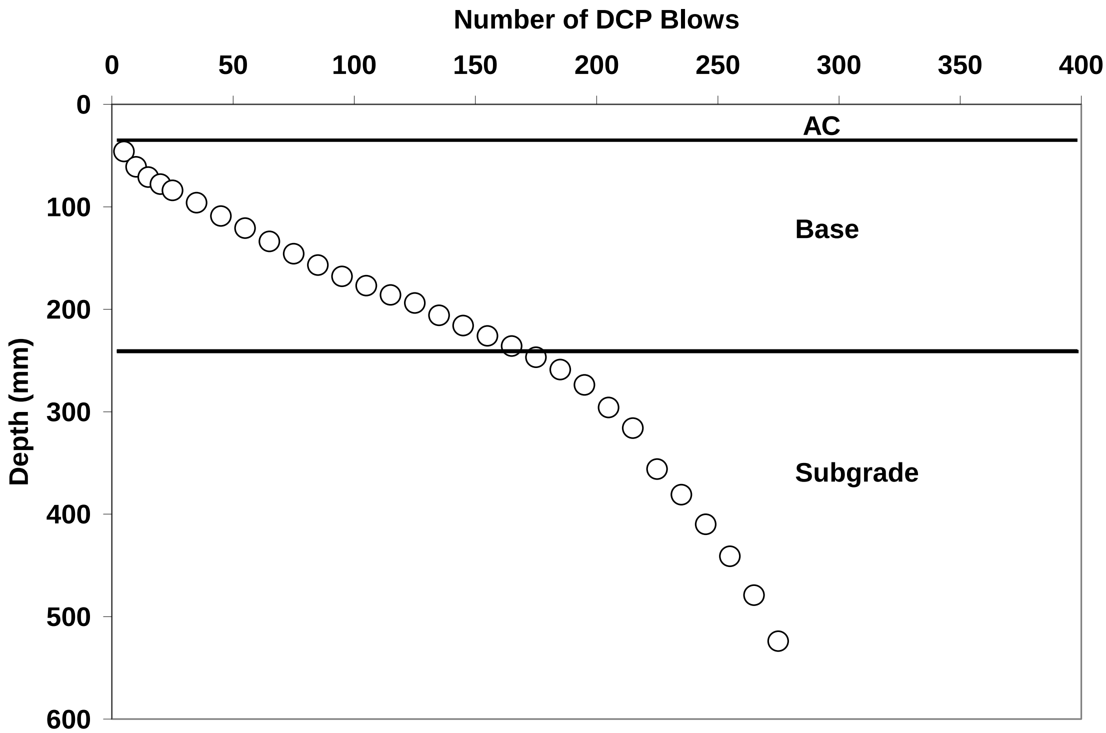

Figure 11. DCP Test Plot; Section 0502, Core No. A 69.

The empirical relations given in Equations 1 and 2 have been used in pavement literature to correlate PI with base and subgrade strength measurements, namely California Bearing Ratio (CBR) and elastic modulus **[2, 3]**.

$$CBR = 292/(PI)^{1.12}$$ Equation (1)

$$E = 17.58*(CBR)^{0.64}$$ Equation (2)

Where, *PI* is the DCP penetration rate in mm/blows; and *E* is the elastic modulus in MPa.

The CBR and modulus values computed from the DCP tests are presented in Table 8. Test sections 0502 and 0505 exhibited stiffer base material. Due to the hardness of the layer materials, few DCP tests were performed at section 0505. The subgrade material for each of the test sections was in good condition with high penetration resistance at section 0505.

Table 8. CBR and Modulus Values from DCP Tests.

Section	CBR		Modulus (MPa)	
	Base	Subgrade	Base	Subgrade
0502	24.9	7.8	137.5	65.3
0505	30.9	20.9	158.1	109.6
0506	9.7	11.8	75.2	85.3
0509	14.7	6.8	98.4	59.9

STANDARD PENETRATION TEST (SPT)

The Standard Penetration Test (SPT) can be used to characterize the strength of subsurface soils and provides undisturbed and disturbed samples that can be visually inspected. It is the most common method of soil exploration for foundation designs.

SPT testing was performed as part of the forensic investigation to measure the soil resistance to penetration. SPT locations are shown in Table 9. Four SPT tests were performed for each of the test sections. SPT tests were conducted, using the ADOT SPT device (Figure 12), by driving the split spoon sampler into the soil as per the ASTM D 1586 standards. The numbers of hammer blows were recorded for each of three 6 inch intervals, totaling 18 inches. SPT-N values were established for base and subgrade layers using the number of blows at 12 inches and 18 inches, respectively.

The SPT-N values for each of the test sections are presented in Table 10. These values correspond to stiff granular materials. This indicates the pavement subsurface soil materials are in good condition and can resist traffic vehicle loading. The materials extracted from the sample were also visually inspected. The undisturbed and disturbed SPT samples for test section 0505 are shown in Figures 13 and 14, respectively. In general, uniform soil materials were observed for each of the test sections.

.

Table 9. SPT Test Locations.

Section	Core No.	Offset (m)	Station (m)	Remark
0502	A61	0.8	2.7	6 in diameter cores.
	A66	0.9	35.0	
	A73	0.9	103.2	
	A80	1.0	148.0	
0505	A42	1.1	10.2	
	A44	1.8	55.7	
	A45	0.8	85.7	
	A48	1.6	135.9	
0506	A21	1.0	4.1	
	A29	1.3	60.5	
	A31	1.2	96.4	
	A40	0.5	153.4	
0509	A1	0.8	6.2	
	A4	1.7	23.3	
	A7	1.7	47.4	
	A12	0.6	102.1	

Figure 12. SPT Testing.

Table 10. SPT Test Results.

Section	SPT-N Values	
	Base	Subgrade
0502	21	18
0505	19	19
0506	9	10
0509	17	14

Figure 13. Undisturbed SPT Sample; Section 0505, Core No. 44.

Figure 14. Disturbed SPT Sample; Section 0505, Core No. 44.

TRENCH OPERATION

Trench excavations were conducted in order to determine which layer (s) in the pavement structure contributed to the rutting mechanism. As per the LTPP guidelines, trenches were cut and removed at station 2+50 (76 m) on test sections 0509 (Trench No. 1) and 0506 (Trench No. 2). The trench size was 1.2 m wide and 3.6 m long. Prior to excavation, transverse profile measurements, DCP, FWD, and Nuclear Density Gauge (NDG) tests were completed. The saw-cut pattern of the trench and test locations for DCP, FWD, and NDG are shown in Figure 15.

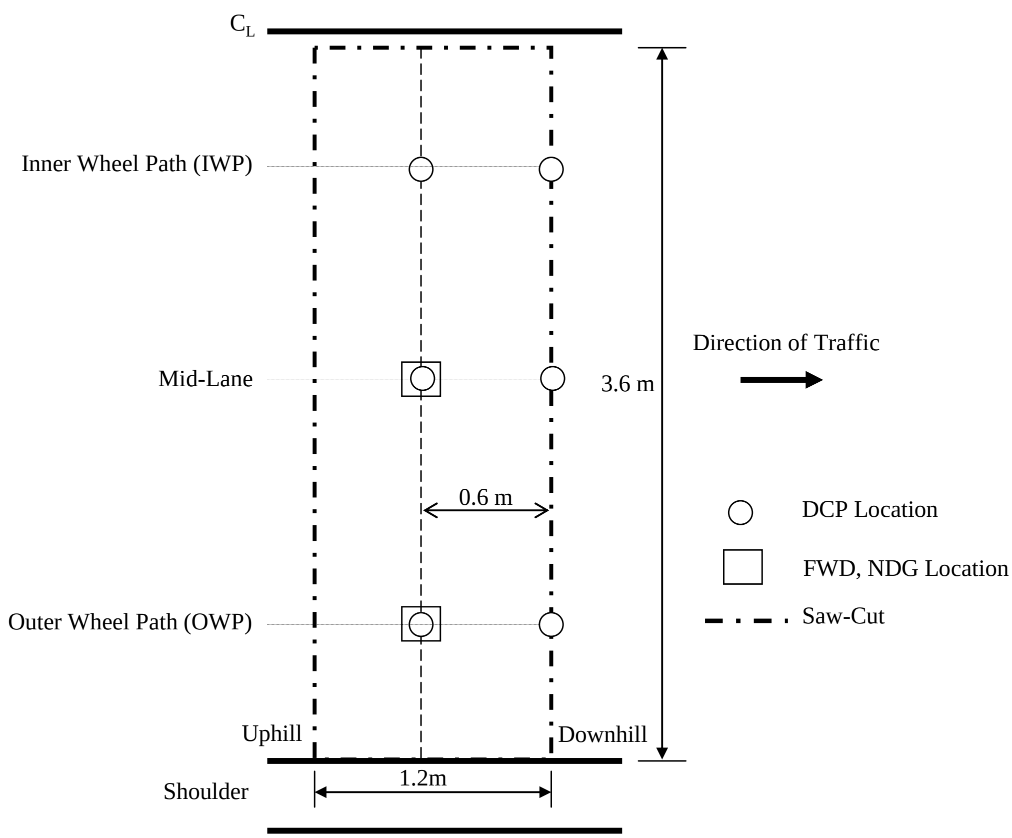

Figure 15. DCP, FWD, NDG and Saw-cut Locations.

The trench cutting was laid out with spray paint, and the trenches were cut with a diamond saw (the trench excavation operation is shown in Figure 16). For both of the test sections, the saw cut was deep enough to penetrate through the AC layers. Nails and string lines were used to delineate each pavement layer, and the pavement layer interfaces were clearly identified. Following excavation, a visual assessment was made at the exposed layers and photographs were taken throughout the operation. No reflective cracks (i.e., cracks from underlying pavement layers propagating to surface layers) were observed at the bottom of the AC slab layer, reconfirming the crack mechanism as top-down cracking.

Figure 16. Trench Excavation.

As per the LTPP recommendation, layer thickness profiles were collected at 1 ft (0.305 m) intervals with a standard tape measure along the length of the trench. For consistency, the same person measured all layer thickness profiles. The layer thickness profiles for test section 0509 and 0506 are presented in Tables 11 and 12, respectively. The subsurface profiles measured in these test sections are shown in Figures 17 and 18, respectively. The layer profiles show the rutting contributed by each layer (Figure 19 and 20). Close-up views of the surface layer along the wheel paths are shown in Figures 21 and 22, respectively. It is clearly shown that rutting was mainly in the top AC layer and virtually no rutting was detected in the lower layers (AC inlay and base layer). Similar observations were found using downhill subsurface profiles.

While layer profiles show how much rutting is contributed by each layer, surface profile yields the total amount of rutting. The transverse surface profiles collected using a Dipstick™ device at the trench locations confirm rutting along the wheel paths (Figures 23). An average rut depth of 6.5 mm was obtained for both trenches. In general, the original AC layer was falling apart when recovered. Along this forensic investigation, testing was also performed concurrently by the NCHRP contractor and no testing results were received

Table 11. Pavement Layer Thickness; Section 0509 (Trench No. 1).

Offset (m)	**Downhill**						**Uphill**					
	Overlay		**Inlay**		**Base**		**Overlay**		**Inlay**		**Base**	
	(in)	**(mm)**	**(in)**	**(mm)**	**(in)**	**(mm)**	**(in)**	**(mm)**	**(in)**	**(mm)**	**(in)**	**(mm)**
0.000	1.66	42.04	3.13	79.38	14.00	355.60	1.66	42.04	3.38	85.73	13.50	342.90
0.305	1.66	42.04	3.44	87.33	13.81	350.82	1.66	42.04	3.75	95.25	13.75	349.25
0.610	1.63	41.50	3.44	87.30	13.63	346.08	1.63	41.50	3.63	92.08	13.75	349.25
0.915	1.78	45.09	3.25	82.55	13.88	352.43	1.78	45.09	3.00	76.20	14.25	361.95
1.220	1.74	44.30	3.11	79.04	14.08	357.51	1.74	44.30	3.00	76.20	14.13	358.78
1.525	1.59	40.28	3.06	77.77	14.13	358.78	1.59	40.28	3.00	76.20	14.38	365.13
1.830	1.73	43.97	3.13	79.38	14.06	357.20	1.73	43.97	2.88	73.03	14.50	368.30
2.135	1.76	44.75	3.25	82.55	13.88	352.43	1.76	44.75	3.44	87.33	13.88	352.43
2.440	1.79	45.54	3.38	85.73	13.88	352.43	1.79	45.54	3.19	80.98	14.00	355.60
2.745	1.67	42.37	3.25	82.55	13.94	354.03	1.67	42.37	3.31	84.15	13.88	352.43
3.050	1.67	42.42	3.69	93.65	13.69	347.68	1.67	42.42	3.25	82.55	14.00	355.60
3.355	1.67	42.42	3.81	96.82	13.63	346.08	1.67	42.42	3.25	82.55	14.13	358.78

Table 12. Pavement Layer Thickness; Section 0506 (Trench No. 2).

Offset (m)	**Downhill**						**Uphill**					
	Overlay		**Inlay**		**Base**		**Overlay**		**Inlay**		**Base**	
	(in)	**(mm)**	**(in)**	**(mm)**	**(in)**	**(mm)**	**(in)**	**(mm)**	**(in)**	**(mm)**	**(in)**	**(mm)**
0.000	2.19	55.65	2.94	74.60	12.75	323.85	2.19	55.65	3.19	80.95	13.00	330.20
0.305	2.19	55.65	3.00	76.20	12.63	320.68	2.19	55.65	3.13	79.38	13.00	330.20
0.610	2.20	55.91	3.13	79.38	12.75	323.85	2.20	55.91	3.06	77.77	13.06	331.80
0.915	2.19	55.55	3.13	79.38	12.56	319.10	2.19	55.55	2.94	74.60	13.06	331.80
1.220	2.15	54.71	3.25	82.55	12.56	319.07	2.15	54.71	3.00	76.20	13.06	331.77
1.525	2.19	55.65	3.06	77.77	12.81	325.45	2.19	55.65	2.94	74.60	13.13	333.38
1.830	2.23	56.59	3.19	80.98	12.63	320.68	2.23	56.59	2.88	73.03	13.19	334.98
2.135	2.22	56.31	3.38	85.73	12.50	317.50	2.22	56.31	2.75	69.85	13.19	334.95
2.440	2.10	53.29	3.06	77.77	12.50	317.50	2.10	53.29	3.00	76.20	13.00	330.20
2.745	2.01	51.05	2.88	73.03	12.75	323.85	2.01	51.05	2.94	74.60	13.13	333.38
3.050	1.79	45.54	3.31	84.15	12.44	315.90	1.79	45.54	3.00	76.20	13.00	330.20
3.355	1.79	45.54	3.13	79.38	12.63	320.68	1.79	45.54	3.06	77.77	12.75	323.85

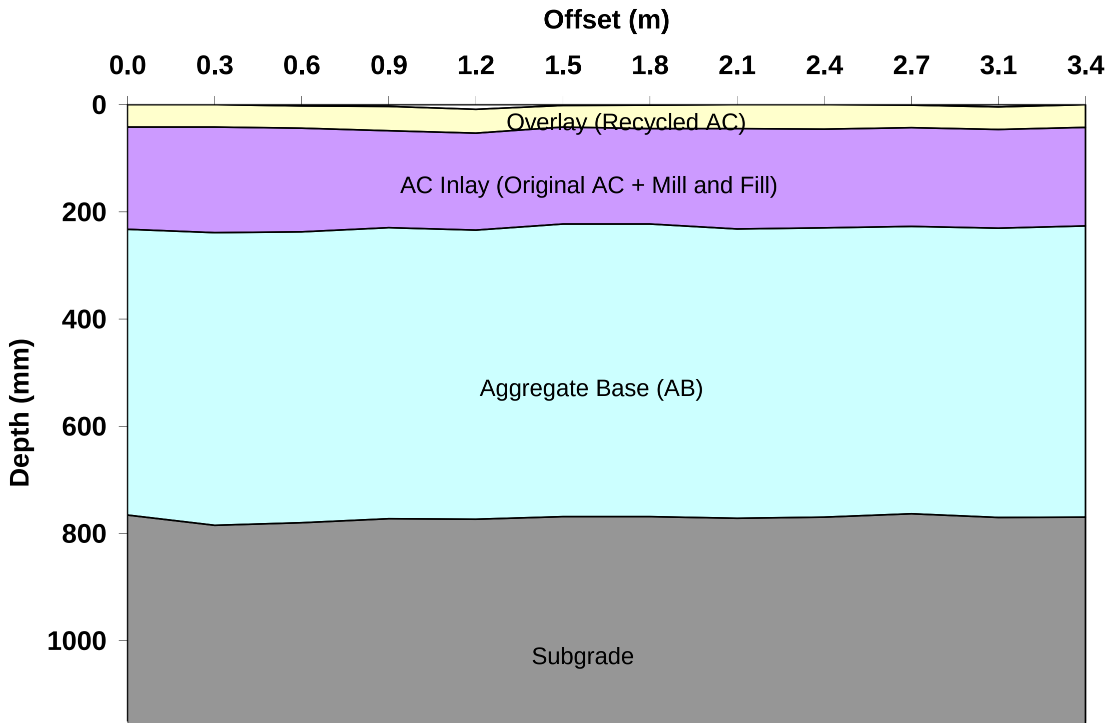

Figure 17. Subsurface Profiles; Section 0509 Uphill.

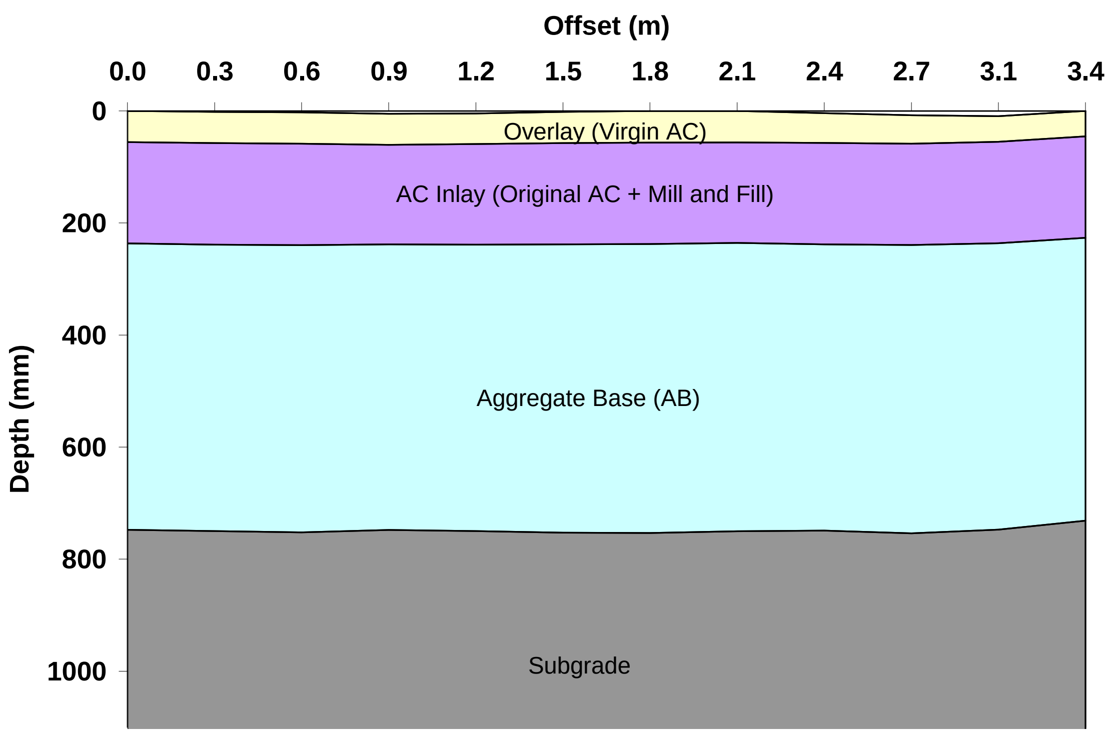

Figure 18. Subsurface Profiles; Section 0506 Uphill.

Figure 19. Trench Profiles; Section 0509.

Figure 20. Trench Profiles; Section 0506.

Figure 21. OWP Rutting; Section 0509.

Figure 22. IWP Rutting; Section 0506.

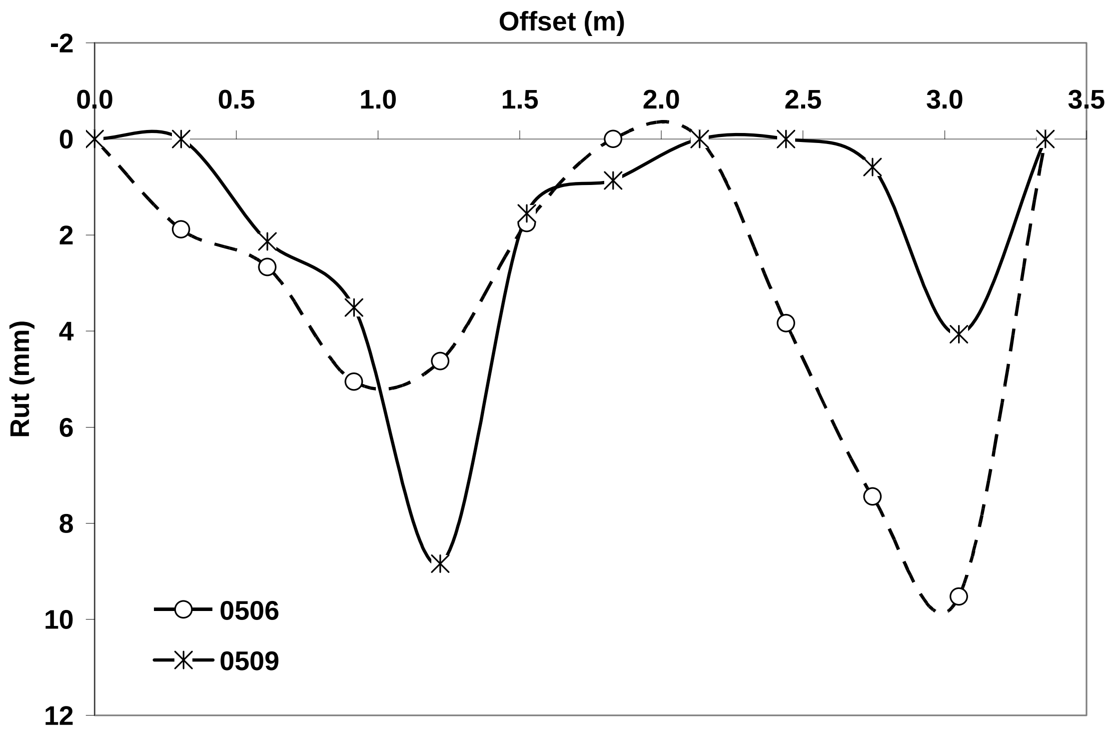

Figure 23. AC Surface Rut Depth.

NUCLEAR DENSITY GAUGE (NDG) TESTS

Pavement design procedures assume that the layers in the pavement structure have been compacted to a specified density. The stiffness of a pavement layer can change as a result of seasonal variations in moisture level. As part of the forensic investigation, NDG tests were conducted on the top of the base and subgrade layers at trench locations in order to measure the in-situ density and moisture content. The NDG test locations were shown in Figure 15.

Prior to testing, the surface was leveled and smoothed. Shovels and brooms were used to smooth the base and subgrade surfaces for NDG testing (Figure 24). The NDG test results are presented in Table 13. These results are the average of four readings at each location. Higher densities and lower moisture content for the base layer were obtained as compared to the subgrade layer. In general, NDG measurements resulted in consistent densities and moisture contents indicating uniform base and subgrade material properties. Relatively higher NDG values were recorded for test section 0509.

Figure 24. NDG Testing.

Table 13. Dry Density and Moisture Content from NDG Tests.

Section	Layer	Dry Density (kg/m^3)			Moisture Content (%)		
		OWP	IWP	Average	OWP	IWP	Average
0506	Base	1858.1	1867.8	1863.0	5.2	4.5	4.9
	Subgrade	1819.6	1768.2	1793.9	8.1	7.9	8.0
0509	Base	1943.3	1977.0	1960.1	4.1	4.4	4.3
	Subgrade	1907.9	1906.3	1907.1	8.4	8.6	8.5

LABORATORY TESTS ON BASE AND SUBGRADE MATERIALS

For sections 0506 and 0509, laboratory tests were conducted to determine the engineering properties of the base and subgrade materials. Bulk soil samples from the trenches were shipped to Arizona DOT for laboratory testing. Results of the soil testing are provided in Table 14. The base material gradations for the two test sections are similar. However, significant variations in gradations are obtained for subgrade material especially for sieve sizes ranging from 12.5mm to 0.075mm; particularly the subgrade material in section 0506, which had a high percentages of fines (19.1%). In general, the laboratory tests resulted in consistent Atterburg properties. Laboratory measured densities and moisture contents were higher than the NDG in-situ measurements.

Table 14. Laboratory Test Results.

Sieve Size		Test Section			
		0506		0509	
		Base	Subgrade	Base	Subgrade
Standard	(mm)	Percent Passing		Percent Passing	
3"	75.0	100	100	100	100
2"	50.0	100	100	100	100
1½"	37.5	100	100	100	100
1"	25.0	100	99	100	99
¾"	19.0	98	98	100	95
½"	12.5	96	95	96	79
3/8"	9.5	95	93	95	73
No. 4	4.75	89	84	90	60
No. 10	2.00	75	70	77	48
No. 40	0.425	50	38	54	21
No. 80	0.180	42	25	45	8
No. 200	0.075	34.4	19.1	36	4.9
Dust Proportion (%)		0.6	1.3	0.6	0.4
Liquid Limit		23	26	---	22
Plasticity Index		7	8	NP[1]	5
Dry Density (kg/m^3)		2066	2163	2082	2179
Optimum Moisture Content (%)		9.0	7.0	9.0	6.0
[1] NP: Non-plastic					

LABORATORY TESTS ON ASPHALT CONCRETES (AC)

Laboratory testing on the AC core samples included sieve analysis, asphalt binder content, and density. These tests were performed by ADOT lab personnel in accordance with LTPP test protocols.

Sieve Analysis

Aggregate gradation affects how the aggregates interlock and rearrange under vehicular loading. Sieve analysis was performed on the core samples in order to characterize the AC mixture aggregate gradations placed in the field. The AC core sets used in the sieve analysis for each test section are presented in Appendix C. The sieve analysis results, including the Job Mix Formula (JMF) requirements, are shown in Tables 15 and 16. Overall, the measured percent passing for test sections 0502 and 0509 deviate from the JMF aggregate gradations, but are relatively close for sections 0505 and 0506.

Table 15. Sieve Analysis Result; Sections 0505 and 0506.

Sieve Size		**Percent Passing**		
Standard	**(mm)**	**JMF**	**0505**	**0506**
1"	25.0	100	100	100
¾"	19.0	100	97.8	99.3
½"	12.5	94	88.2	89.6
3/8"	9.51	79	79	78.4
No. 4	4.75	58	60.3	58.9
No. 10	2.00	44	46.4	44
No. 40	0.425	17	21.7	20.7
No. 80	0.180		8.5	8.4
No .200	0.075	4.8	4.6	5

Table 16. Sieve Analysis Result; Sections 0502 and 0509.

Sieve Size		Percent Passing		
Standard	(mm)	JMF	0502	0509
1"	25.0	100	100	100
¾"	19.0	100	98.1	98.9
½"	12.5	95	86.8	88.1
3/8"	9.51	90	75.3	78.2
No. 4	4.75	37	59.7	59
No. 10	2.00	24	44.8	44.4
No. 40	0.425	13	20.5	20.1
No. 80	0.180		8.3	8.3
No .200	0.075	4.1	4.8	5.4

Asphalt Binder Content

The binding properties of asphalt cement in AC mixtures significantly affect the AC pavement performance. The AC core sets used for asphalt binder content test on each test section are presented in Appendix C. The average measured asphalt binder contents for each test section are given in Table 17. The measured average percent binder contents for the test sections (except section 0505) are higher when compared to the JMF specified values.

Table 17. Average Asphalt Binder Content.

Section	Asphalt Binder Content (%)	
	Measured	JMF
0502	4.9	3.5
0505	4.5	4.7
0506	5.0	4.7
0509	4.9	3.5

Density

Density is an intrinsic property of the AC mixtures. It affects the amount of aggregates, air voids, and asphalt binder used in the mixture composition. The AC core sets used for density tests on each test section are presented in Appendix C. The maximum theoretical specific gravity (G_{mm}) and bulk specific gravity (G_{mb}) of the AC core samples are presented in Table 18. The percentage of air voids in the AC core samples was calculated using G_{mm} and G_{mb}. In general, the calculated percent air void is higher than the JMF values, and it is significantly highest for test section 0505. This phenomenon may be a contributing factor to pavement rutting.

Table 18. Density Test Results.

Section	**Average G_{mm}**	**Average G_{mb}**	**Air Void (%)**		
			Calculated	**JMF**	**Specification**
0502	2.441	2.281	6.6	5.4	5.0 - 7.0
0505	2.448	2.225	9.1	6.1	5.8 - 6.2
0506	2.430	2.277	6.3	6.1	5.8 - 6.2
0509	2.437	2.268	6.9	5.4	5.0 - 7.0

NON-DESTRUCTIVE TESTING

PAVEMENT CONDITION SURVEY

Pavement distresses at the test sections were recorded and summarized in Table 19 in accordance with the LTPP Distress Identification Manual **[4]**. The pavement distress maps are provided in Appendix D. Typical snapshot view of the test sections are presented in Figure 25. The predominant distresses identified in the test sections included rutting, fatigue cracking, longitudinal cracking, transverse cracking, and pumping.

Fatigue cracking is caused by repeated traffic loading. High severity fatigue cracking was observed for test sections 0502 and 0505. Low to high severity transverse and longitudinal cracking were observed for test sections 0505, 0506, and 0509. Neither transverse nor longitudinal cracking was rated on test section 0502 because of the extent of block and fatigue cracking. Low severity block cracking was observed in test section 0505. Based on the visual assessment, the patterns of the non-wheel path longitudinal cracking consistently occurred at the mid-lane. Low to moderate severity patch deterioration was observed in section 0506. Pavement distress in the form of pumping was also noticed in each of the four test sections, particularly in sections 0502 and 0505.

Table 19. Pavement Distress Summary (September 2008).

Distress Type		Severity Level	Quantity			
			040502	040505	040506	040509
Fatigue cracking (m^2)		Low	-	6.9	4.1	18.8
		Moderate	-	68.4	1.3	44.3
		High	342.3	322.8	0.57	21.4
Block cracking (m^2)		Low	-	112.0	-	-
		Moderate	236.9	-	-	-
		High	-	-	-	-
Longitudinal cracking (m)	Wheel path	Low	-	-	0.3	1.0
		Moderate	-	-	-	-
		High	-	-	-	-
	Non-wheel path	Low	-	2.1	26.1	55.6
		Moderate	-	43.6	33.8	98.3
		High	-	2.0	62.1	4.3
Transverse cracking (m)		Low	-	21.5	11.3	69.5
		Moderate	-	8.6	9.0	57.0
		High	-	-	46.4	57
Patch/Patch deterioration (m^2)		Low	-	-	0.1	-
		Moderate	-	-	0.1	-
		High	-	-	-	-
Water bleeding and pumping (m)		NA*	152.4	132.0	1.0	37

* Not Applicable

Figure 25. Pavement Conditions at Selected SPS-5 Test Sections.

Historical development of fatigue cracking, transverse cracking, and pumping are plotted in Figures 26 through 28. The growth of these distresses increased over time for each of the test sections. Comparatively, the extent of fatigue cracking and transverse cracking is minimal for test sections 0506 and 0502, respectively. Maintenance activities (fog seals and crack sealing) appear to have reduced the severity level of fatigue and transverse cracks. However, after the maintenance operations, an increase in transverse cracks is still apparent for test sections 0506 and 0509. Upon pavement degradation, some portion of high severity transverse cracks in test sections 0502 and 0505 were converted into fatigue or block cracks and therefore the transverse cracking in these test sections is masked.

During the September 2008 visit, disintegration and loss of AC materials were also noticed in some locations of the test sections. In most cases, the transverse cracks covered the entire width of the lane. Section 0502 exhibited low severity transverse cracks over the monitored history. In addition, the extent of water bleeding and pumping increased over time for test sections 0502 and 0505. Since 2004, an increase in the pumping level was observed in test section 0509. Test section 0506 demonstrated very little pumping over time.

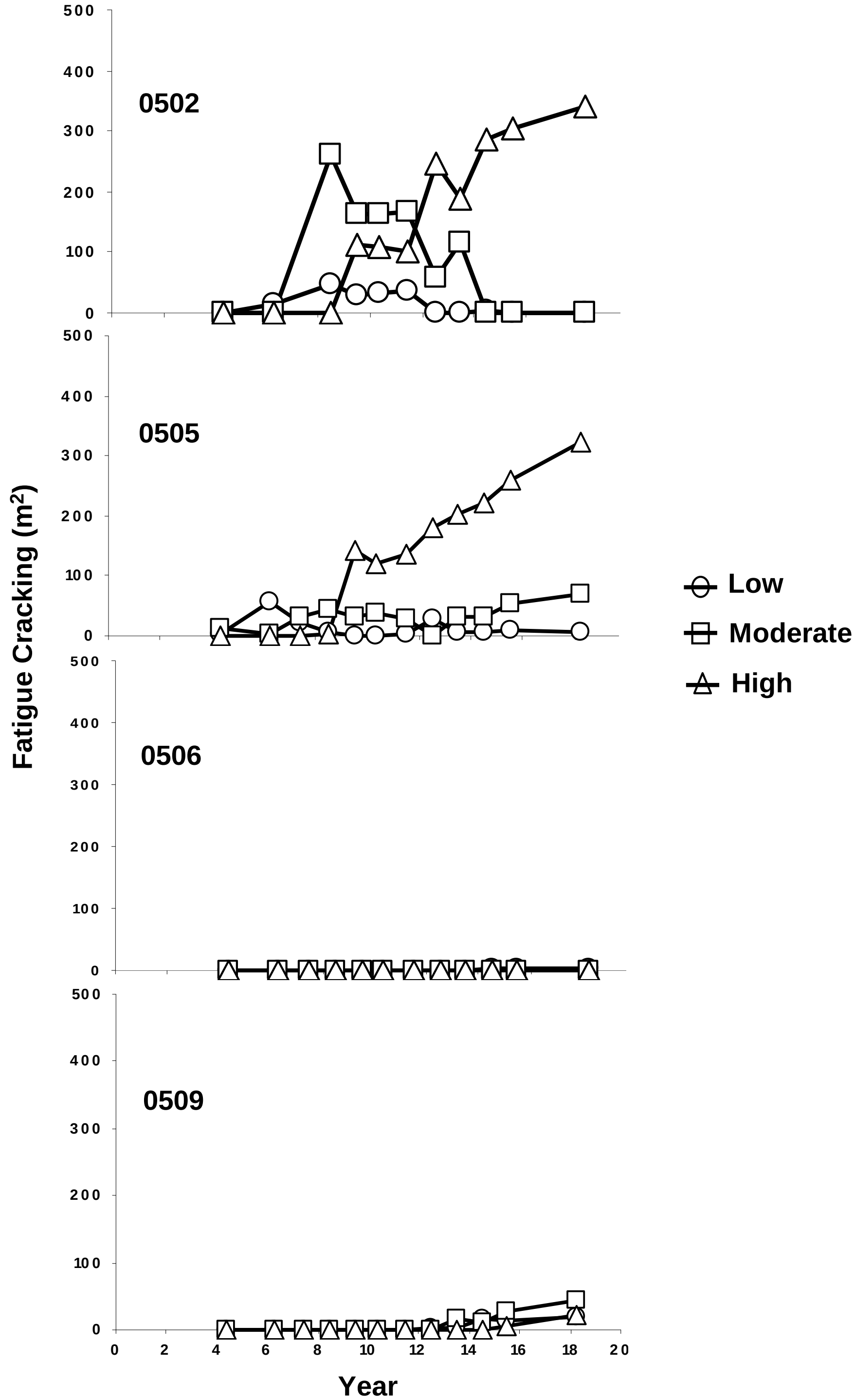

Figure 26. Fatigue Cracking Progression.

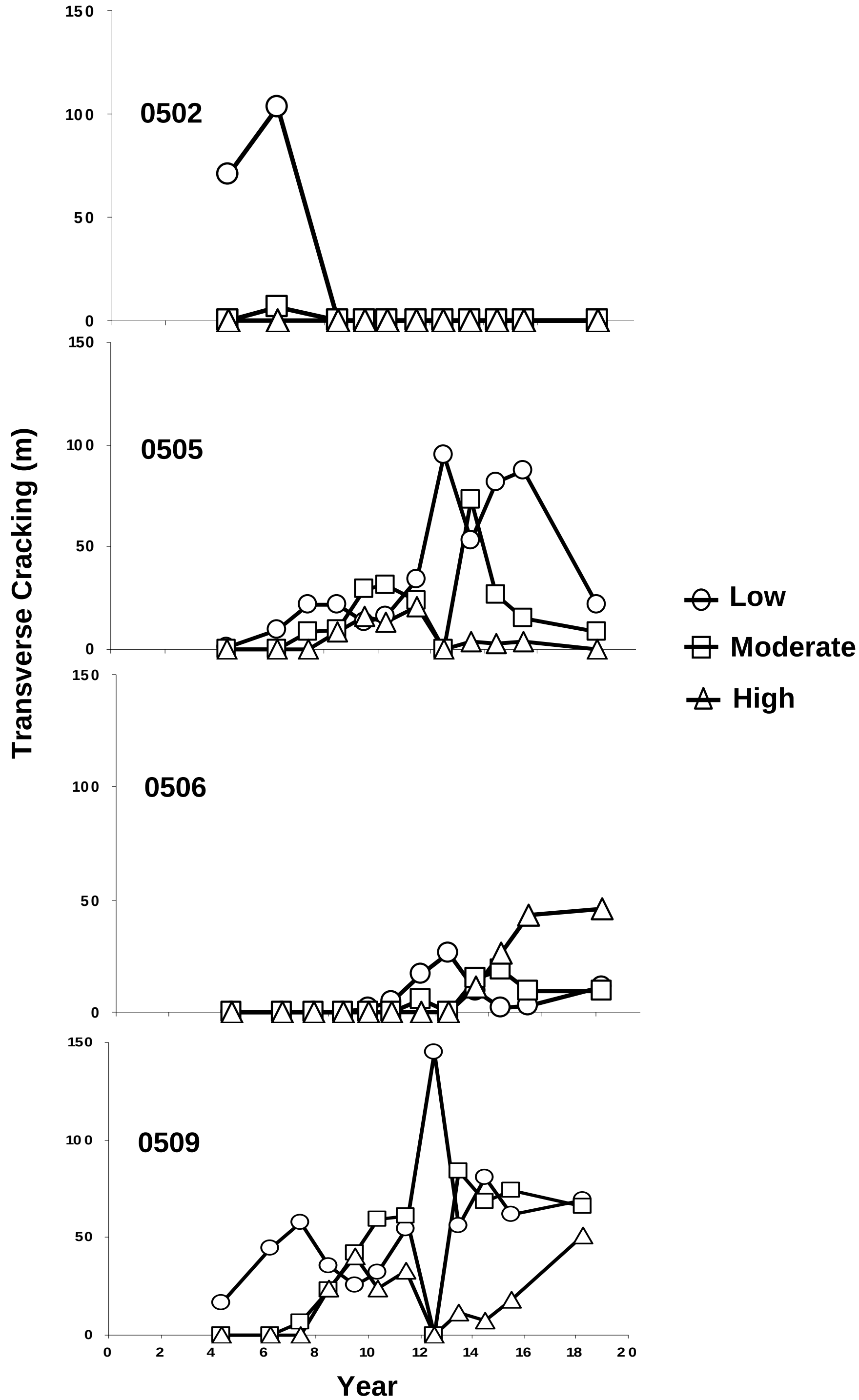

Figure 27. Transverse Cracking Progression.

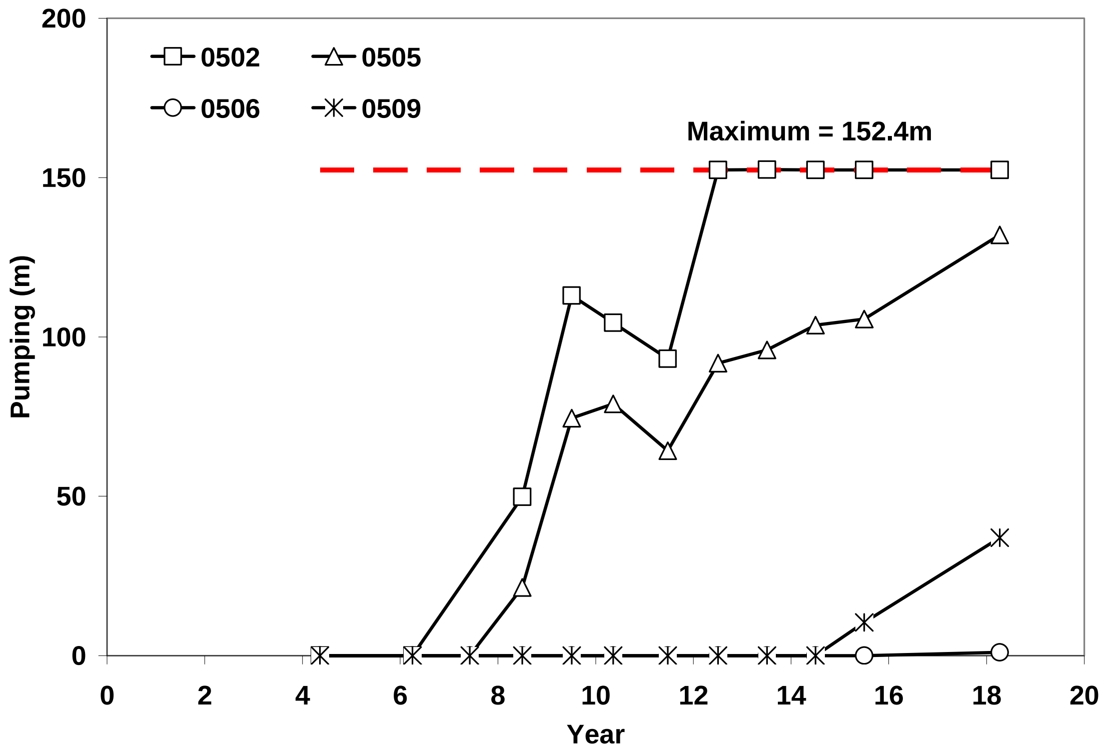

Figure 28. Pumping Progression.

According to an industry survey, rutting is the most serious pavement distress. Fatigue cracking was rated as the second most serious problem, followed by thermal cracking **[5]**. These distresses are influenced by material properties, loading history, and environment. They can be further compounded by poor design procedures and/or pavement maintenance and rehabilitation practices.

Pavement rutting is a surface depression along wheel paths caused by the plastic deformation of the AC materials, which is a common problem in hot climates. At higher temperature, AC pavements become softer due to a reduction in asphalt binder viscosity. This phenomenon increases the rutting potential of AC pavements. Rutting in AC pavements is a load-induced permanent deformation of pavement layer(s). It develops with an increasing number of traffic load applications and material aging over time. Rutting is typically caused by a combination of densification and shear related deformation and may occur in any layer of a pavement structure. The layer(s) in which rutting occurs is a function of loading magnitude and the relative strength of the pavement layers. Two main problems associated with rutting in pavements are: (1) vehicle steering difficulty, and (2) hydroplaning (water in the ruts), particularly for light passenger cars **[6]**.

In recent years, the AZ SPS-5 test sections have experienced an increase in rutting. One of the objectives of this forensic investigation was to study rutting performance. The LTPP program uses the Dipstick™ device to obtain reference elevations across the pavement lane and quantify the rutting of pavements. Dipstick™ measurements at 1ft (0.305m) intervals were taken to trace the transverse profiles. A complete view of rut depth along the Inner Wheel Path (IWP) and Outer Wheel Path (OWP) for each of the test sections is presented in Figures 29 and 30, respectively. For most of the stations, the OWP rutting is higher than the IWP rutting. In general, test sections 0505 and 0506 with virgin AC overlay exhibited higher rutting resistance than test sections 0502 and 0509 with the recycled AC overlay.

The rut depth progression for the test sections along IWP and OWP during their monitored period are presented in Tables 20 through 23. In these tables, routine maintenance activities (i.e., fog seal coats) contributed to a decrease in average rut depth are represented by star (*). The historical average rut depth is shown in Figures 31 through 34. The rutting performance of the test sections after four and eighteen years of service are presented. It is evident that the test sections' rutting increased over time, especially for test sections 0502, 0505 and 0509. The rutting progression for test section 0506 is very minimal.

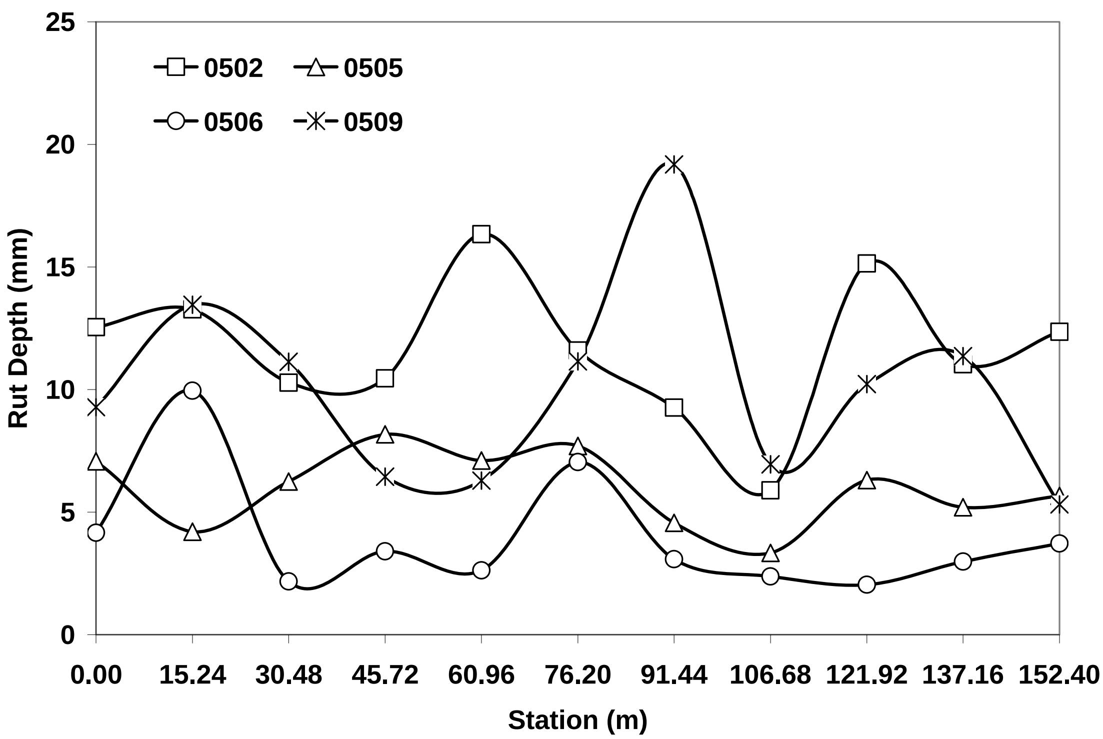

Figure 29. Inner Wheel Path (IWP) Rutting.

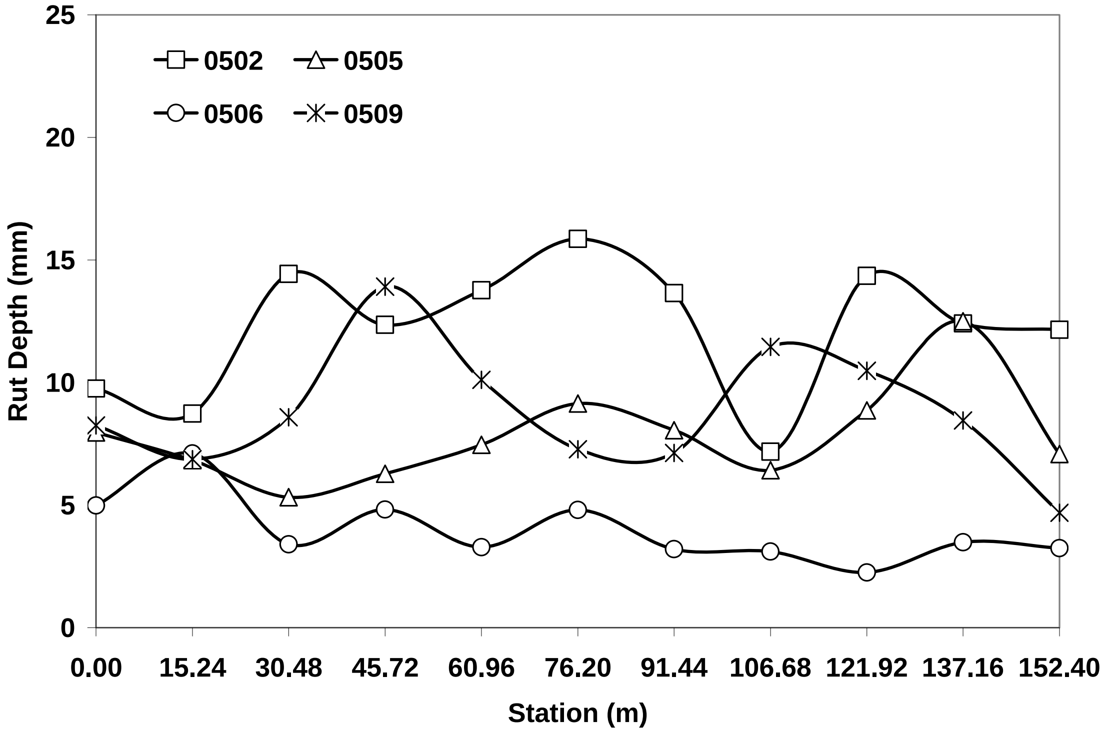

Figure 30. Outer Wheel Path (OWP) Rutting.

Table 20. Rut Depth Progression; Section 0502.

Test Date	Average Rut Depth (mm)		
	IWP	OWP	Average
19 Oct 94	5.37	5.87	5.62
13 Nov 97	6.92	7.03	6.98
10 Dec 98	6.67	7.62	7.15
13 Dec 99	8.28	10.99	9.64
17 Oct 00	6.98	6.37	6.67*
29 Nov 01	7.41	8.10	7.75
11 Dec 02	7.76	8.20	7.98
11 Dec 03	8.27	8.64	8.46
8 Dec 04	9.40	10.74	10.07
8 Dec 05	9.59	10.74	10.17
15 Sep 08	11.65	12.24	11.94

Table 21. Rut Depth Progression; Section 0505.

Test Date	Average Rut Depth (mm)		
	IWP	OWP	Average
20 Oct 94	1.25	2.01	1.63
12 Jul 96	1.64	5.87	3.75
13 Nov 97	1.87	2.91	2.39
10 Dec 98	2.18	3.05	2.62
14 Dec 99	3.28	5.41	4.35
18 Oct 00	2.65	3.20	2.93*
29 Nov 01	2.95	4.51	3.73
12 Dec 02	3.47	4.31	3.89
12 Dec 03	3.36	4.82	4.09
8 Dec 04	3.72	5.48	4.60
8 Dec 05	4.51	5.62	5.07
15 Sept 08	5.96	7.81	6.88

Table 22. Rut Depth Progression; Section 0506.

Test Date	Average Rut Depth (mm)		
	IWP	OWP	Average
19 Oct 94	1.02	0.99	1.01
12 Sep 96	1.56	1.24	1.40
13 Nov 97	2.68	2.10	2.39
10 Dec 98	2.22	1.94	2.08
14 Dec 99	2.70	5.32	4.01
17 Oct 00	2.26	2.06	2.16*
29 Nov 01	2.45	3.60	3.03
12 Dec 02	2.04	2.36	2.20*
11 Dec 03	1.96	1.92	1.94*
8 Dec 04	2.88	3.28	3.08
8 Dec 05	3.60	3.76	3.68
15 Sep 08	7.04	4.80	5.92

Table 23. Rut Depth Progression; Section 0509.

Test Date	Average Rut Depth (mm)		
	IWP	OWP	Average
19 Oct 94	6.61	5.96	6.29
12 Sep 96	8.53	7.54	8.04
13 Nov 97	8.22	5.97	7.10
13 Dec 99	10.23	10.18	10.21
17 Oct 00	7.02	5.67	6.35*
29 Nov 01	7.29	5.96	6.63
11 Dec 02	7.40	6.10	6.75
11 Dec 03	6.98	6.73	6.86
8 Dec 04	6.98	7.43	7.21
5 Dec 05	7.14	6.45	6.80*
15 Sep 08	11.15	7.28	9.22

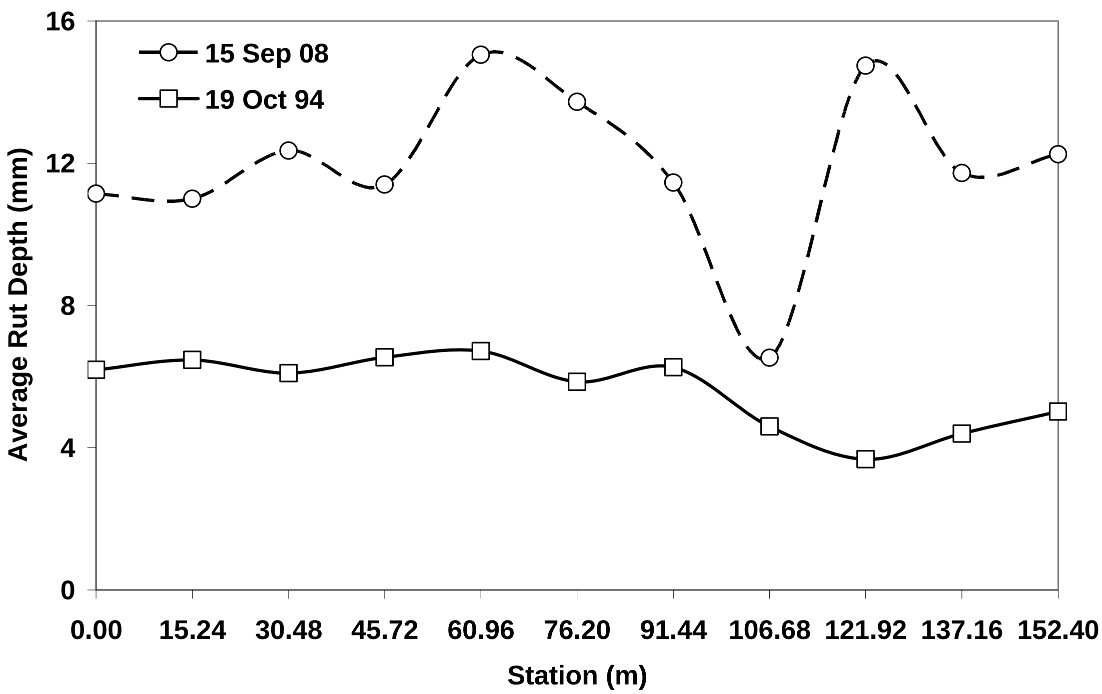

Figure 31. Rutting Performance; Section 0502.

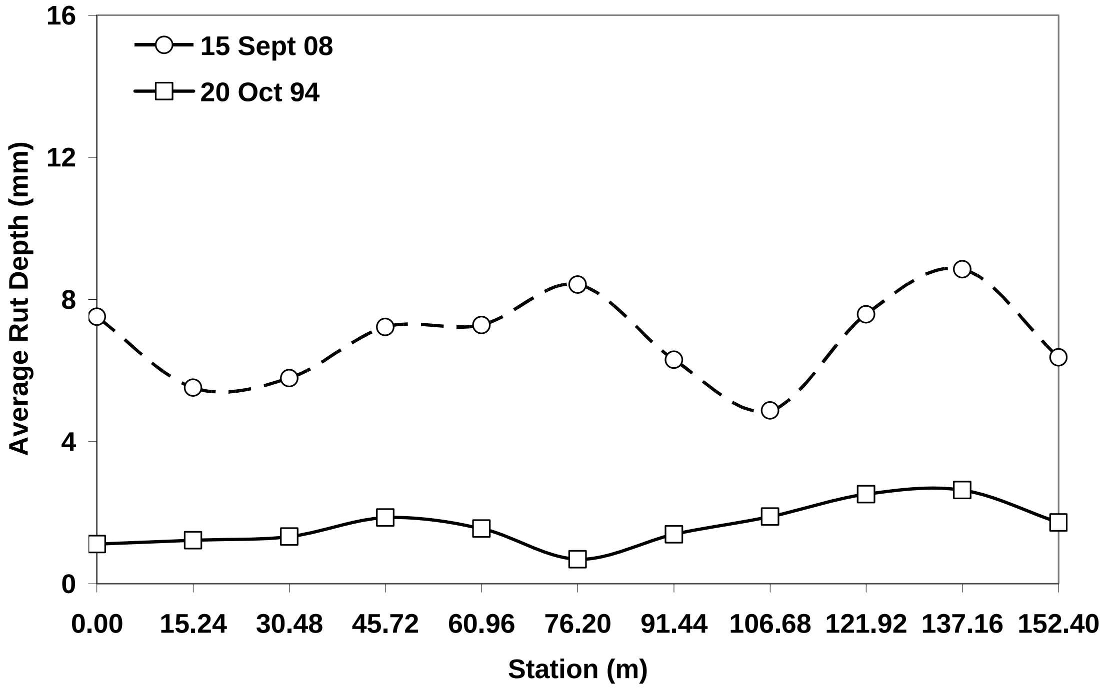

Figure 32. Rutting Performance; Section 0505.

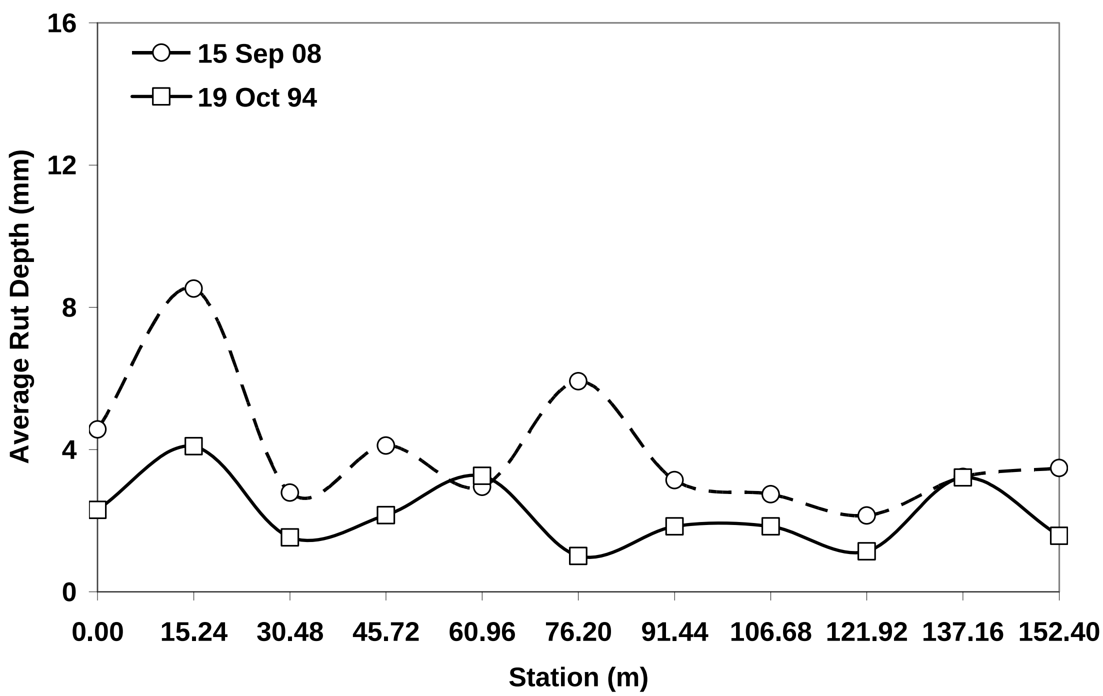

Figure 33. Rutting Performance; Section 0506.

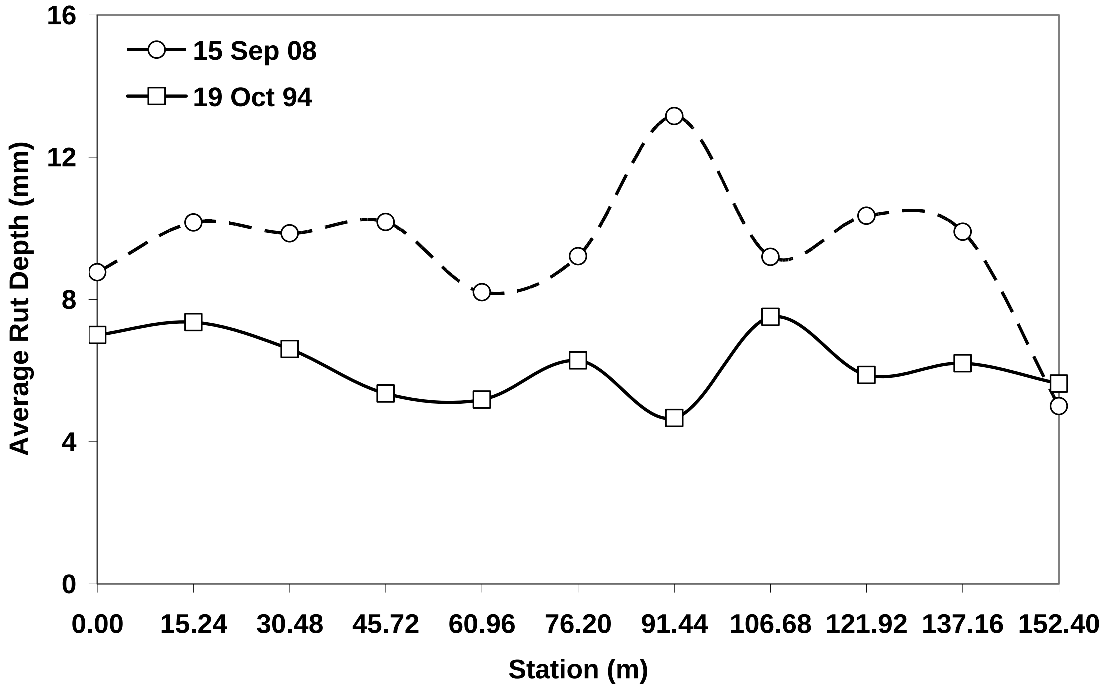

Figure 34. Rutting Performance; Section 0509.

ROUGHNESS

Pavement roughness is considered one of the dominant attributes of pavement condition affecting the public perception of serviceability. High speed inertial profilometers provide routine collection of pavement roughness profile data on LTPP test sites. As part of the forensic investigation, the pavement longitudinal profile data were recorded using the ICC inertial profiler provided by FHWA for LTPP data collection (Figure 35). A constant vehicle speed of 50 miles per hour was maintained during the profile measurement runs. The longitudinal surface elevations were collected at 6 in (150mm) intervals.

The LTPP ProQual software was used to evaluate the acceptability of profile runs based on LTPP criteria. From the collected profile data, the International Roughness Index (IRI) values along IWP and OWP, as well as the mean IRI of the two wheel paths, were computed. In this forensic study, the effect of pavement distresses on roughness IRI were investigated.

The profile characteristics of each pavement section and the change in the IWP and OWP IRI with time are presented in Figures 36 through 39. The mean IRI values for each of the test sections over their monitored period are given in Figure 40. The historical IRI summary statistics are presented in Table 24. Section 0502 showed improvement in OWP IRI after rehabilitation. In addition, the IWP roughness after rehabilitation was much higher than that of OWP. This was almost certainly caused by the presence of distresses along the IWP. The IWP and OWP IRI values are slightly decreased after the placement of fog seal coats and crack sealing. Sections 0502 and 0509 exhibited significant increase in IRI over their post-rehabilitation monitoring history. The roughness level in 2008 is almost twice the roughness level before rehabilitation in 1990 for each test section. The drastic growth in roughness for these test sections is due primarily to the existence of fatigue cracking and pumping in test section 0502 and transverse cracking in test section 0509. In most cases, the transverse cracks covered the entire width of the lane. Section 0505 also exhibited a large increase in roughness with time. The change in roughness growth at this test section was minimal throughout the post-rehabilitation monitoring history. This section experienced high severity fatigue cracking and transverse cracking with a high level of pumping contributing to an increase in the roughness level. Section 0506 increased in roughness at a steady rate after rehabilitation until 2004. In this section, the roughness increased more rapidly in the last 3 years than over the previous 14 years with the development of high severity transverse cracks.

As discussed previously, each of the test sections received crack sealing and fog seal coats. These rehabilitation activities did not cause an immediate change of the IRI values. In general, based on the longitudinal profile roughness analyses, it was found that recycled overlay test sections 0502 and 0509 exhibited the largest post-rehabilitation increase in roughness IRI over their monitoring history.

Figure 35. LTPP Inertial Profiler.

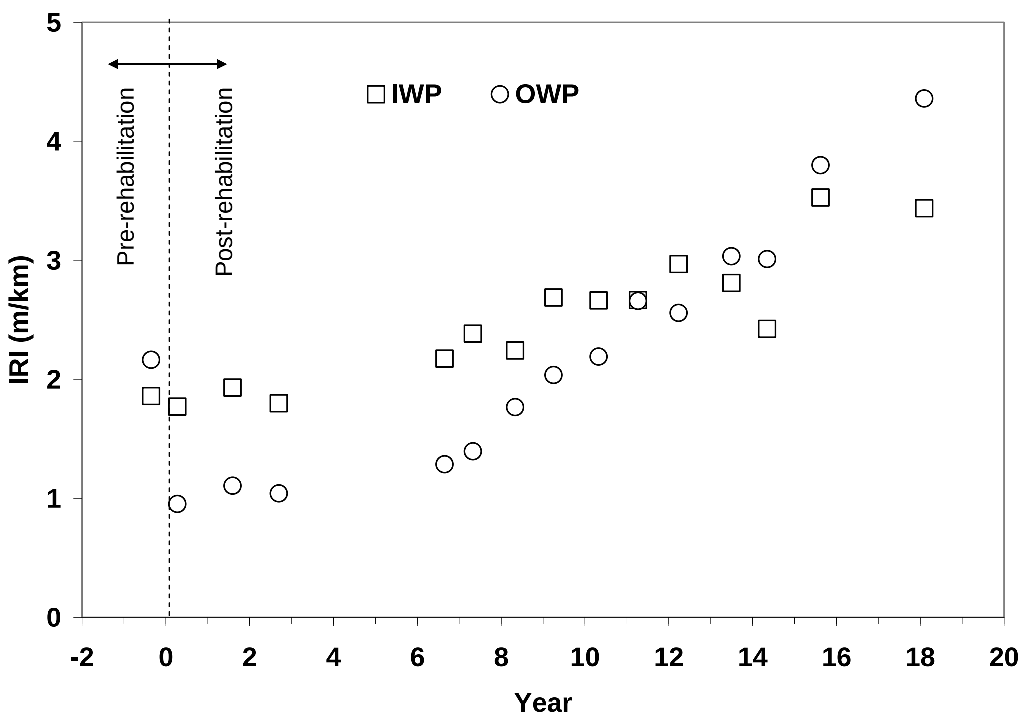

Figure 36. IRI Progression; Section 0502.

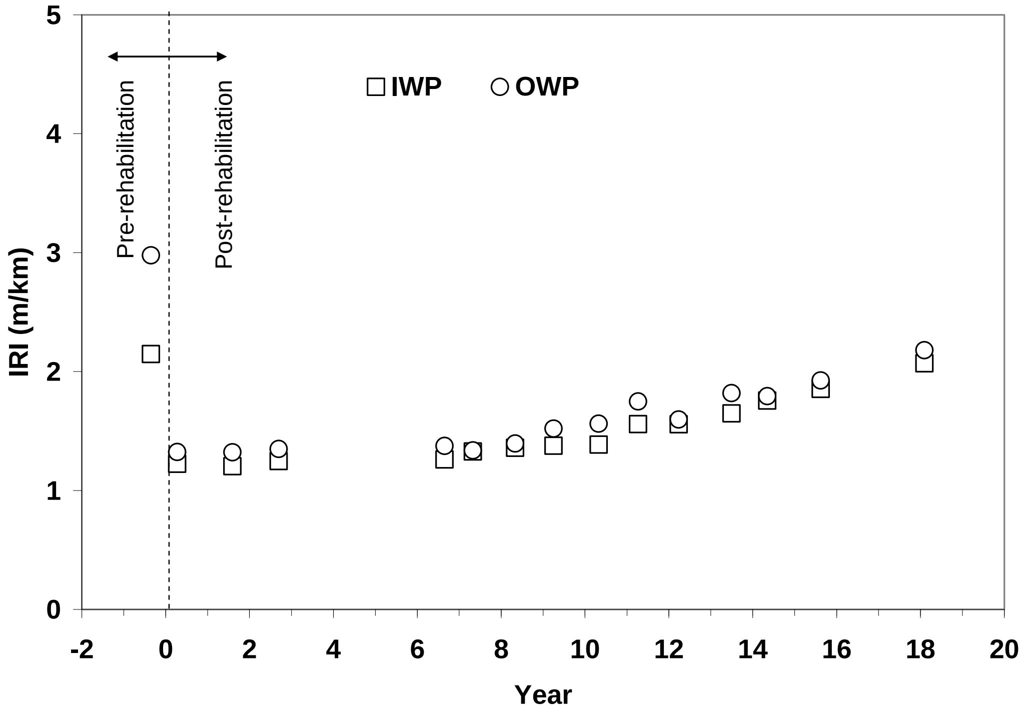

Figure 37. IRI Progression; Section 0505.

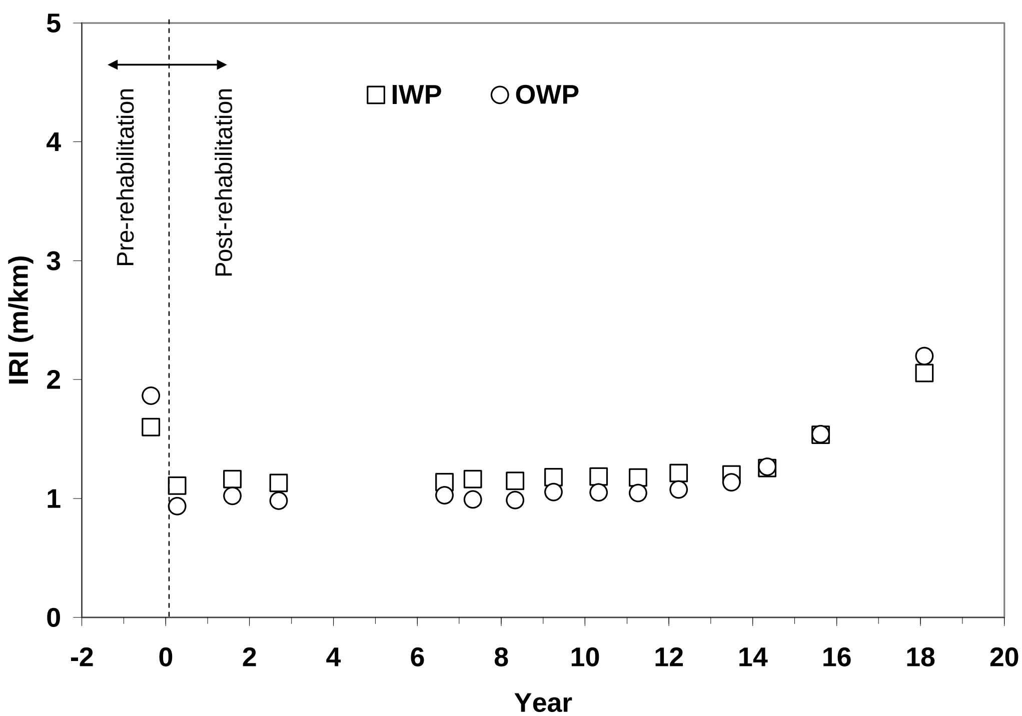

Figure 38. IRI Progression; Section 0506.

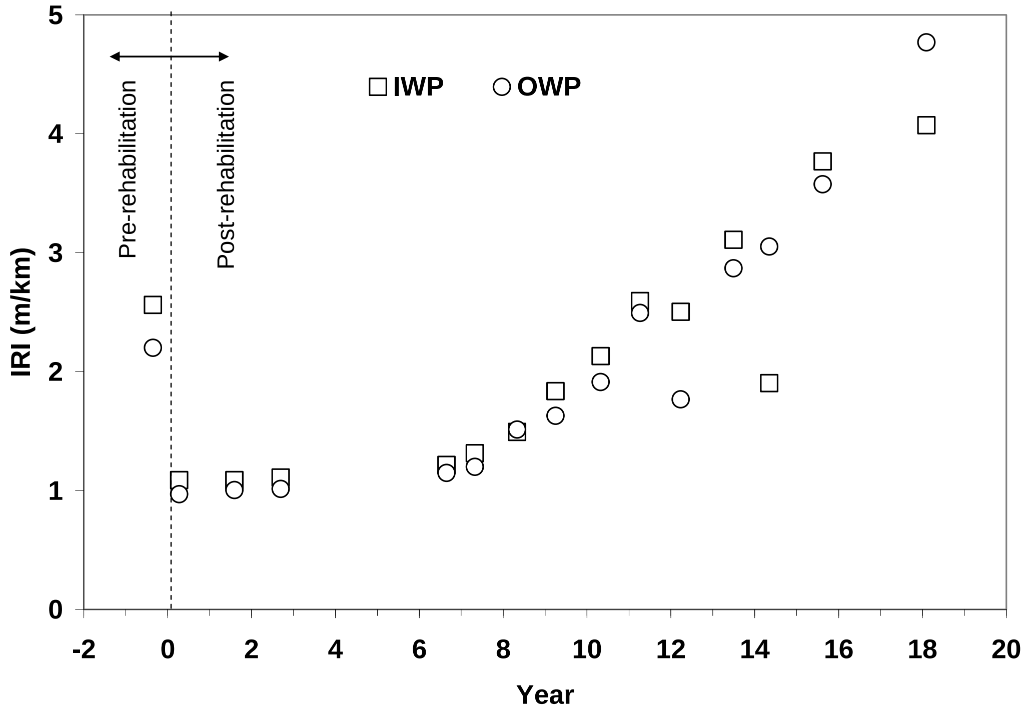

Figure 39. IRI Progression; Section 0509.

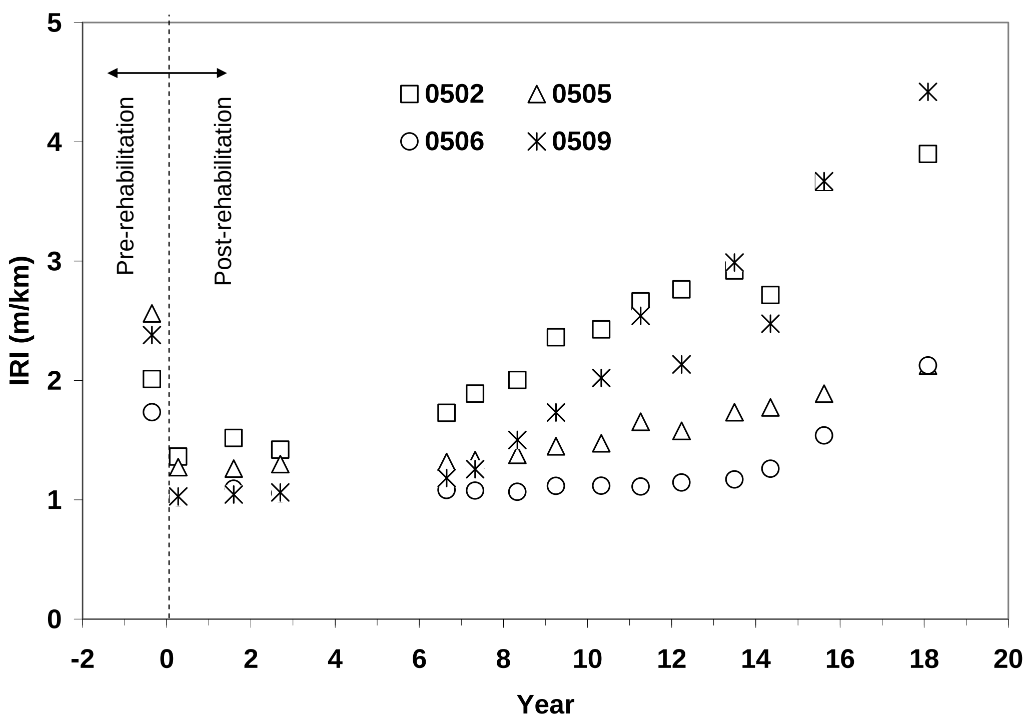

Figure 40. Mean IRI Progression.

Table 24. IRI Summary Statistics.

Test Date	Year	Test Section							
		0502		0505		0506		0509	
		IRI (m/km)							
		Mean	Standard Deviation	Mean	Standard Deviation	Mean	Standard Deviation	Mean	Standard Deviation
5 Feb 90*	-0.4*	2.012	0.120	2.562	0.011	1.733	0.103	2.380	0.034
21 Sept 90	0.3	1.362	0.029	1.273	0.007	1.020	0.011	1.027	0.012
15 Jan 92	1.6	1.518	0.056	1.262	0.019	1.091	0.038	1.044	0.012
22 Feb 93	2.7	1.419	0.031	1.298	0.010	1.055	0.015	1.061	0.016
3 Feb 97	6.6	1.729	0.037	1.316	0.016	1.081	0.008	1.181	0.005
9 Dec 97	7.3	1.889	0.050	1.333	0.013	1.077	0.020	1.256	0.014
11 Dec 98	8.3	2.004	0.024	1.377	0.007	1.067	0.017	1.501	0.016
11 Nov 99	9.3	2.361	0.055	1.448	0.023	1.115	0.012	1.732	0.013
6 Dec 00	10.3	2.427	0.026	1.473	0.033	1.117	0.005	2.020	0.016
15 Nov 01	11.3	2.662	0.029	1.653	0.021	1.111	0.010	2.542	0.039
4 Nov 02	12.2	2.762	0.156	1.577	0.066	1.144	0.029	2.134	0.285
6 Feb 04	13.5	2.922	0.088	1.733	0.052	1.169	0.011	2.988	0.108
14 Dec 04	14.3	2.717	0.088	1.775	0.035	1.260	0.030	2.476	0.227
24 Mar 06	15.6	3.663	0.042	1.890	0.064	1.538	0.006	3.671	0.092
11 Sep 08	18.1	3.898	0.053	2.124	0.093	2.126	0.034	4.419	0.162

* Pre-rehabilitation test

FALLING WEIGHT DEFLECTOMETER (FWD) TESTING

Pavement's structural condition can be assessed through several different measurements. The most comprehensive approach is to use Falling Weight Deflectometer (FWD) data. Since the early 1990's, the FWD has been used widely in the LTPP program to measure pavement layer deflections. The FWD is capable of producing a wide range of loads. The geophones located at specified distances from the load plate measure surface deflections to determine the in-situ elastic modulus of the pavement layers.

For the forensic investigation, FWD deflection testing was performed on September 15 to 17, 2008. Eleven deflection tests per pass were collected on each test section at 50 ft (15.24 m) testing intervals along the OWP and mid-lane. The FWD testing locations are shown in Figure 41.

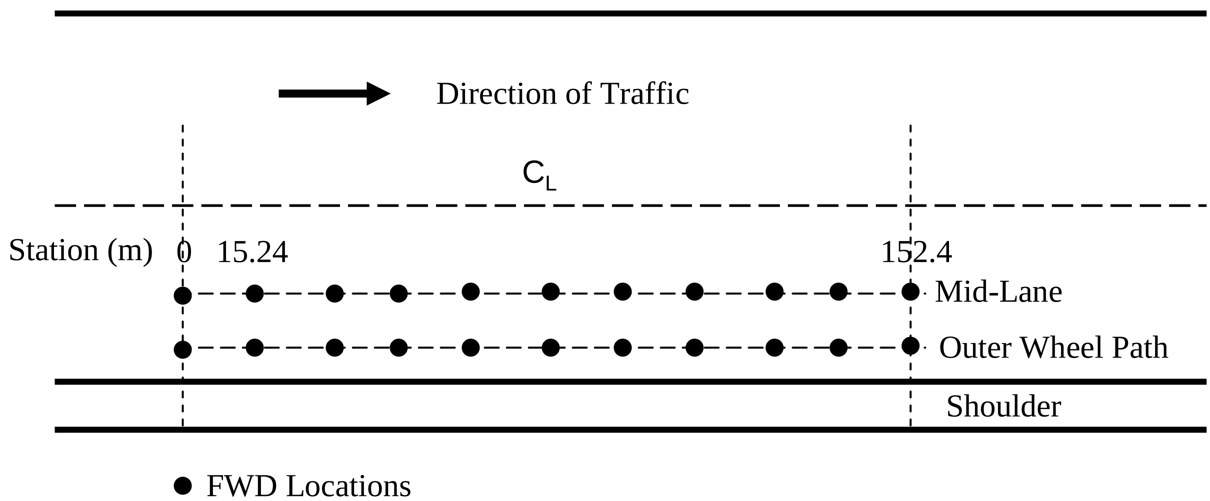

Figure 41. FWD Test Locations.

To assess the performance of the AC surface layer, the FWD maximum deflections along the OWP and mid-lane were analyzed and are presented in Figures 42 and 43, respectively. As illustrated in these figures, the FWD maximum deflection value varies from station to station. The OWP has generally higher deflections when compared to the deflection at the mid-lane. Test sections 0502 and 0509, with low rutting resistance performance, measured higher FWD maximum deflections, whereas test sections 0505 and 0506 exhibited lower deflections. This phenomenon is apparent for FWD deflections along the OWP. Referring to Figure 43, the large deflection spike at station 76.20 m (section 0506) is due to the presence of high severity transverse cracking.

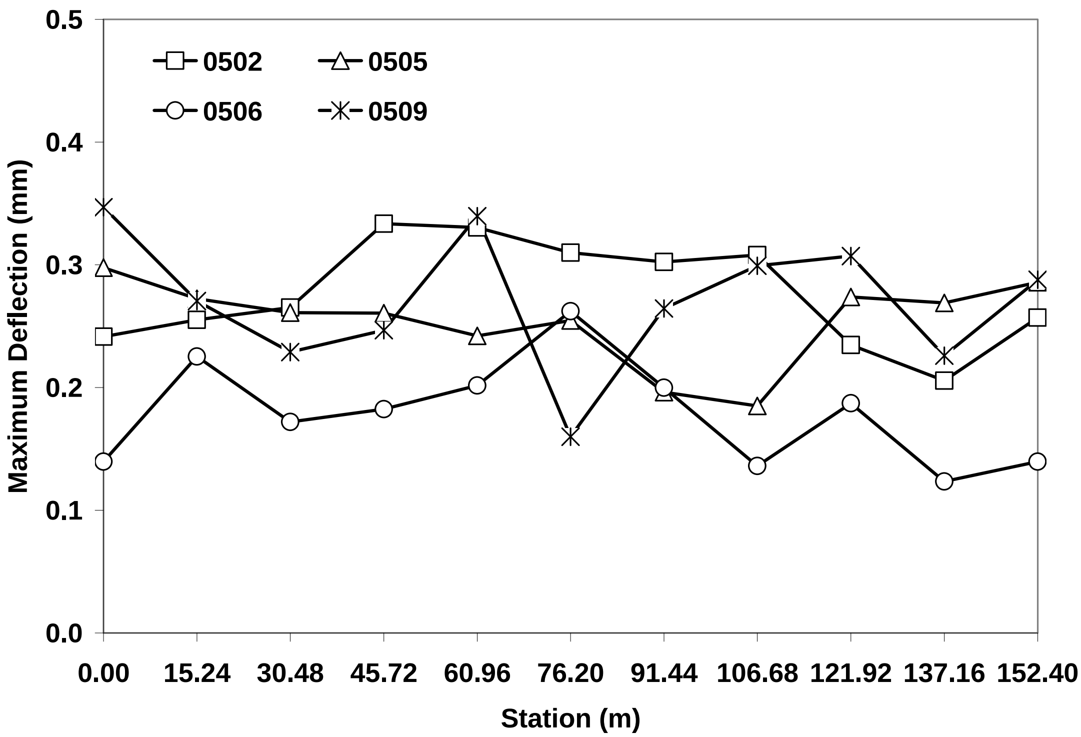

Figure 42. FWD Maximum Deflections; OWP.

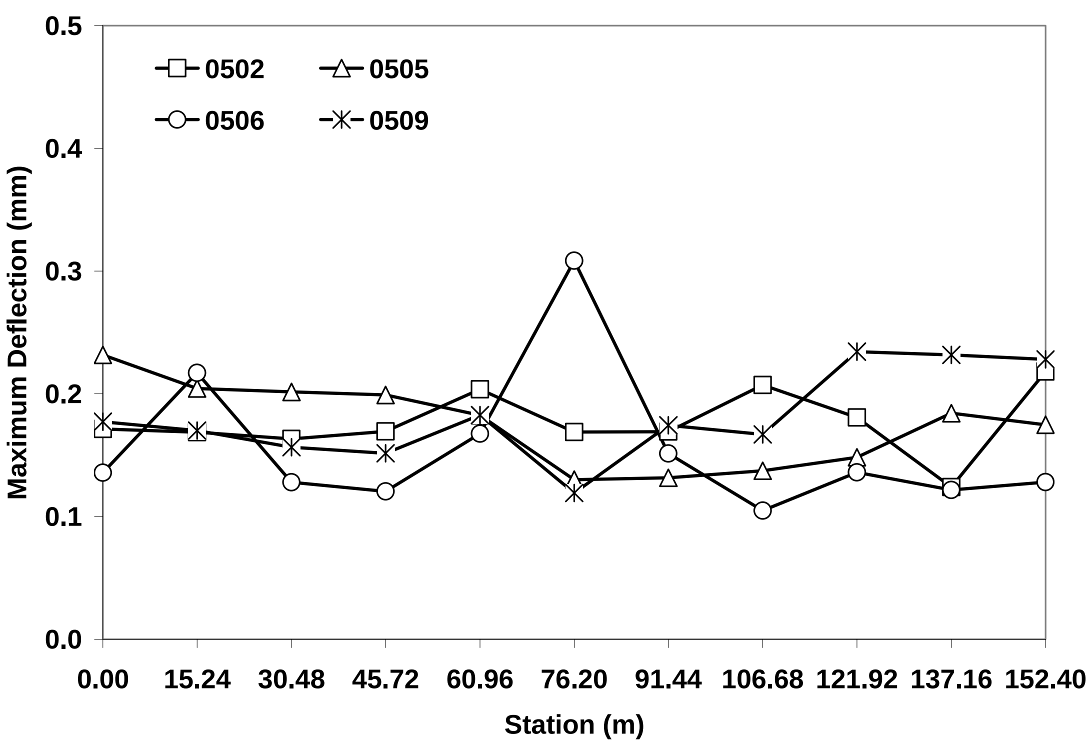

Figure 43. FWD Maximum Deflections; Mid-Lane.

The test sections layer modulus values were back-calculated from FWD deflection data using the EVERCALC back-calculation program developed by Washington State Department of Transportation **[7]**. The input parameters for the analyses include sensor locations, layer thickness, initial modulus ranges, and Poisson's ratio. The initial modulus and Poisson's ratio values used in the analysis are shown in Table 25.

For FWD back-calculation analysis, the AC layer refers the combinations of inlay (original AC and mill & fill) and overlay layers. The back-calculated layer moduli values using the FWD deflection data measured in September 2008 are summarized in Table 26. In general, higher modulus values correlate with better performing pavement layers and vice versa. The AC layer moduli values for test sections 0506 and 0509 are higher, indicating stiffer AC layers. These test sections exhibited low severity fatigue cracking with very little pumping. The AC layer moduli values for test sections 0502 and 0505 are lower, suggesting deteriorated or weakened AC surface layer. These findings are consistent with the rutting and cracking performance of each test section presented earlier.

It is evident that the base and subgrade layer modulus values are relatively high for AC pavements indicating high strength materials. The modulus values were estimated to be in the ranges of 300 to 500 MPa and 50 to 300 MPa, respectively. These values are reasonable and higher than would be anticipated for conventional flexible pavement subgrade materials. In general, the FWD back-calculation results indicated that the base and subgrade materials are all in good condition.

Table 25. Initial Input Parameters EVERCALC **[7]**.

Material Type	Initial Modulus Range (MPa)	Poisson's Ratio
AC	1,000-15,000	0.35
Base	70-4,000	0.40
Subgrade	35-2,000	0.45

Table 26. Back-calculated Layer Moduli (September 2008).

Section	Layer Modulus (MPa)		
	AC* **[E1]**	**Base** **[E2]**	**Subgrade** **[E3]**
0502	2419.5	343.3	280.6
0505	1659.3	455.8	148.1
0506	5869.2	386.1	57.7
0509	4886.9	310.2	251.5

* Refers the combinations of inlay (original AC and mill & fill) and overlay layers.

Back-calculated AC layer moduli values for the test sections over their monitored history are presented in Figure 44. Stiffer AC responses are observed in test sections 0506 and 0509. The AC layer strength for test sections 0502 and 0505 are almost identical.

In general, reduction in AC layer stiffness with time occurs due to deterioration of the pavement structure. Over time, the test sections received extensive crack sealing and fog seal coats to improve conditions of the surface layer. A slight increase in the AC layer stiffness is shown with these maintenance activities. Periodic maintenance and repairs can provide temporary improvement of the surface condition, but do not typically remedy structural deficiencies associated with the pavement layers. Over time, the AC stiffness in each of the test sections became inadequate to handle the existing traffic volume. Overall, the final structural condition of pavement layers was lower than the pre-rehabilitation strength, indicating the need for immediate pavement rehabilitation activities.

The back-calculated base and subgrade layer moduli values over their monitored period are shown in Figures 45 and 46, respectively. The stiffness of these materials significantly reduced over the past years. Upon degradation of the surface layers, water can easily percolate through cracks. Water damage and loss of materials from pumping may have contributed to the loss of material strength.

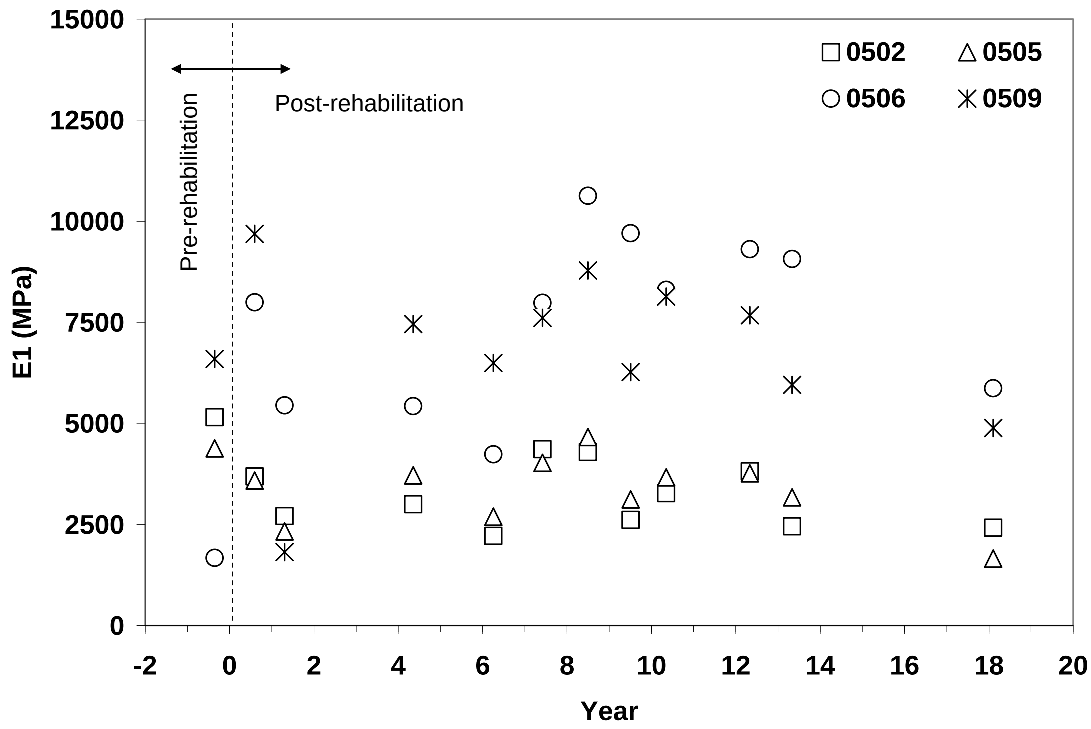

Figure 44. AC Layer Moduli Progression.

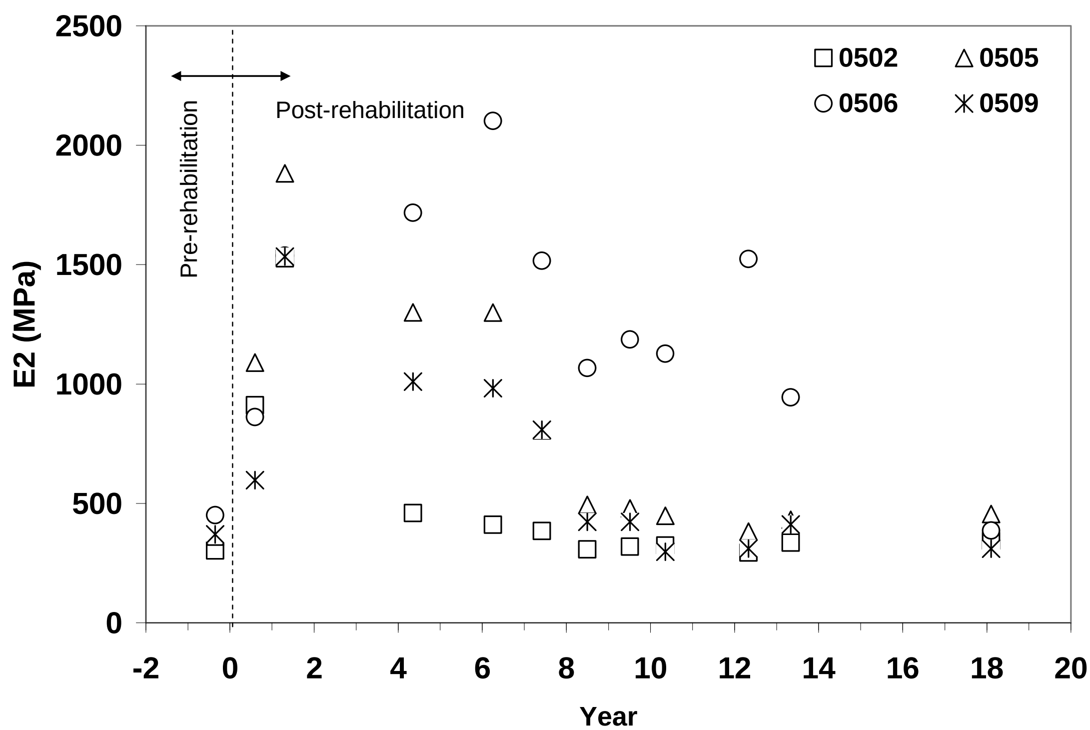

Figure 45. Base Layer Moduli Progression.

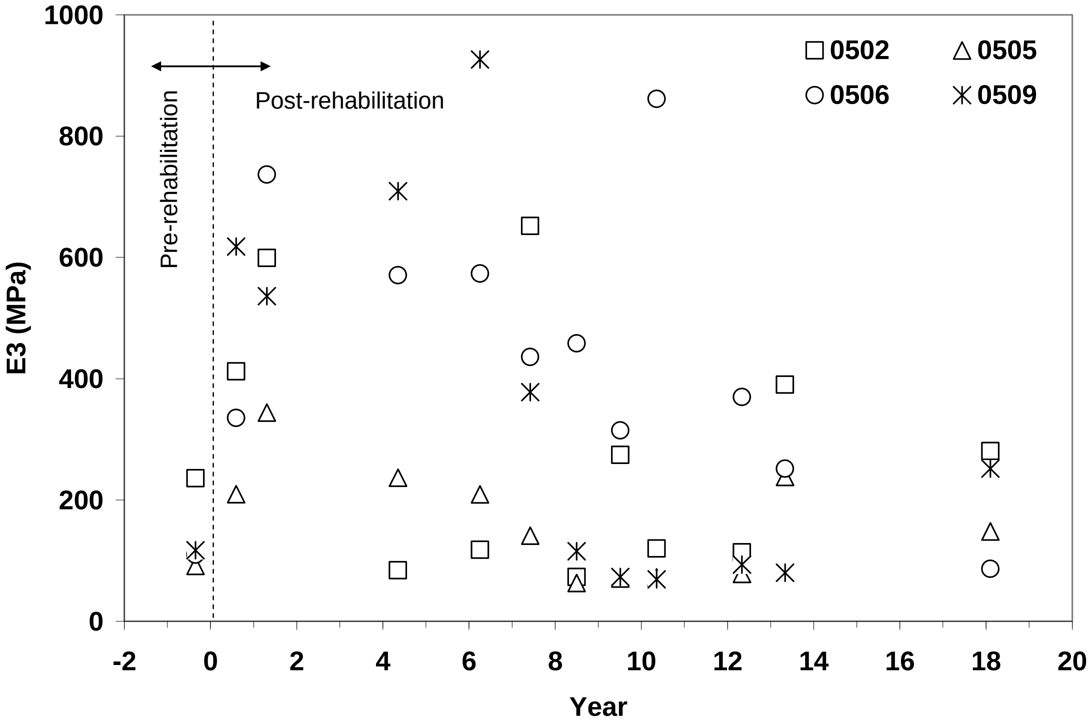

Figure 46. Subgrade Layer Moduli Progression.

In addition, the 1993 AASHTO design guide was used to calculate the effective modulus of the pavement (E_P). The input parameters included deflection measured at the center of the load, the subgrade resilient modulus, and the total thickness of all pavement layers above the subgrade (D). The effective Structural Number (SN_{eff}) was computed using the following equation:

$$SN_{eff} = 0.0045D\sqrt[3]{E_P} \quad \text{Equation (3)}$$

The structural strength of the test sections using the FWD deflection data measured in September 2008 are given in Figure 47. The average SN_{eff} values for each test sections are presented Table 27. Test section 0506 exhibited higher structural strength than the other test sections.

The structural strength of each pavement section over their monitored period are presented in Figure 48. As discussed previously, each of the test sections received crack sealing in May 2002 and fog seal coats in May 1998, August 2001, and April 2003. These maintenance activities did not significantly improve the post-rehabilitation structural performance. In general, the pavement structural capacity for each of the test sections deteriorated with time.

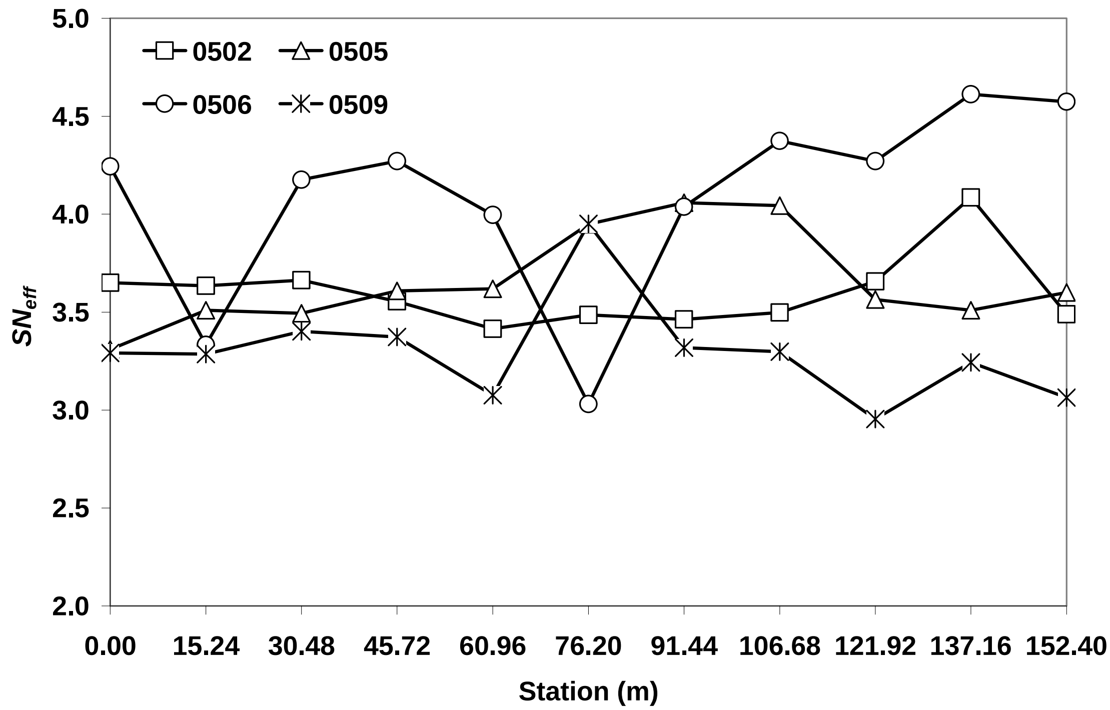

Figure 47. Structural Strength of Test Sections (September 2008).

Table 27. Average Structural Number (September 2008).

Section	**Average SN_{eff}**
0502	3.6
0505	3.7
0506	4.1
0509	3.3

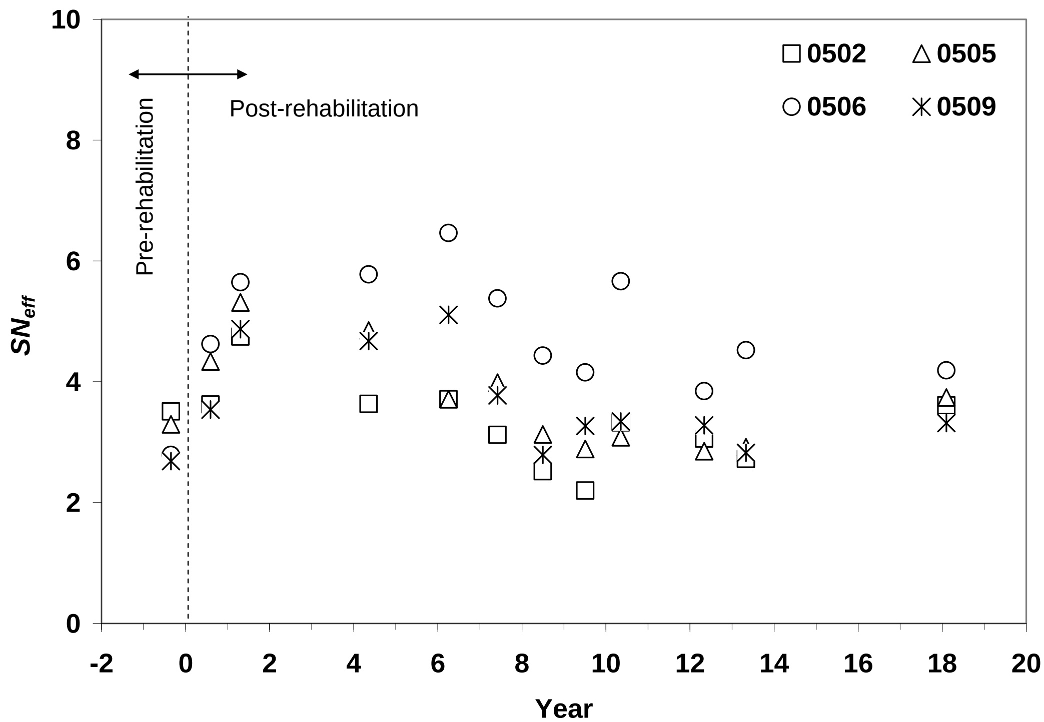

Figure 48. Structural Strength Progression.

Modulus Comparison

The modulus values from different test methods may vary due to testing procedures and local conditions. The comparisons of base and subgrade moduli using FWD and DCP are presented in Table 28. The moduli values from these tests are not identical since each device estimates the modulus in different ways; however, they do follow similar trends. Overall, the FWD back-calculation analyses resulted in higher modulus values. No meaningful correlation was found that relates the SPT-N values to the base and subgrade elastic moduli values, since the granular layers in pavements are relatively thinner than deep foundations used in most geotechnical projects

Table 28. Comparison of Base and Subgrade Modulus Values.

Section	Base Modulus (MPa)		Percent Difference	Subgrade Modulus (MPa)		Percent Difference
	FWD	DCP		FWD	DCP	
0502	343.3	137.5	59.9	280.6	65.3	76.7
0505	455.8	158.1	65.3	148.1	109.6	26.0
0506	386.1	75.2	80.5	57.7	85.3	32.4
0509	310.2	98.4	68.3	251.5	59.9	76.2

SUMMARY AND CONCLUSIONS

An in-depth forensic investigation consisting of destructive and non-destructive tests following LTPP protocols was performed on selected Arizona SPS-5 test sections (0502, 0505, 0506, and 0509). Based on preliminary discussions with ADOT and FHWA, the project objectives included identifying the causes of pavement failures, examining the pavement structural and functional performances, measuring within-section layer thicknesses and material properties, and testing end-state physical properties.

Core holes were drilled to attempt determine the point of crack initiation and to check whether the crack extended completely through the bound surface layer. Several core samples exhibited medium to high severity cracks initiated at the pavement surface and extending to the inlay layer, showing a top-down cracking pattern. The main contributing factors for this type of cracking may include heavy axle loads, aging of asphalt binder, and reductions in AC surface layer stiffness. Moreover, thickness measurements from core samples were used to assess, if any, construction variability during rehabilitation activities. In general, the average thickness of the AC pavement layers (overlay and original inlay layers) in each test section remained constant over the 500 ft section length and was consistent with the rehabilitation design thicknesses.

As per LTPP recommendations, trench excavations were conducted in two test sections (0506 and 0509) to determine which layer (s) in the pavement structure contributed to the higher than expected rutting. Regardless of pavement type used, it was found that rutting was mainly in the top AC layer and virtually no rutting was detected in the lower layers. Rutting along wheel paths was also dominant for each test section. The AC surface rutting was also quantified using reference elevations across the pavement lane collected using a Dipstick™ device. It was determined that test sections 0505 and 0506 with virgin AC overlay exhibited higher rutting resistance than sections 0502 and 0509 with recycled AC overlay. The combined effects of high volume traffic loading and temperature were identified as primary causes of rutting. Pavement sections constructed with recycled AC mixtures (0502 and 0509) exhibited significant percentages of air voids that could also be a contributing factor for pavement rutting.

Based on visual assessment of entire trench operations, no reflective cracks were observed at the bottom of the AC slab layer, reconfirming the crack mechanism as top-down cracking. Nonetheless, the original AC layer placed during 1968 pavement construction was appeared to be “dry” mix and consequently falling apart upon extraction of cores and trench chunks. This indicates that the original AC mixture retained inadequate binder content associated with high percent air voids that consequently reduced mixture bonding.

NDG tests were conducted on top of the base and subgrade layers at trench locations to measure in-situ densities. DCP and SPT tests were also conducted to characterize the relative strength of these layers. Testing results from these devices indicated uniform base/subgrade material properties and were found to be in good conditions (i.e., high strength materials). Comparatively, higher densities for the base materials were obtained indicating optimum compaction efforts during pavement reconstruction/rehabilitation.

In addition, laboratory tests were conducted to determine the engineering properties of the base and subgrade materials at trench locations. The base material gradations for these test sections were similar. However, significant variations in gradation were obtained for subgrade material, especially for sieve sizes ranging from 12.5mm to 0.075mm (i.e., the subgrade material in section 0506 had a much higher percentages of fines). Laboratory testing on AC core samples were also performed in accordance with LTPP test protocols. Overall, the measured percent passing for test sections 0502 and 0509 deviated significantly from the JMF aggregate gradations, but were relatively close for sections 0505 and 0506. The measured average percent binder contents for the test sections (except section 0505) were higher when compared to the JMF specified values. The rutted test sections are found to be associated with high binder content. The poor gradations associated with material selection with no subsequent adjustment in the mix design were found to permit moisture infiltration which potentially led to rapid pavement deterioration.

Pavement distresses were recorded in accordance with the LTPP Distress Identification Manual. The main pavement distresses identified in September 2008 forensic investigation included fatigue cracking, longitudinal cracking, transverse cracking, rutting, block cracking, and pumping. The extent and severity levels of these distresses for the test sections are summarized below:

- High severity fatigue cracking was observed for test sections 0502 and 0505. Neither transverse nor longitudinal cracking was rated on test section 0502 because of the extent of block and fatigue cracking.
- Low to high severity transverse and longitudinal cracking were observed for test sections 0505, 0506, and 0509. In most cases, the transverse cracks covered the entire width of the lane. The patterns of the non-wheel path longitudinal cracking consistently occurred at the mid-lane.
- During the September 2008 visit, surface disintegration and loss of AC materials were also noticed in some locations of the test sections.
- Pavement distress in the form of pumping was also observed in each of the four test sections, particularly 0502 and 0505.
- In general, upon degradation of the pavement surface layer, the growth of these distresses increased over time for each of the test sections.
- Maintenance activities (fog seals and crack sealing) applied over the years appeared to have reduced the propagation of fatigue and transverse cracks temporarily.

Based on the longitudinal profile data, significant growth in roughness levels were observed for each test section. The aforementioned maintenance activities, did not cause significant changes of the IRI values. In general, recycled overlay test sections 0502 and 0509 exhibited the largest post-rehabilitation increase in roughness IRI over their monitoring history due to their associated high severity distress levels.

The back-calculated surface layer moduli values varied from station to station within a test section, indicating non-uniform structural strength. It was found that the surface layer moduli for test sections 0506 and 0509, exhibiting low severity fatigue cracking with very little pumping, were high. On the other hand, lower surface modulus values were obtained for sections 0502 and 0505, suggesting a deteriorated or weakened pavement structures. These findings were consistent with the rutting and cracking performance of each test section. The moduli from DCP and FWD analysis were high for base and subgrade layers, indicating pavement deterioration was not associated with these layers.
In summary, based on the field and laboratory forensic investigations, it was determined that continued deterioration of pavement structural strength and the consequent decline in ride quality were observed for each test section.

From this forensic investigation, the following conclusions can be drawn:

- Base thicknesses were measured in the trench and on the split spoon samples taken along the section at core locations. They were uniform throughout the sections.
- Most of the cracks were top-down cracks (high severity at top and low severity at the bottom of the layer). A significant number of the cracks were full-depth.
- A couple of non-vertical cracks were observed at the trench edges, possibly the effect of the top-down cracking mechanism.
- Rutting was observed in the overlay layer only.
- The original asphalt layer was deteriorated and lost its viscous properties.
- The asphalt layers in the trench slabs were intact and no separation/slippage of layers were observed. No voids were observed at the edges of the slabs or trenches.

ACKNOWLEDGMENTS

This work could not have been completed without the assistance of Mr. Jack Springer of the Federal Highway Administration (FHWA). NCE would also like to express sincere appreciation to Dr. Murari Pradhan and field crew members of the Arizona Department of Transportation (ADOT) for their support.

REFERENCES

1. Hossain, M., Lattin D., Scofield L.(1996) “SPS-5: Rehabilitation of Asphalt Concrete Pavements. Construction Report.” Arizona Department of Transportation, 390 pages.
2. Dar-Hao C., T. Scullion, J. Bilyeu, D. Yuan, and S. Nazarian. (2002) “Forensic Study of Warranty Project on US82” Journal of Performance of Constructed Facilities.
3. Dar-Hao C., J. Bilyeu, T. Scullion, Deng-Fong L., and Fujie, Z. (2003) “Forensic Evaluation of Premature Failures of Texas Specific Pavement Study – 1 Sections” Journal of Performance of Constructed Facilities.
4. John S. Miller and William Y. Bellinger. (2003) “Distress Identification Manual for the Long-Term Pavement Performance Program (LTPP)”. FHWA-RD-03-031.
5. Witczak, M., Kaloush, K., Pellinen, T., El-Basyouny, M., Von Quintus, H. (2002) “Simple Performance Test for Superpave Mix Design.” National Cooperative Highway Research Program, NCHRP Report 465, Transportation Research Board, Washington, D.C.
6. Sousa, J.B., Craus, J., C.L., Monismith (1991) “Summary Report on Permanent Deformation in Asphalt Concrete.” Strategic Highway Research Program, National Research Council, Washington, D.C., Report No. SHRTP-A/IR-91-104.
7. Everseries User’s Guide Pavement Analysis Computer Software and Case Studies Washington State Department of Transportation, 170 pages.

Appendix A

As-Sampled Field Sampling and Testing Plan

FORENSIC EVALUATION

Field Sampling and Testing Plan

for

LTPP SPS-5 Project (040500)

I-8 Eastbound
Casa Grande, Arizona

As-Sampled

October 21, 2008

Western Regional Support Contractor
Nichols Consulting Engineers, Chtd.

Forensic Evaluation Plan
For LTPP SPS-5 Project (040500)

I-8 Eastbound, Casa Grande, Arizona

Introduction

The need for forensic evaluation of LTPP test sites has been discussed for nearly the entire life of the program. There is a widespread agreement that forensic investigation on LTPP test sections should be pursued, especially for the Specific Pavement Study (SPS) test sections reaching terminal serviceability. It has also been said that premature failures, as well as the exceptional performers, must be examined closely if we are to fully understand *why* pavements have performed as they have.

The plan for conducting the investigations was discussed at the Transportation Research Board (TRB) LTPP Special Activities Expert Task Group Meeting on April 2 and April 3 in Woods Hole, MA. The investigations will follow the guidelines in the "Framework for LTPP Forensic Investigations - Final" (Appendix A) developed in April 2004 to promote consistency and uniformity and to maximize their benefits. Key elements of the guidelines include distress mechanism investigations and surveys, the collection of missing/ desirable data, measurements of material properties, within-section layer thicknesses, end-state physical properties, deflection, and profile.

Figure 1. Photograph of a forensic trench in Arizona.

FHWA initiated forensic evaluations at one LTPP SPS project in each of the four regions. The Arizona SPS-5 was selected for the Western Region. This selection was based on the distress mechanisms and outstanding agency support to perform the forensic activities.

The Arizona SPS-5 test site is located at milepost 159.01 near Casa Grande on Interstate-8 in the eastbound direction. This roadway was originally opened to traffic in 1968. The SPS-5 rehabilitation was performed in 1990. Table 1 shows the Arizona SPS-5 site rehabilitation alternatives. Figure 2 shows the project layout and layer structures for each section in the Arizona SPS-5 project.

Table 1: Arizona SPS-5 Rehabilitation Alternatives.

Section	Surface Preparation	Overlay Material	Overlay Thickness (Inch)
0501	Routine maintenance		-
0502	Minimum	Recycled Asphalt	2
0503	Minimum	Recycled Asphalt	5
0504	Minimum	Virgin Asphalt	5
0505	Minimum	Virgin Asphalt	2
0506	Intensive	Virgin Asphalt	2
0507	Intensive	Virgin Asphalt	5
0508	Intensive	Recycled Asphalt	5
0509	Intensive	Recycled Asphalt	2
0559	Intensive	Recycled Asphalt	2
0560	Minimum	Asphalt Rubber Asphalt Concrete	2.5

The Arizona SPS-5 site was originally constructed with 12.0 -21.0 inches of granular base, 4.0 inches of asphalt concrete, and 0.9 inches of open graded friction course. The section 040506 was overlaid with virgin asphalt. The section 040509 was overlaid with recycled asphalt and is expected to show minimal or no rutting. Looking at the LTPP performance data, the section 040506 shows virtually no fatigue cracking and no rutting. Some high severity transverse cracks with loss of materials were observed. The section 040509 shows moderate severity fatigue cracks throughout the section. Moderate severity transverse cracks were observed in this section. Significant rutting is observed at the outer wheel path.

Arizona Department of transportation preferred to have a recycled asphalt pavement section in the forensic evaluation. The unexpected performance behavior of the sections and the ADOT's request were the key for the selection of these two sections for the forensic evaluation.

For section 040506, the open graded friction course and 1.0 inch of existing asphalt concrete layer were milled off and two overlay layers of 2.8 and 2.4 inches were placed during the SPS-5 rehabilitation in 1990. For section 040509, the open graded friction course and 2.1 inch existing asphalt pavement were milled off and two overlay layers of 2.6 and 1.3 inches were placed during the SPS-5 rehabilitation is 1990. Both sections received fog seal in 1998, 2001 and 2003. The Subgrade material is predominantly silty gravel with sand for both sections. The current layer structure can be found in Table 2.

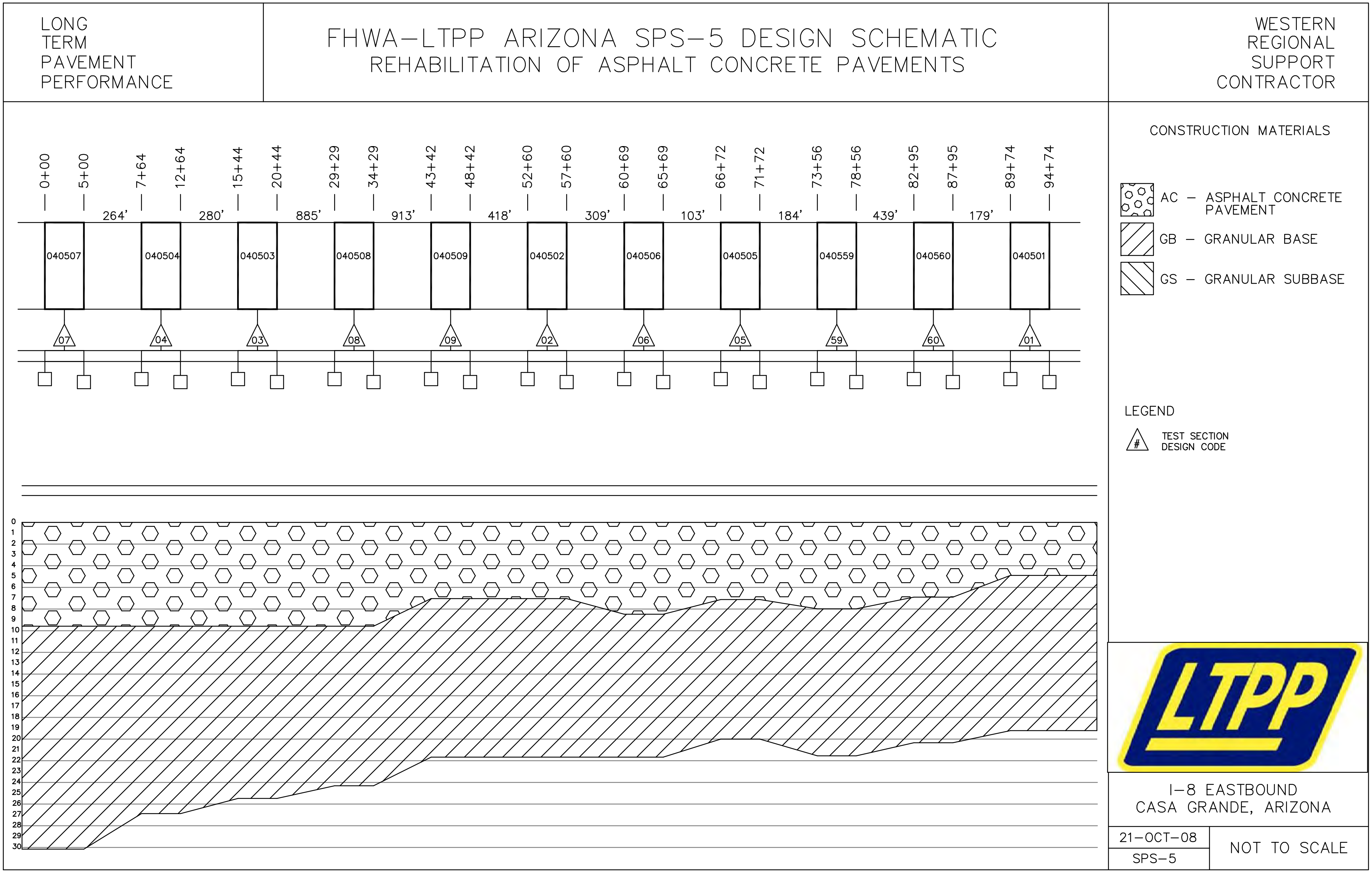

FIGURE 2. FORENSIC SAMPLING AND TESTING PLAN FOR 040500 PROJECT

Table 2: Layer Structure of the Project Sections.

Section	Layer	Thickness (inch)	Construction Year
040506	Granular Base	12.8	1968
	Asphalt Concrete	3.0	1968
	Asphalt Concrete	2.8	1990
	Asphalt Concrete	2.4	1990
	Fog seal	0.1	1998
	Fog seal	0.1	2001
	Fog seal	0.1	2003
040509	Granular Base	14.8	1968
	Asphalt Concrete	2.6	1968
	Recycled Asphalt Concrete	2.6	1990
	Recycled Asphalt Concrete	1.3	1990
	Fog seal	0.1	1998
	Fog seal	0.1	2001
	Fog seal	0.1	2003

In addition to the forensic evaluation on sections 040506 and 040509, the WRSC plans to perform distress surveys on the remaining sections. Additional coring is planned on the other asphalt sections to see the crack origination. These activities will be taken place only if time permits.

Project Details

This plan is prepared for the LTPP SPS-5 project 040500, located on the I-8 eastbound truck lane near Casa Grande, Arizona. Forensic investigations will be conducted on sections 040506 and 040509. The plan layouts are shown in figures 3 and 4.

The minimum field activities include the distress mechanism investigations and ideally will include tests on samples to find the end-state physical properties supplement to the forensic evaluation. The following activities will take place at the site:

- Two trenches of the size of 4 X12 ft, one for each section, will be excavated. The unbound layers will be tested with Dynamic Core Penetrometer (DCP). Also the moisture samples will be collected. Both bound and unbound layer profiles will be marked. Photographs will be taken.

- Cores will be taken at fatigue, longitudinal, and transverse crack locations. Also cores will be taken at FWD locations.

- Depending on the specific features of the site, drainage evaluation will be conducted. This can provide valuable supplemental information on distress mechanisms.

- Manual distress, Dipstick, FWD, profile, Dynamic Cone Penetrometer (DCP) testing will be completed at the field.

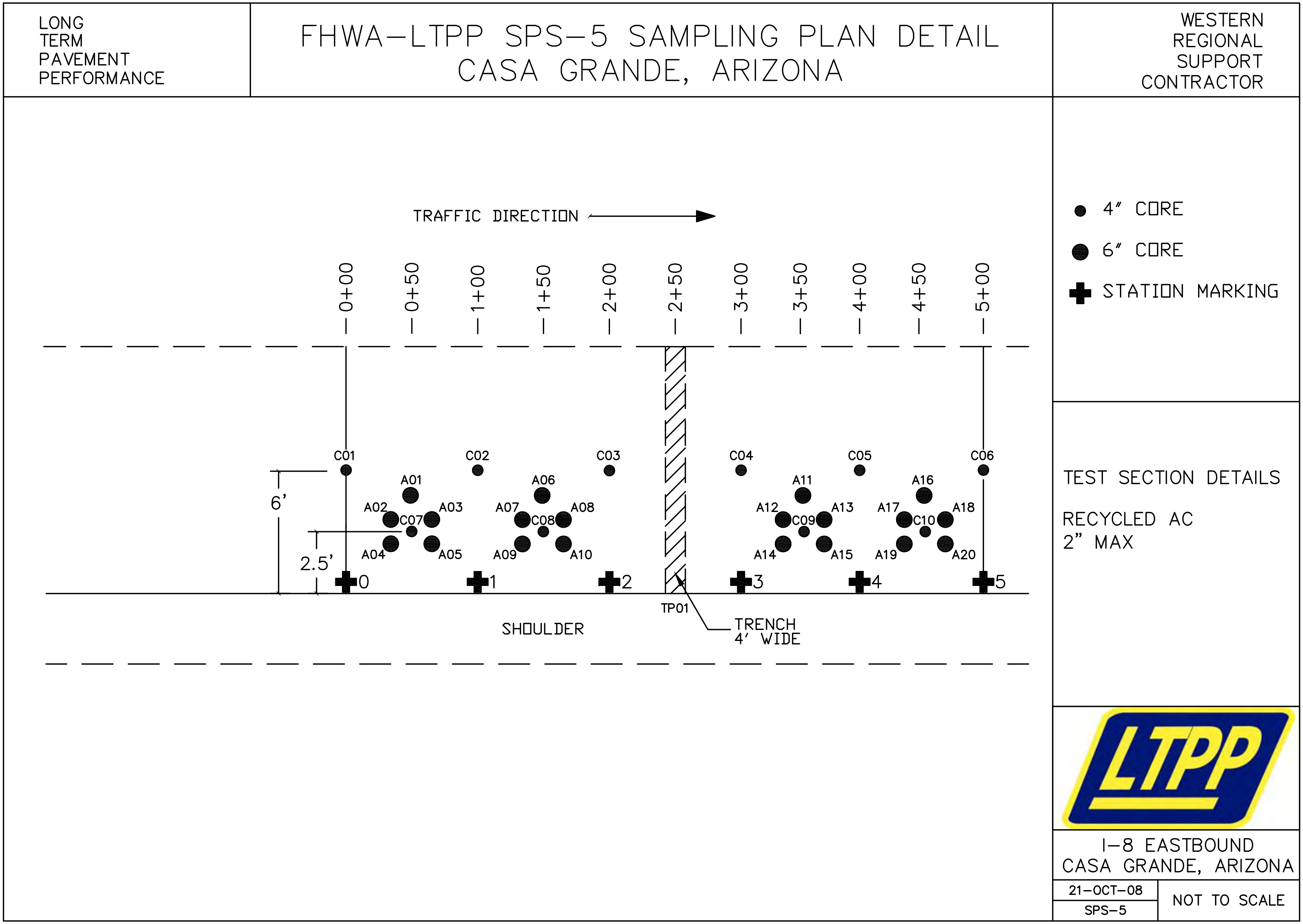

FIGURE 3. FORENSIC SAMPLING AND TESTING PLAN FOR SECTION 040509

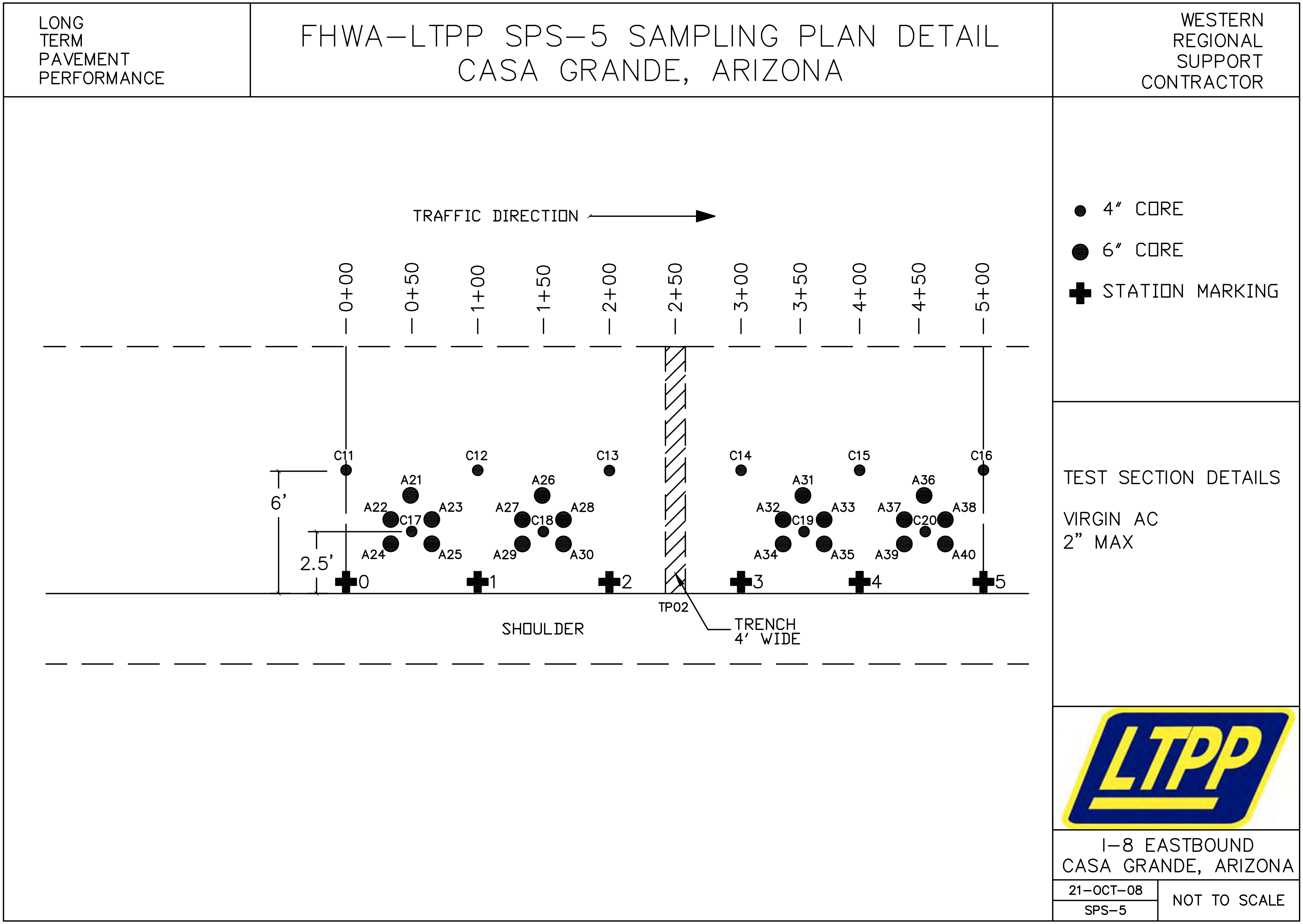

FIGURE 4. FORENSIC SAMPLING AND TESTING PLAN FOR SECTION 040506

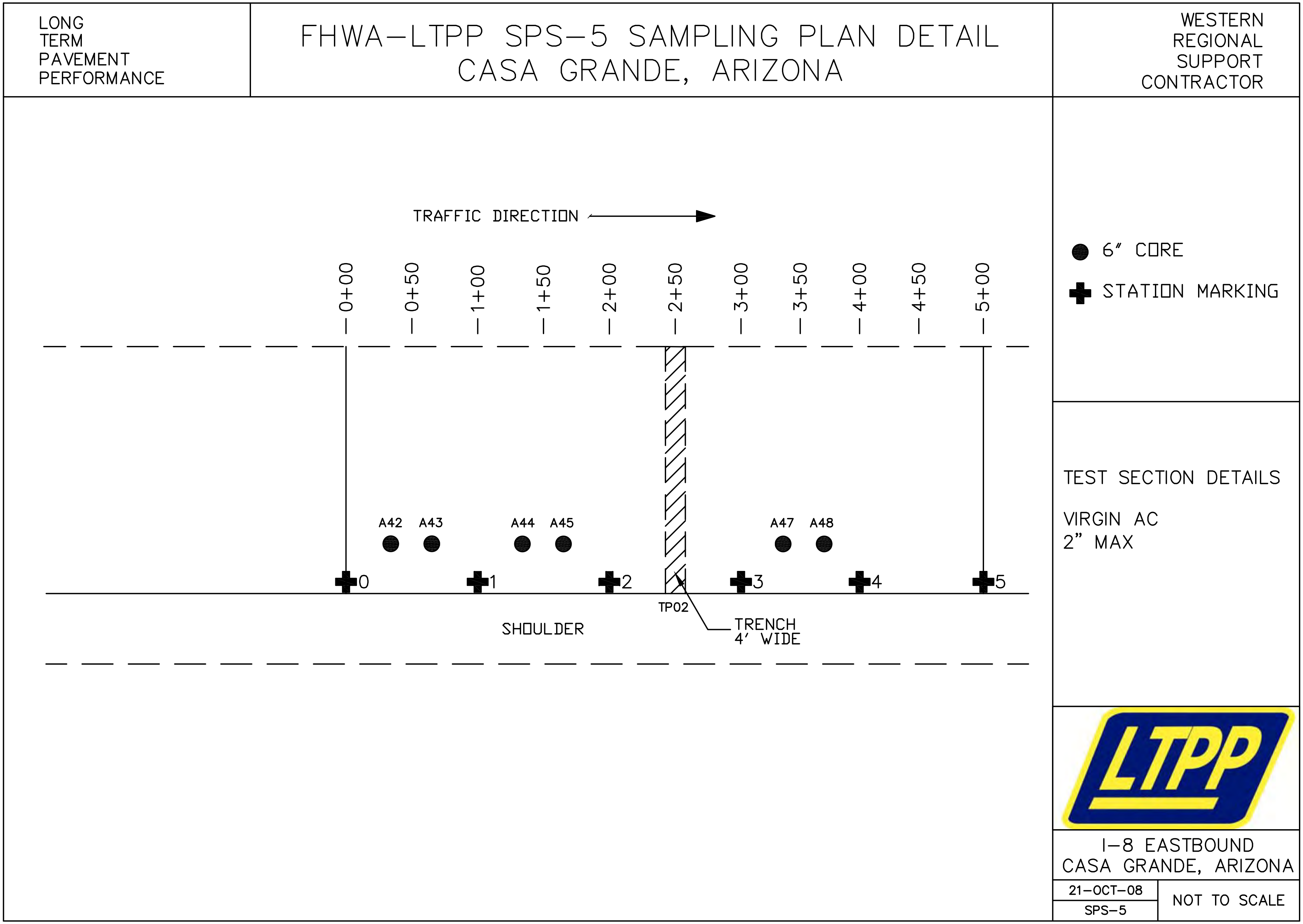

FIGURE 5. FORENSIC SAMPLING AND TESTING PLAN FOR SECTION 040505

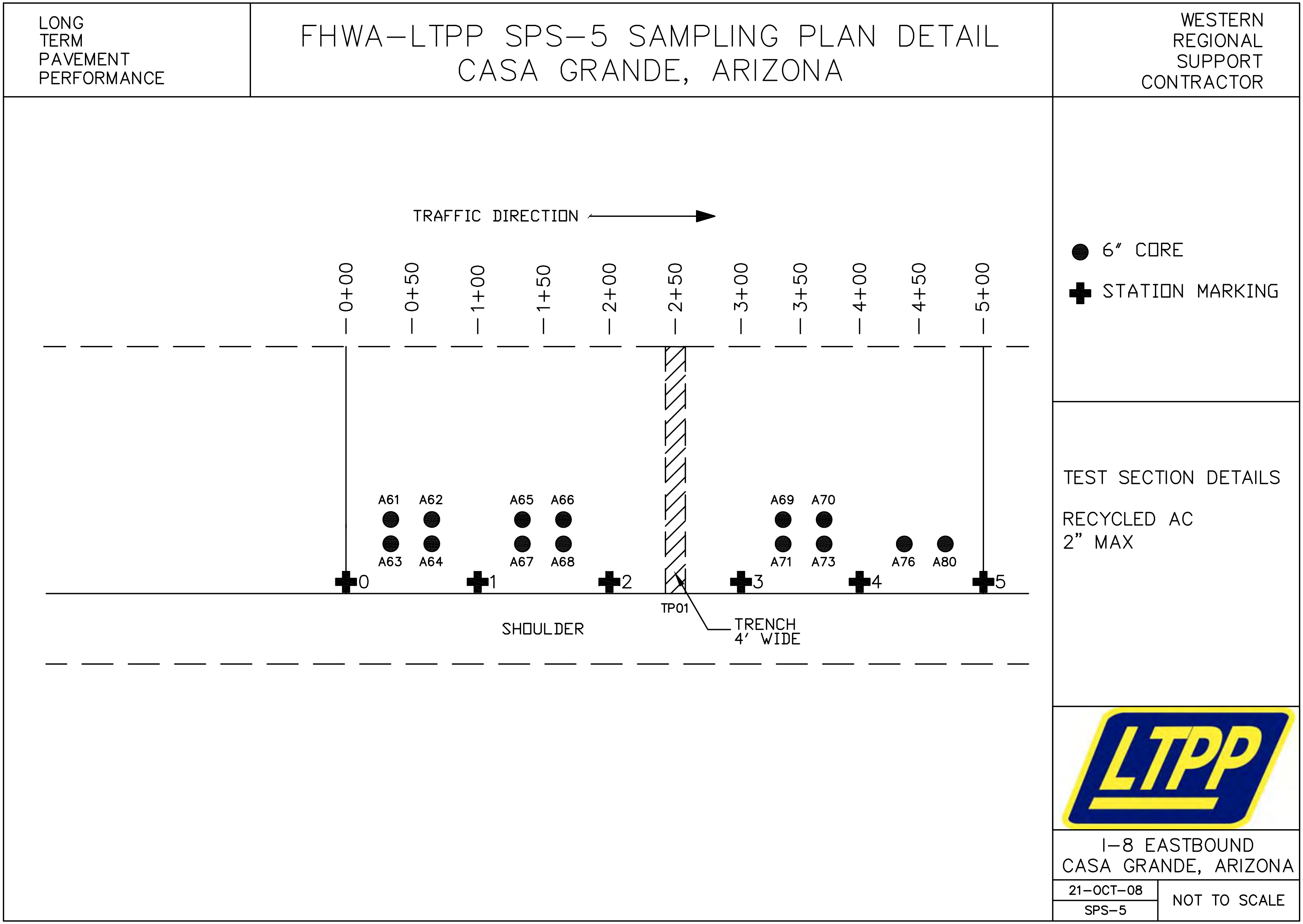

FIGURE 6. FORENSIC SAMPLING AND TESTING PLAN FOR SECTION 040502

- Walking in video of the sections will be taken.

The supplemental lab tests are detailed in Table 3. Tables 4 and 5 detail the number of tests and the required samples respectively.

Table 3: Supplemental Lab Tests for End-State Properties.

Material	Laboratory Tests
Unbound Base	Moisture Density Relationship
	Engineering Properties: Atterberg Limit, Gradation
	Specific Gravity
Subgrade	Moisture Density Relationship
	Engineering Properties: Atterberg Limit, Gradation
	Specific Gravity
AC	Mix Properties: Density, Voids, AC Content, Volumetric Analysis

Table 4. Forensic Sampling and Testing for Arizona SPS-5

LO5B Project Layer (Material Code)	**A (265)**	**C (308)**	**D (1)**	**F(13)**	**G(13)**	**H (1)**	**I (1)**	**K(73)**	**L (73)**	**M (73)**
Required Tests for sections 040506 & 040509	**Subgrade**	**Granular Base**	**AC**	**AC**	**AC**	**AC**	**AC**	**AC**	**AC**	**AC**
Granular Base and Subgrade										
Gradation (SS01/UG01/UG02)	2	2								
Atterburg Limit (SS03/UG04)	2	2								
Moisture Density Relationship (SS05/UG05)	2	2								
Specific Gravity (SS13/UG13)	2	2								
Dynamic Core Penetrometer (SS14/UG14)	14	14								
Asphalt Concrete										
Layer Thickness (AC01)			20	10	10	10	10			
Bulk Specific Gravity (AC02)			6	3	6	3	6			
Maximum Specific Gravity (AC03)			10	3	6	3	4			
Asphalt Content (AC04)			10	3	4	3	4			
Volumetric Analysis (SP02)			10	3	4	3	4			

Table 5: Summary of Forensic Sampling for Arizona SPS- 5

Materials and Sample Description	040506 (Virgin Asphalt)	040509 (Recycled Asphalt)	040502 (Recycled Asphalt)	040505 (Virgin Asphalt)	Total
1. AC Layer					
4" diameter cores	10	10	0	0	20
6" diameter cores	20	20	14	6	60
12 ft x 4 ft trench	1	1	0	0	2
2. Unbound Base (50 lb bag)	4	4	0	0	8
3. Subgrade (50 lb bag)	4	4	0	0	8

Table 6: Asphalt Concrete Testing

Sample Location	Sample Number	Project Layer	Layer No.	Test Section	Test No.	Tests Involved in Laboratory Handling & Testing Sequence	
						1	2
C01	CA01	D	3	040509	3	AC01	AC02
		F	5			AC01	AC02
		G	6			AC01	AC02
		K	7			AC01	
		L	8			AC01	
		M	9			AC01	
C1A	CA02	D	3	040509	3	AC01	
		F	5			AC01	
		G	6			AC01	
		K	7			AC01	
		L	8			AC01	
		M	9			AC01	
C03	CA03	D	3	040509	3	AC01	AC02
		F	5			AC01	AC02
		G	6			AC01	AC02
		K	7			AC01	
		L	8			AC01	
		M	9			AC01	
C04	CA04	D	3	040509	3	AC01	
		F	5			AC01	
		G	6			AC01	
		K	7			AC01	
		L	8			AC01	
		M	9			AC01	
C05	CA05	D	3	040509	3	AC01	AC02
		F	5			AC01	AC02
		G	6			AC01	AC02
		K	7			AC01	
		L	8			AC01	
		M	9			AC01	
C06	CA06	D	3	040509	3	AC01	
		F	5			AC01	
		G	6			AC01	
		K	7			AC01	
		L	8			AC01	
		M	9			AC01	
C07	CA07	D	3	040509	3	AC01	
		F	5			AC01	
		G	6			AC01	
		K	7			AC01	
		L	8			AC01	
		M	9			AC01	
C08	CA08	D	3	040509	3	AC01	
		F	5			AC01	
		G	6			AC01	
		K	7			AC01	
		L	8			AC01	
		M	9			AC01	
C09	CA09	D	3	040509	3	AC01	
		F	5			AC01	
		G	6			AC01	
		K	7			AC01	

Table 6: Asphalt Concrete Testing

Sample Location	Sample Number	Project Layer	Layer No.	Test Section	Test No.	Tests Involved in Laboratory Handling & Testing Sequence	
						1	2
		L	8			AC01	
		M	9			AC01	
C10	CA10	D	3	040509	3	AC01	
		F	5			AC01	
		G	6			AC01	
		K	7			AC01	
		L	8			AC01	
		M	9			AC01	
A01	CA51	D	3	040509	3	AC03	
		F	5			AC03	
		G	6			AC03	
		K	7				
		L	8				
		M	9				
AX01(A02+A03+A04+A05+A06)	CAX01	D	3	040509	3	AC04	SP02
		F	5			AC04	SP02
		G	6			AC04	SP02
		K	7				
		L	8				
		M	9				
A07	CA57	D	3	040509	3	AC03	
		F	5			AC03	
		G	6			AC03	
		K	7				
		L	8				
		M	9				
AX02(A08+A09+A10+A11+A12)	CAX02	D	3	040509	3	AC04	SP02
		F	5			AC04	SP02
		G	6			AC04	SP02
		K	7				
		L	8				
		M	9				
A13	CA63	D	3	040509	3	AC03	
		F	5			AC03	
		G	6			AC03	
		K	7				
		L	8				
		M	9				
AX03(A14+A15+A16+A17+A18)	CAX03	D	3	040509	3	AC04	SP02
		F	5			AC04	SP02
		G	6			AC04	SP02
		K	7				
		L	8				
		M	9				
C11	CA11	D	3	040506	3	AC01	AC02
		H	5			AC01	AC02
		I	6			AC01	AC02
		K	7			AC01	
		L	8			AC01	
		M	9			AC01	
		D	3			AC01	
		H	5			AC01	

Table 6: Asphalt Concrete Testing

Sample Location	Sample Number	Project Layer	Layer No.	Test Section	Test No.	Tests Involved in Laboratory Handling & Testing Sequence	
						1	2
C12	CA12	I	6	040506	3	AC01	
		K	7			AC01	
		L	8			AC01	
		M	9			AC01	
C13	CA13	D	3	040506	3	AC01	AC02
		H	5			AC01	AC02
		I	6			AC01	AC02
		K	7			AC01	
		L	8			AC01	
		M	9			AC01	
C14	CA14	D	3	040506	3	AC01	
		H	5			AC01	
		I	6			AC01	
		K	7			AC01	
		L	8			AC01	
		M	9			AC01	
C15	CA15	D	3	040506	3	AC01	AC02
		H	5			AC01	AC02
		I	6			AC01	AC02
		K	7			AC01	
		L	8			AC01	
		M	9			AC01	
C16	CA16	D	3	040506	3	AC01	
		H	5			AC01	
		I	6			AC01	
		K	7			AC01	
		L	8			AC01	
		M	9			AC01	
C17	CA17	D	3	040506	3	AC01	
		H	5			AC01	
		I	6			AC01	
		K	7			AC01	
		L	8			AC01	
		M	9			AC01	
C18	CA18	D	3	040506	3	AC01	
		H	5			AC01	
		I	6			AC01	
		K	7			AC01	
		L	8			AC01	
		M	9			AC01	
C19	CA19	D	3	040506	3	AC01	
		H	5			AC01	
		I	6			AC01	
		K	7			AC01	
		L	8			AC01	
		M	9			AC01	
C20	CA20	D	3	040506	3	AC01	
		H	5			AC01	
		I	6			AC01	
		K	7			AC01	
		L	8			AC01	
		M	9			AC01	

Table 6: Asphalt Concrete Testing

Sample Location	Sample Number	Project Layer	Layer No.	Test Section	Test No.	Tests Involved in Laboratory Handling & Testing Sequence	
						1	2
A21	CA71	D	3	040506	3	AC03	
		H	5			AC03	
		I	6			AC03	
		K	7				
		L	8				
		M	9				
AX04(A22+A23+A24+A25+A26)	CAX04	D	3	040506	3	AC04	SP02
		H	5			AC04	SP02
		I	6			AC04	SP02
		K	7				
		L	8				
		M	9				
A27	CA77	D	3	040506	3	AC03	
		H	5			AC03	
		I	6			AC03	
		K	7				
		L	8				
		M	9				
AX05(A28+A29+A30+A31+A32)	CAX05	D	3	040506	3	AC04	SP02
		H	5			AC04	SP02
		I	6			AC04	SP02
		K	7				
		L	8				
		M	9				
A33	CA83	D	3	040506	3	AC03	
		H	5			AC03	
		I	6			AC03	
		K	7				
		L	8				
		M	9				
AX06(A34+A35+A36+A37+A38)	CAX06	D	3	040506	3	AC04	SP02
		H	5			AC04	SP02
		I	6			AC04	SP02
		K	7				
		L	8				
		M	9				
A42	CA92	D	3	040505	3	AC03	
		I	5			AC03	
		K	6				
		L	7				
		M	8				
AX07(A43+A44+A45+A46+A47)	CAX07	D	3	040505	3	AC04	SP02
		I	5			AC04	SP02
		K	6				
		L	7				
		M	8				
A61	CA111	D	3	040502	3	AC03	
		G	5			AC03	
		K	6				
		L	7				
		M	8				
		D	3			AC04	SP02

Table 6: Asphalt Concrete Testing

Sample Location	Sample Number	Project Layer	Layer No.	Test Section	Test No.	Tests Involved in Laboratory Handling & Testing Sequence	
						1	2
AX08(A62+A63+A64+A65)	CAX08	G	5	040502	3	AC04	SP02
		K	6				
		L	7				
		M	8				
A66	CA116	D	3	040502	3	AC03	
		G	5			AC03	
		K	6				
		L	7				
		M	8				
AX09(A67+A68+A69+A70)	CAX09	D	3	040502	3	AC04	SP02
		G	5			AC04	SP02
		K	6				
		L	7				
		M	8				
A71	CA121	D	3	040502	3	AC03	
		G	5			AC03	
		K	6				
		L	7				
		M	8				
AX10(A73+A76+A80)	CAX10	D	3	040502	3	AC04	SP02
		G	5			AC04	SP02
		K	6				
		L	7				
		M	8				

Table 7. Granular Base Testing

Sample Location	Sample Number	Project Layer	Layer No.	Test Section	Test No.	Tests Involved in Laboratory Handling and Testing Sequence			
						1	2	3	4
TP01	BG01	C	2	040509	3	UG01/UG02	UG04	UG05	UG13
TP02	BG02	C	2	040506	3	UG01/UG02	UG04	UG05	UG13

Table 8. Subgrade Testing

Sample Location	Sample Number	Project Layer	Layer No.	Test Section	Test No.	Tests Involved in Laboratory Handling and Testing Sequence			
						1	2	3	4
TP01	BS01	A	1	040509	3	SS01	SS03	SS05	SS13
TP02	BS02	A	1	040506	3	SS01	SS03	SS05	SS13

Roles and Responsibilities

The roles, responsibilities, and contact information of the partners in completing this project are summarized in Table 6.

Table-6: Roles, Responsibilities, and Contact Details.

Organization/Contact	Responsibility
Agency: Arizona Murari Man Pradhan, (602) 712-6574 mpradhan@azdot.gov	Traffic control. Trenching support with required equipment and crew. Coring unit with 4” diameter barrels. Boring unit with split spoon. Dry core unit with 6” diameter barrel. Nuclear gauge. Patching the trench and core holes where the samples will be taken. Transport the cores to the agency lab. Laboratory tests listed in Table 4.
Regional Support Contractor: NCE Kevin Senn, (775) 329-4955 ksenn@nce.reno.nv.us Yathi V. Yatheepan (775) 329-4955 yathi@nce.reno.nv.us	Developing site specific forensic evaluation plan. Coordinating all activities with Arizona. Be present during sampling operation. Identifying sampling locations. Falling Weight Deflectometer (FWD) testing. Manual distress survey. Transverse profiles. Longitudinal profiles. Dynamic Cone Penetrometer (DCP). Walking in video. Evaluation of the trenches (Photos). Inspect drainage system. Visual examination & thickness of Cores (Stripping – Photos). Labeling and packing the samples. Moisture content testing. Completing the sampling data sheets. Perform data analysis and submit a forensic report to FHWA and ADOT.
FHWA-LTPP Jack Springer, (202) 493-3144 jack.springer@fhwa.dot.gov	Overall responsibility for the LTPP forensic operations.

Appendix B

AC Core Sample Photos

Core A61

Core A62

Core A63

Core A64

Core A65

Core A67

Figure B1. AC Core Samples; Section 0502.

Core A68

Core A69

Core A71

Core A73

Core A76

Core A80

Figure B1. AC Core Samples; Section 0502 (Continued).

Core A42

Core A45

Core A48

Core A49

Figure B2. AC Core Samples; Section 0505.

Core A21

Core A23

Core A26

Core A27

Core A28

Core A30

Figure B3. AC Core Samples; Section 0506.

Core A31

Core A32

Core A33

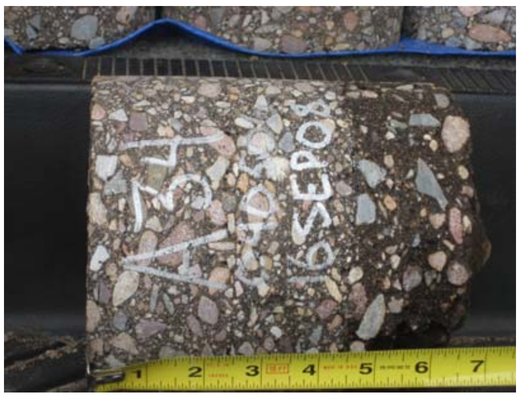

Core A34

Core A35

Core A36

Figure B3. AC Core Samples; Section 0506 (Continued).

Core A37

Core A38

Core A39

Core A40

Core C11

Core C12

Figure B3. AC Core Samples; Section 0506 (Continued).

Core C13

Core C14

Core C16

Core C17

Core C18

Core C19

Figure B3. AC Core Samples; Section 0506 (Continued).

Core C20

Figure B3. AC Core Samples; Section 0506 (Continued).

Core A2

Core A3

Core A4

Core A5

Core A6

Core A8

Figure B4. AC Core Samples; Section 0509.

Core A9

Core A10

Core A11

Core A12

Core A14

Core A15

Figure B4. AC Core Samples; Section 0509 (Continued).

Core A16

Core A18

Core A19

Core C1

Core C1A

Core C4

Figure B4. AC Core Samples; Section 0509 (Continued).

Core C5

Core C6

Core C7

Core C8

Core C10

Figure B4. AC Core Samples; Section 0509 (Continued).

Appendix C

AC Laboratory Test Results

Table C1. Gradation; Section 0502.

Core No.	Sample No.	Sieve Size Standard (mm)									
		1 ½” (37.5)	**1” (25.0)**	**¾” (19.0)**	**½” (12.5)**	**3/8” (9.5)**	**No. 4 (4.75)**	**No. 10 (2.00)**	**No. 40 (0.425)**	**No. 80 (0.180)**	**No. 200 (0.075)**
		Percent Passing									
A61	CA111	100	100	99	84	85	62	44	20	8	4.5
A61	CA111	100	100	98	87	78	60	46	22	9	5.1
A62	CA112	100	100	99	87	79	59	44	20	8	4.7
A62	CA112	100	100	96	84	76	58	45	21	9	5
A63	CA113	100	100	98	87	80	60	43	18	6	2.8
A64	CA114	100	100	100	93	85	62	44	20	8	4.9
A65	CA115	100	100	100	92	81	58	41	20	9	6.3
A66	CA116	100	100	100	91	80	59	42	19	8	5
A67	CA117	100	100	98	85	75	54	40	17	5	1.8
A67	CA117	100	100	98	84	76	61	48	18	4	0.8
A68	CA118	100	100	100	94	86	64	46	21	9	5.7
A69	CA119	100	100	98	89	80	60	45	22	9	5
A69	CA119	100	100	99	85	77	62	50	24	10	5.6
A70	CA120	100	100	98	89	80	59	44	20	8	4.6
A70	CA120	100	100	96	80	73	58	46	21	8	3.9
A71	CA121	100	100	98	86	76	57	43	20	8	4.8
A76	CA126	100	100	98	89	81	62	47	25	15	12.3
A76	CA126	100	100	97	82	74	60	47	22	9	4.7
A80	CA130	100	100	98	90	82	63	47	21	9	5.7
A80	CA130	100	100	94	78	1	56	44	19	6	2.1

Table C2. Gradation; Section 0505.

Core No.	Sample No.	Sieve Size Standard (mm)									
		1 ½" (37.5)	1" (25.0)	¾" (19.0)	½" (12.5)	3/8" (9.5)	No. 4 (4.75)	No. 10 (2.00)	No. 40 (0.425)	No. 80 (0.180)	No. 200 (0.075)
		Percent Passing									
A42	CA92	100	100	100	95	83	58	42	20	8	4.7
A42	CA92	100	100	95	79	72	58	46	21	7	2.7
A43	CA93	100	100	100	91	77	55	40	19	8	4.6
A43	CA93	100	100	97	85	78	64	51	23	8	3.7
A44	CA94	100	100	100	89	78	57	42	19	7	3.5
A44	CA94	100	100	95	84	78	64	51	23	8	3.8
A45	CA95	100	100	100	95	84	59	45	22	10	6.6
A45	CA95	100	100	95	81	73	60	47	22	8	3.7
A47	CA97	100	100	99	93	84	61	46	23	12	8.8
A47	CA97	100	100	98	87	80	65	52	24	9	4.1
A48	CA98	100	100	100	94	82	58	43	20	8	4.6
A48	CA98	100	100	95	85	79	65	52	24	9	4.6

Table C3. Gradation; Section 0506.

Core No.	**Sample No.**	**Sieve Size Standard (mm)**									
		1 ½" (37.5)	**1" (25.0)**	**¾" (19.0)**	**½" (12.5)**	**3/8" (9.5)**	**No. 4 (4.75)**	**No. 10 (2.00)**	**No. 40 (0.425)**	**No. 80 (0.180)**	**No. 200 (0.075)**
		Percent Passing									
A21	CA71	100	100	100	91	80	60	44	20	9	5.7
A22	CA72	100	100	100	94	82	60	43	19	8	4.8
A23	CA73	100	100	100	91	77	55	40	18	8	5.1
A23	CA73	100	100	99	81	71	58	46	21	7	3.2
A24	CA74	100	100	100	90	79	58	43	20	8	4.7
A24	CA74	100	100	96	82	74	60	49	23	8	4.1
A25	CA75	100	100	100	88	75	54	40	19	8	4.8
A26	CA76	100	100	100	90	75	54	40	18	7	4
A27	CA77	100	100	100	92	81	58	42	20	9	5.9
A27	CA77	100	100	96	81	74	62	50	24	9	4.5
A28	CA78	100	100	100	90	89	69	53	39	15	11.8
A29	CA79	100	100	100	91	78	57	42	20	9	5.9
A30	CA80	100	100	100	92	81	59	43	20	9	6
A31	CA81	100	100	100	93	79	58	42	20	9	5.8
A32	CA82	100	100	100	93	81	58	41	18	7	3.8
A33	CA83	100	100	100	93	80	59	42	18	6	2.8
A33	CA83	100	100	98	86	79	65	52	23	8	3.9
A34	CA84	100	100	100	91	79	58	42	20	9	6
A35	CA85	100	100	100	92	80	58	42	19	8	4.9

Table C3. Gradation; Section 0506 (Continued).

Core No.	**Sample No.**	**Sieve Size Standard (mm)**									
		1 ½” (37.5)	**1” (25.0)**	**¾” (19.0)**	**½” (12.5)**	**3/8” (9.5)**	**No. 4 (4.75)**	**No. 10 (2.00)**	**No. 40 (0.425)**	**No. 80 (0.180)**	**No. 200 (0.075)**
		Percent Passing									
A36	CA86	100	100	100	91	79	57	41	18	7	4
A37	CA87	100	100	100	94	82	60	43	19	8	4.8
A37	CA87	100	100	97	83	76	64	51	25	10	5
A38	CA88	100	100	100	92	81	59	43	19	8	5
A39	CA89	100	100	100	89	76	55	40	18	8	5
A40	CA90	100	100	100	90	77	55	40	18	8	5
A40	CA90	100	100	95	89.1	74	61	49	22	8	4

Table C4. Gradation; Section 0509.

Core No.	Sample No.	Sieve Size Standard (mm)									
		1 ½” (37.5)	1” (25.0)	¾” (19.0)	½” (12.5)	3/8” (9.5)	No. 4 (4.75)	No. 10 (2.00)	No. 40 (0.425)	No. 80 (0.180)	No. 200 (0.075)
		Percent Passing									
A02	CA52	100	100	100	90	81	60	44	20	8	4.8
A03	CA53	100	100	99	86	77	56	42	20	9	6
A03	CA53	100	100	96	80	73	59	47	23	9	4.1
A04	CA54	100	100	100	88	76	55	40	19	8	5
A05	CA55	100	100	100	92	82	59	43	19	7	3.8
A05	CA55	100	100	99	88	81	66	53	25	10	5.9
A06	CA56	100	100	100	90	80	59	43	19	7	3.8
A06	CA56	100	100	100	86	78	63	49	20	7	4
A08	CA58	100	100	100	89	78	56	41	19	8	5.1
A08	CA58	100	100	98	81	71	57	45	20	8	7.7
A10	CA60	100	100	99	90	79	57	41	18	7	5.8
A10	CA60	100	100	99	87	79	64	51	24	11	9.2
A11	CA61	100	100	99	90	80	58	42	19	9	8
A12	CA62	100	100	99	86	75	53	39	18	8	5.2
A12	CA62	100	100	97	83	75	63	51	24	9	4.6
A14	CA64	100	100	100	91	81	59	43	19	8	5
A15	CA65	100	100	100	93	82	59	43	20	9	6.1
A16	CA66	100	100	99	90	80	59	43	19	7	4
A16	CA66	100	100	97	84	77	62	49	23	8	3.9

Table C4. Gradation; Section 0509 (Continued).

Core No.	Sample No.	Sieve Size Standard (mm)									
		1 ½” (37.5)	1” (25.0)	¾” (19.0)	½” (12.5)	3/8” (9.5)	No. 4 (4.75)	No. 10 (2.00)	No. 40 (0.425)	No. 80 (0.180)	No. 200 (0.075)
		Percent Passing									
A17	CA67	100	100	99	88	78	56	41	18	7	4
A17	CA67	100	100	99	87	79	65	52	26	12	8.2
A18	CA68	100	100	99	89	78	57	42	19	7	4
A18	CA68	100	100	94	85	77	61	48	22	7	2.7
A19	CA69	100	100	100	91	81	60	44	20	13	10.1
A19	CA69	100	100	98	84	76	59	46	21	7	3.1
A20	CA70	100	100	99	90	77	56	41	18	7	4.3
A20	CA70	100	100	97	86	78	61	48	23	9	5.2
A01-A05	CA51-CA55	100	100	100	89	78	58	42	18	6	3
A01-A05	CA51-CA55	100	100	99	89	78	57	42	19	7	4.1
A06-A10	CA56-CA60	100	100	100	90	80	60	44	19	7	3.8
A06-A10	CA56-CA60	100	100	98	86	77	57	42	19	8	5.4
A11-A15	CA61-CA65	100	100	100	91	77	55	40	19	8	4.9
A11-A15	CA61-CA65	100	100	100	92	82	62	46	20	8	4.8
A16-A20	CA66-CA70	100	100	100	89	74	51	37	10	5	4.4
A16-A20	CA66-CA70	100	100	100	93	83	65	50	26	16	13.4

Table C5. G_{mm} Test Results; Sections 0502, 0505, and 0506.

0502			**0505**			**0506**		
Core No.	**Sample No.**	**G_{mm}**	**Core No.**	**Sample No.**	**G_{mm}**	**Core No.**	**Sample No.**	**G_{mm}**
A61	CA111	2.407	A42	CA92	2.429	A21	CA71	2.423
A61B	CA111B	2.452	A42B	CA92B	2.467	A22	CA72	2.423
A62	CA112	2.411	A43	CA93	2.432	A23	CA73	2.429
A62B	CA112B	2.478	A43B	CA93B	2.471	A23B	CA73B	2.462
A63	CA113	2.414	A44	CA94	2.428	A24	CA74	2.422
A64	CA114	2.407	A44B	CA94B	2.479	A24B	CA74B	2.460
A65	CA115	2.420	A45	CA95	2.423	A25	CA75	2.429
A66	CA116	2.421	A45B	CA95B	2.479	A26	CA76	2.423
A67	CA117	2.432	A47	CA97	2.431	A27	CA77	2.430
A67B	CA117B	2.478	A47B	CA97B	2.463	A27B	CA77B	2.322
A68	CA118	2.409	A48	CA98	2.418	A28	CA78	2.424
A69	CA119	2.444	A48B	CA98B	2.459	A29	CA79	2.428
A69B	CA119B	2.476				A30	CA80	2.421
A70	CA120	2.432				A31	CA81	2.428
A70B	CA120B	2.475				A32	CA82	2.423
A71	CA121	2.430				A33	CA83	2.420
A71B	CA121B	2.475				A33B	CA83B	2.470
A73	CA123	2.424				A34	CA84	2.427
A76	CA126	2.423				A35	CA85	2.429
A76B	CA126B	2.491				A36	CA86	2.426
A80	CA130	2.419				A37	CA87	2.424
A80B	CA130B	2.482				A37B	CA87B	2.486
						A38	CA88	2.423
						A39	CA89	2.436
						A40	CA90	2.430
						A40B	CA90B	2.472

Table C6. G_{mm} Test Results; Section 0509.

Core No.	Sample No.	G_{mm}	Core No.	Sample No.	G_{mm}
A02	CA52	2.415	A01-A05	CA51-CA55	2.421
A03	CA53	2.425	A01-A05B	CA51-CA55B	2.389
A03B	CA53B	2.488	A06-A10	CA56-CA60	2.415
A04	CA54	2.427	A06-A10B	CA56-CA60B	2.427
A06	CA56	2.422	A11-A15	CA61-CA65	2.432
A06B	CA56B	2.441	A11-A15B	CA61-CA65B	2.425
A08	CA58	2.434	A16-A20	CA66-CA70	2.438
A08B	CA58B	2.483	A16-A20B	CA66-CA70B	2.425
A10	CA60	2.421			
A10B	CA60B	2.473			
A11	CA61	2.422			
A12	CA62	2.435			
A12B	CA62B	2.482			
A14	CA64	2.402			
A15	CA65	2.418			
A16	CA66	2.416			
A16B	CA66B	2.478			
A17	CA67	2.427			
A17B	CA67B	2.466			
A18	CA68	2.420			
A18B	CA68B	2.475			
A19	CA69	2.419			
A19B	CA69B	2.469			
A20	CA70	2.427			
A20B	CA70B	2.475			

Table C7. G_{mb} Test Results; Sections 0502, 0505, and 0506.

0502			0505			0506		
Core No.	**Sample No.**	**G_{mb}**	**Core No.**	**Sample No.**	**G_{mb}**	**Core No.**	**Sample No.**	**G_{mb}**
A61	CA111	2.299	A42	CA92	2.278	A21	CA71	2.298
A61	CA111	2.256	A42	CA92	2.216	A22	CA72	2.267
A62	CA112	2.291	A43	CA93	2.293	A23	CA73	2.325
A62	CA112	2.273	A43	CA93	2.192	A23	CA73	2.191
A63	CA113	2.288	A44	CA94	2.283	A24	CA74	2.340
A64	CA114	2.303	A44	CA94	2.190	A24	CA74	2.183
A65	CA115	2.324	A45	CA95	2.305	A25	CA75	2.285
A66	CA116	2.292	A45	CA95	2.060	A26	CA76	2.316
A67	CA117	2.208	A47	CA97	2.187	A27	CA77	2.324
A68	CA118	2.307	A48	CA98	2.301	A27	CA77	2.239
A69	CA119	2.316	A48	CA98	2.167	A28	CA78	2.304
A69	CA119	2.254				A29	CA79	2.283
A70	CA120	2.271				A30	CA80	2.323
A70	CA120	2.274				A31	CA81	2.280
A71	CA121	2.287				A32	CA82	2.303
A71	CA121	2.222				A33	CA83	2.325
A73	CA123	2.296				A33	CA83	2.173
A76	CA126	2.308				A34	CA84	2.307
A76	CA126	2.253				A35	CA85	2.300
A80	CA130	2.317				A36	CA86	2.298
A80	CA130	2.259				A37	CA87	2.292
						A37	CA87	2.207
						A38	CA88	2.289
						A39	CA89	2.259
						A40	CA90	2.308
						A40	CA90	2.188

Table C8. G_{mb} Test Results; Section 0509.

Core No.	**Sample No.**	**G_{mb}**	**Core No.**	**Sample No.**	**G_{mb}**	**Core No.**	**Sample No.**	**G_{mb}**
A02	CA52	2.286	A12	CA62	2.300	A18	CA68	2.335
A03	CA53	2.300	A12	CA62	2.323	A18	CA68	2.303
A03	CA53	2.197	A12	CA62	2.220	A18	CA68	2.282
A06	CA56	2.304	A12	CA62	2.280	A18	CA68	2.188
A06	CA56	2.316	A12	CA62	2.213	A19	CA69	2.313
A06	CA56	2.278	A13	CA63	2.287	A19	CA69	2.303
A06	CA56	2.122	A13	CA63	2.281	A19	CA69	2.303
A07	CA57	2.322	A13	CA63	2.265	A19	CA69	2.224
A07	CA57	2.285	A14	CA64	2.293	A20	CA70	2.299
A07	CA57	2.167	A14	CA64	2.300	A20	CA70	2.302
A08	CA58	2.300	A15	CA65	2.281	A20	CA70	2.193
A08	CA58	2.274	A15	CA65	2.326	C01	CA01	2.262
A08	CA58	2.162	A15	CA65	2.154	C02	CA02	2.280
A08	CA58	2.274	A15	CA65	2.316	C03	CA03	2.277
A08	CA58	2.197	A16	CA66	2.310	C04	CA04	2.298
A09	CA59	2.284	A16	CA66	2.282	C05	CA05	2.291
A09	CA59	2.262	A16	CA66	2.284			
A10	CA60	2.316	A16	CA66	2.220			
A10	CA60	2.280	A17	CA67	2.324			
A10	CA60	2.166	A17	CA67	2.295			
A11	CA61	2.280	A17	CA67	2.293			
A11	CA61	2.320	A17	CA67	2.190			
A11	CA61	2.212						
A11	CA61	2.243						

Table C9. Percent Asphalt Binder Content (BC); Sections 0502, 0505, and 0506.

0502			0505			0506		
Core No.	**Sample No.**	**BC (%)**	**Core No.**	**Sample No.**	**BC (%)**	**Core No.**	**Sample No.**	**BC (%)**
A61	CA111	5.9	A42	CA92	5.3	A21	CA71	5.4
A61	CA111	4.5	A42	CA92	3.9	A22	CA72	5.5
A62	CA112	5.7	A43	CA93	5.0	A23	CA73	5.2
A62	CA112	4.0	A43	CA93	3.8	A23	CA73	3.8
A63	CA113	5.7	A44	CA94	5.1	A24	CA74	5.5
A64	CA114	5.9	A44	CA94	3.6	A24	CA74	4.0
A65	CA115	5.6	A45	CA95	5.4	A25	CA75	5.1
A67	CA117	5.2	A45	CA95	3.7	A26	CA76	5.3
A67	CA117	3.8	A47	CA97	5.1	A27	CA77	5.3
A68	CA118	5.9	A47	CA97	3.9	A27	CA77	3.7
A69	CA119	5.0	A48	CA98	5.3	A28	CA78	5.4
A69	CA119	3.7	A48	CA98	4.1	A29	CA79	5.3
A70	CA120	5.4				A30	CA80	5.4
A70	CA120	3.7				A31	CA81	5.4
A71	CA121	3.7				A32	CA82	5.4
A73	CA123	5.6				A33	CA83	5.5
A76	CA126	5.5				A33	CA83	4.0
A76	CA126	3.3				A34	CA84	5.4
A80	CA130	5.6				A35	CA85	5.4
A80	CA130	3.4				A36	CA86	5.4
						A37	CA87	5.5
						A37	CA87	3.2
						A38	CA88	5.5
						A39	CA89	5.1
						A40	CA90	5.3
						A40	CA90	3.8

Table C10. Percent Asphalt Binder Content (BC); Section 0509.

Core No.	Sample No.	BC (%)	Core No.	Sample No.	BC (%)
A02	CA52	5.6	A01-A05	CA51-CA55	5.4
A03	CA53	5.4	A01-A05	CA51-CA55	5.5
A03	CA53	3.3	A06-A10	CA56-CA60	5.1
A04	CA54	5.5	A06-A10	CA56-CA60	5.2
A05	CA55	5.6	A11-A15	CA61-CA65	5.7
A05	CA55	4.2	A11-A15	CA61-CA65	5.1
A06	CA56	5.6	A16-A20	CA66-CA70	5.2
A06	CA56	3.6	A16-A20	CA66-CA70	5.6
A08	CA58	5.3			
A08	CA58	3.2			
A10	CA60	5.5			
A10	CA60	4.0			
A11	CA61	5.5			
A12	CA62	5.1			
A12	CA62	3.7			
A14	CA64	5.9			
A15	CA65	5.7			
A16	CA66	5.5			
A16	CA66	4.2			
A17	CA67	5.7			
A17	CA67	4.1			
A18	CA68	5.4			
A18	CA68	3.8			
A19	CA69	5.5			
A19	CA69	4.0			
A20	CA70	5.3			
A20	CA70	4.0			

Appendix D

Pavement Distress Maps

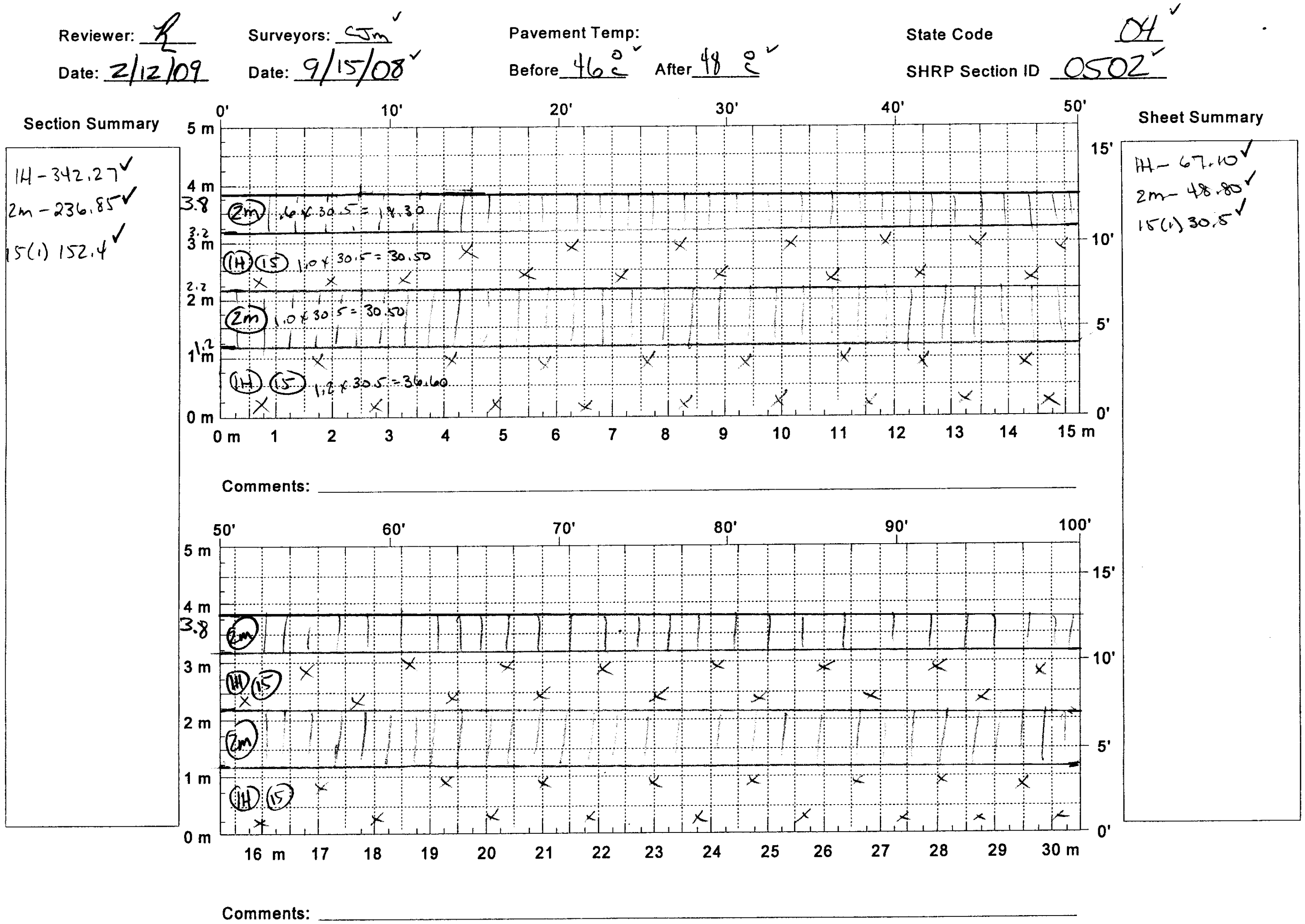

Figure D1. Pavement Distress Map; Station 0+00 to 1+00; Section 0502.

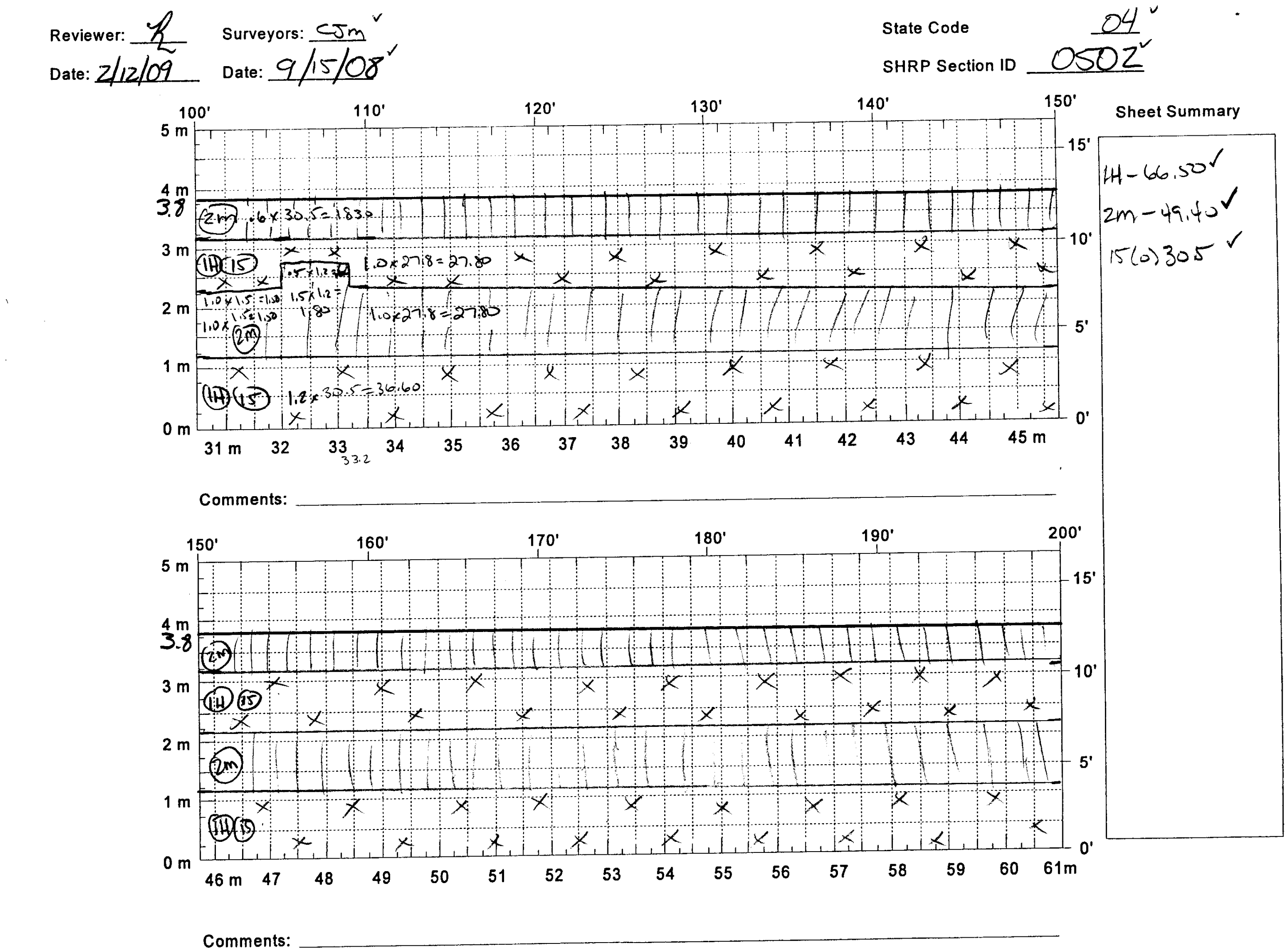

Figure D1. Pavement Distress Map; Station 1+00 to 2+00; Section 0502.

Figure D1. Pavement Distress Map; Station 2+00 to 3+00; Section 0502.

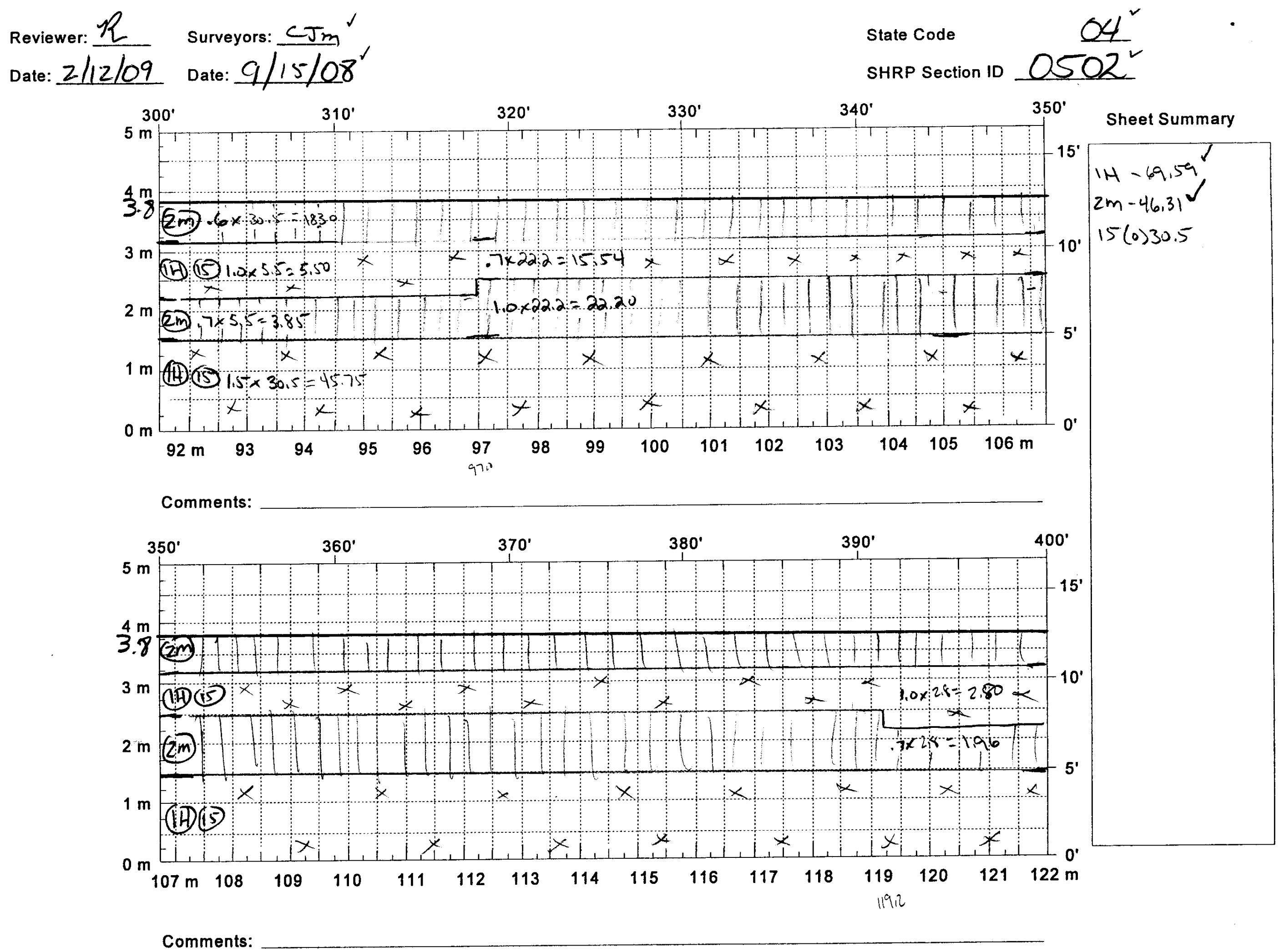

Figure D1. Pavement Distress Map; Station 3+00 to 4+00; Section 0502.

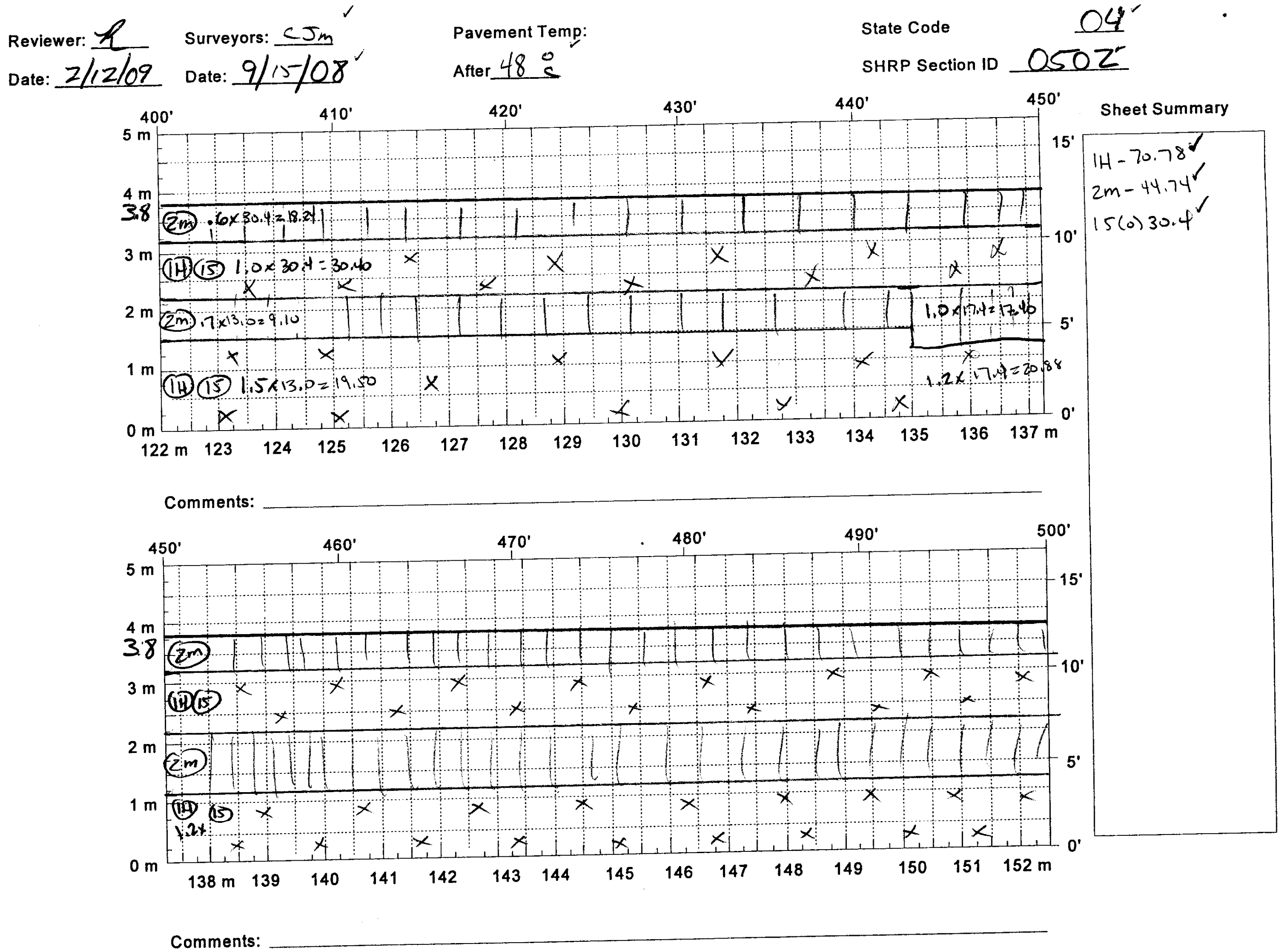

Figure D1. Pavement Distress Map; Station 4+00 to 5+00; Section 0502.

Figure D2. Pavement Distress Map; Station 0+00 to 1+00; Section 0505.

Figure D2. Pavement Distress Map; Station 1+00 to 2+00; Section 0505.

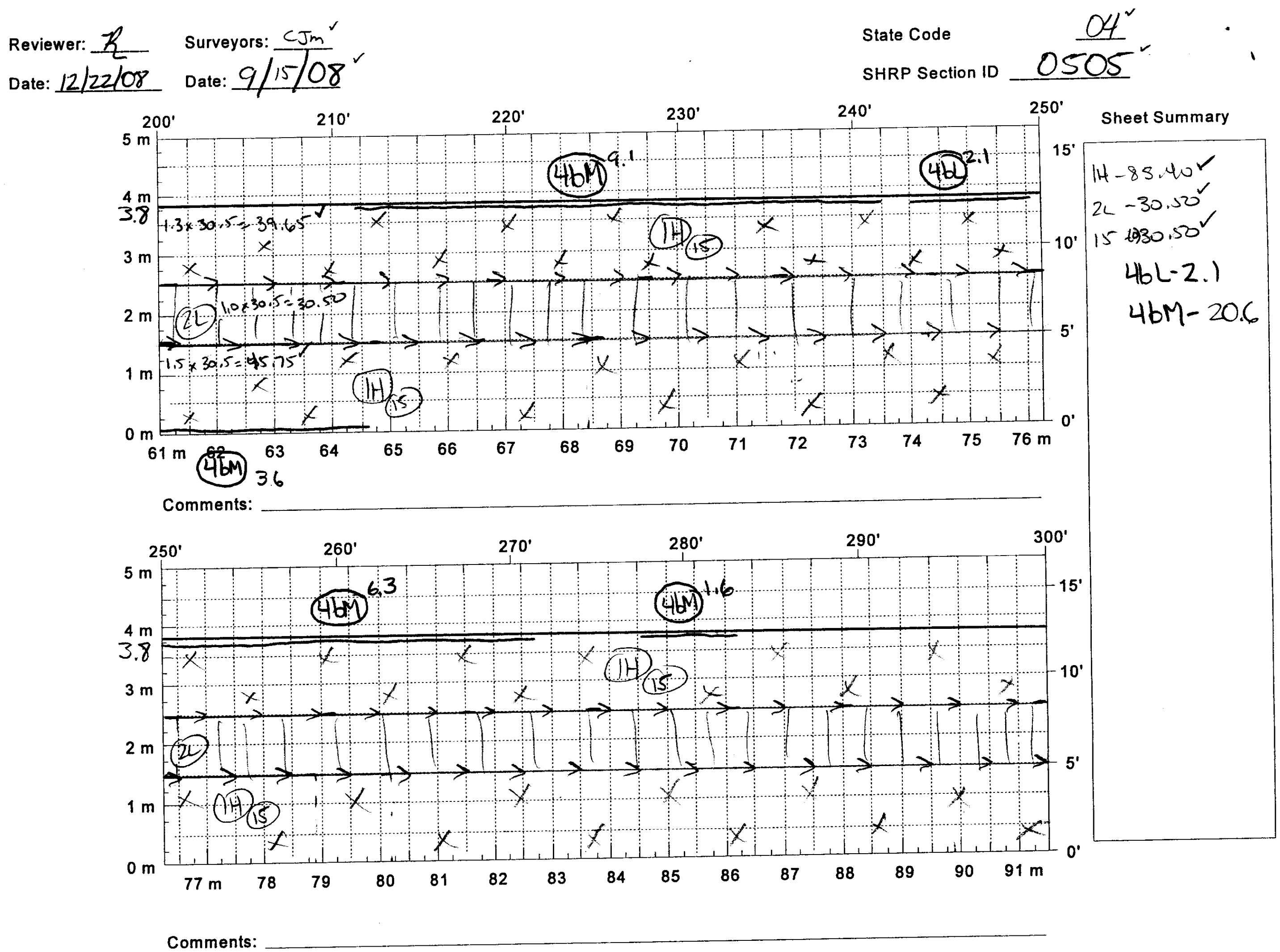

Figure D2. Pavement Distress Map; Station 2+00 to 3+00; Section 0505.

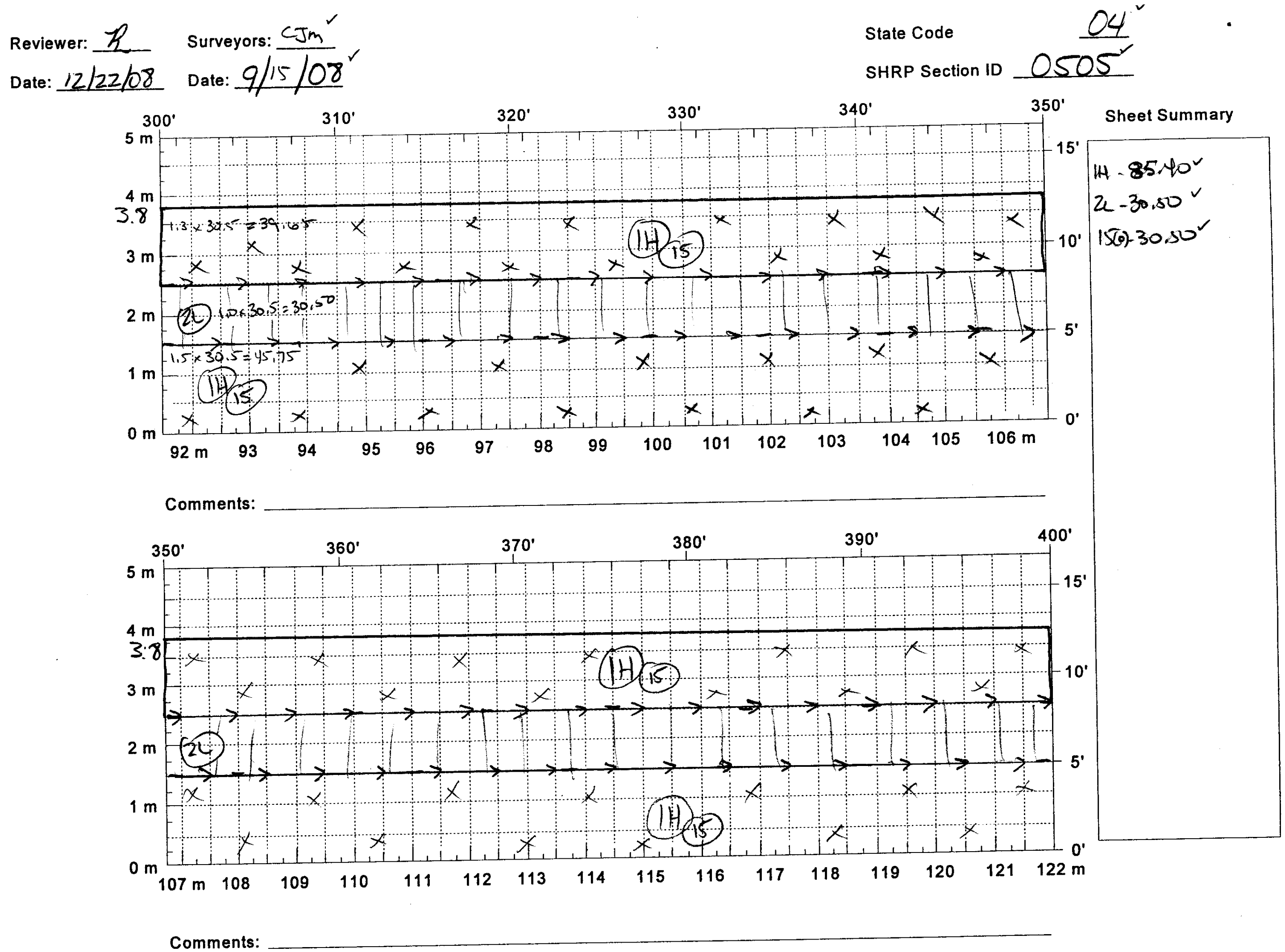

Figure D2. Pavement Distress Map; Station 3+00 to 4+00; Section 0505.

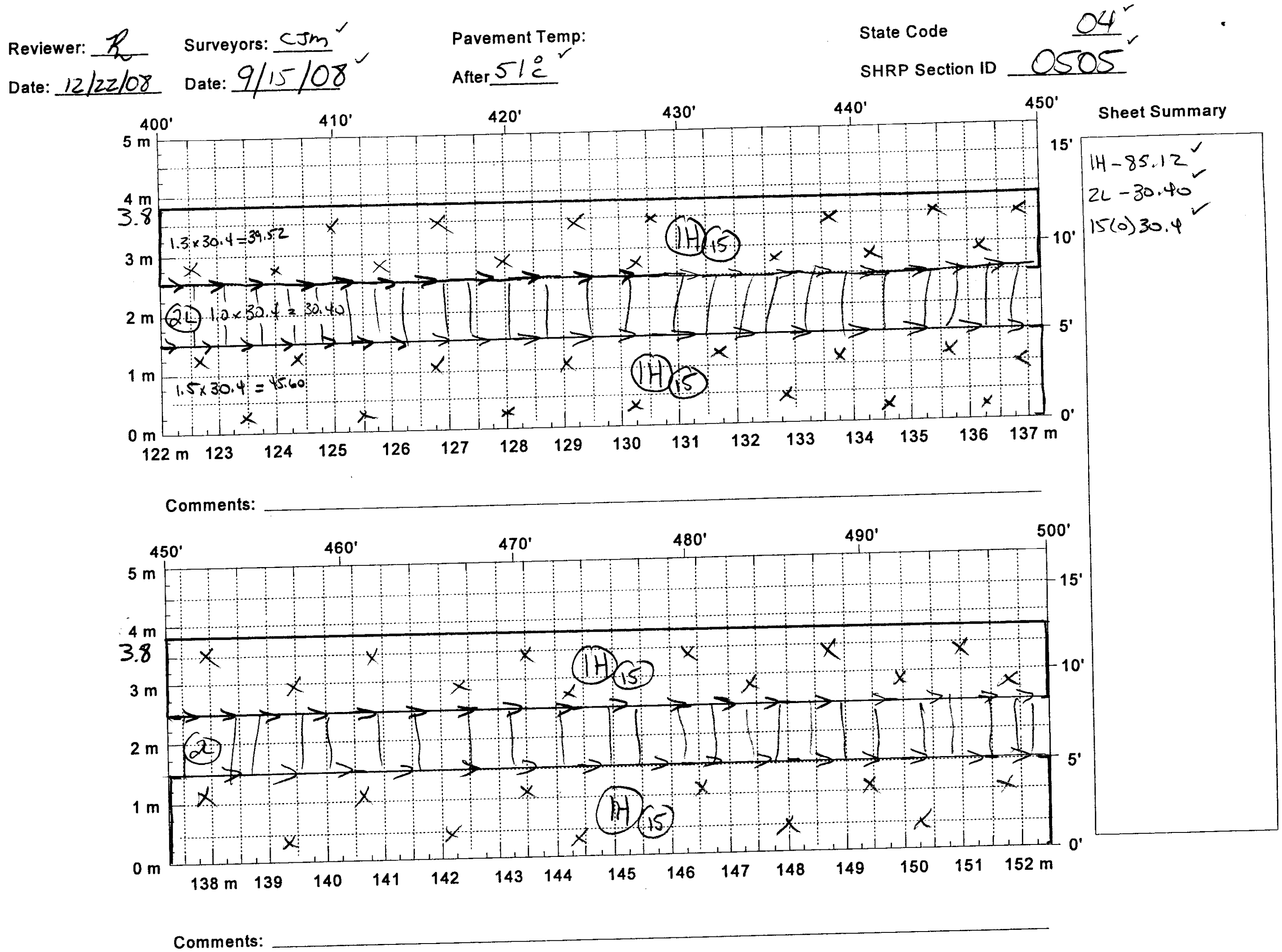

Figure D2. Pavement Distress Map; Station 4+00 to 5+00; Section 0505.

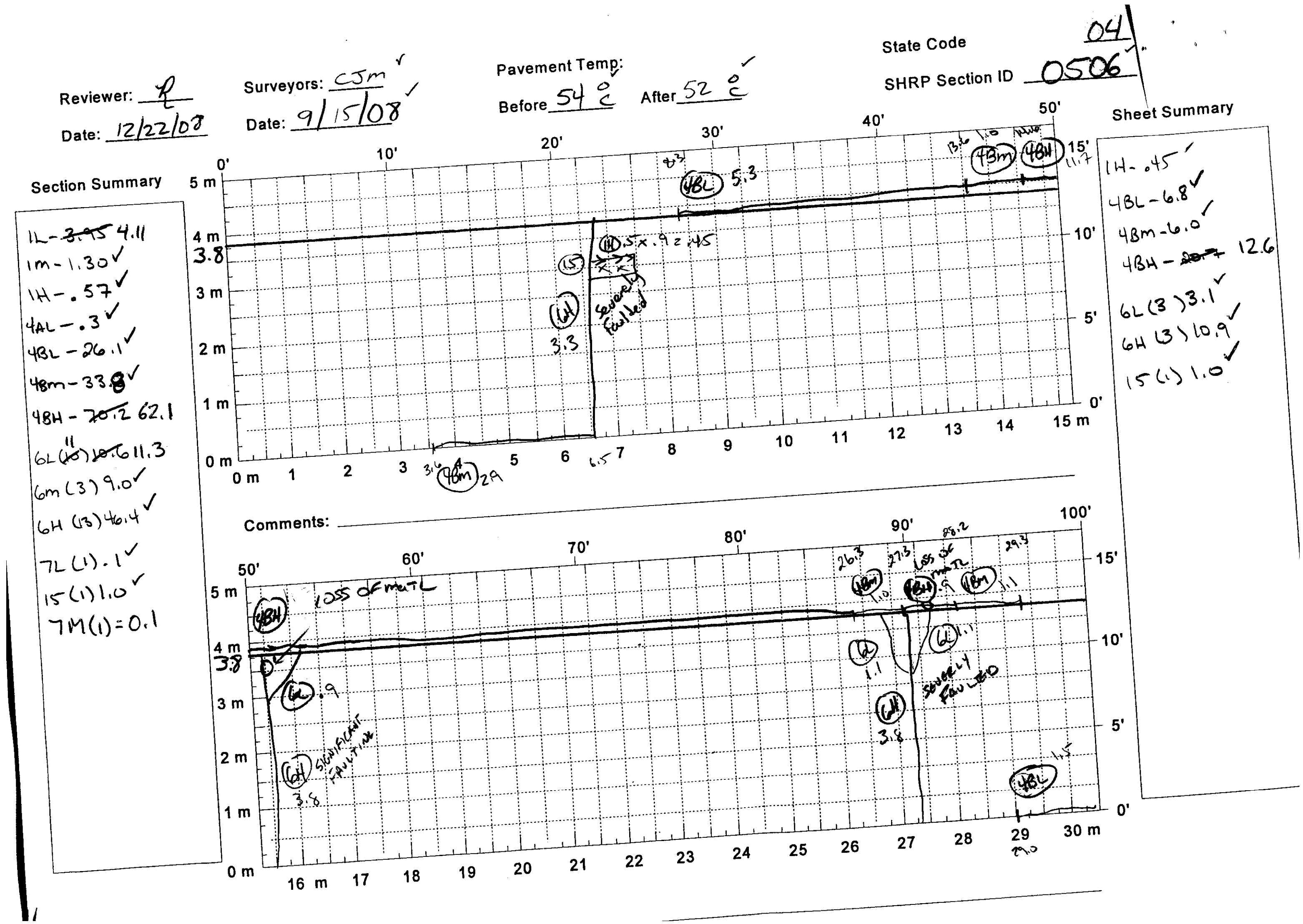

Figure D3. Pavement Distress Map; Station 0+00 to 1+00; Section 0506.

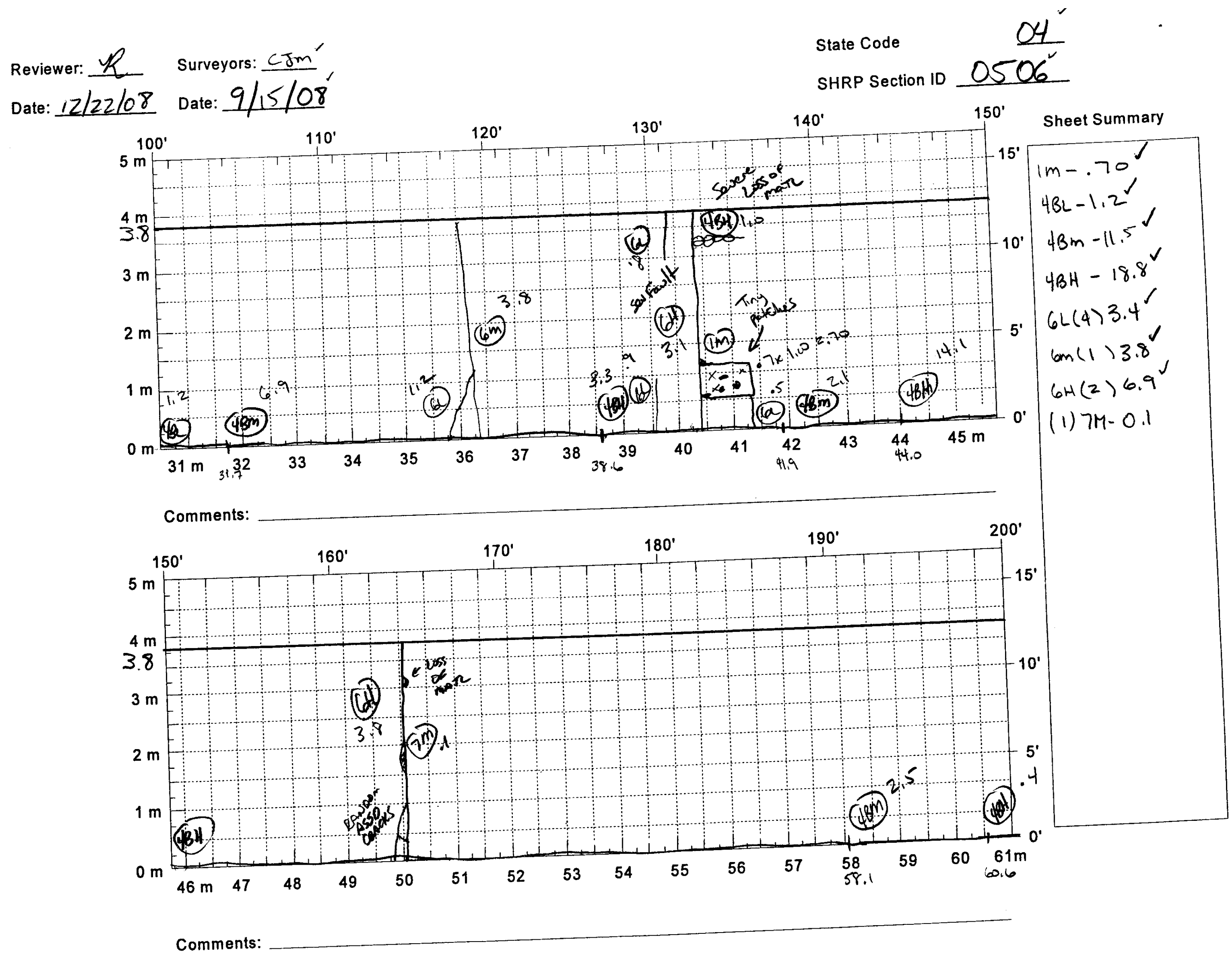

Figure D3. Pavement Distress Map; Station 1+00 to 2+00; Section 0506.

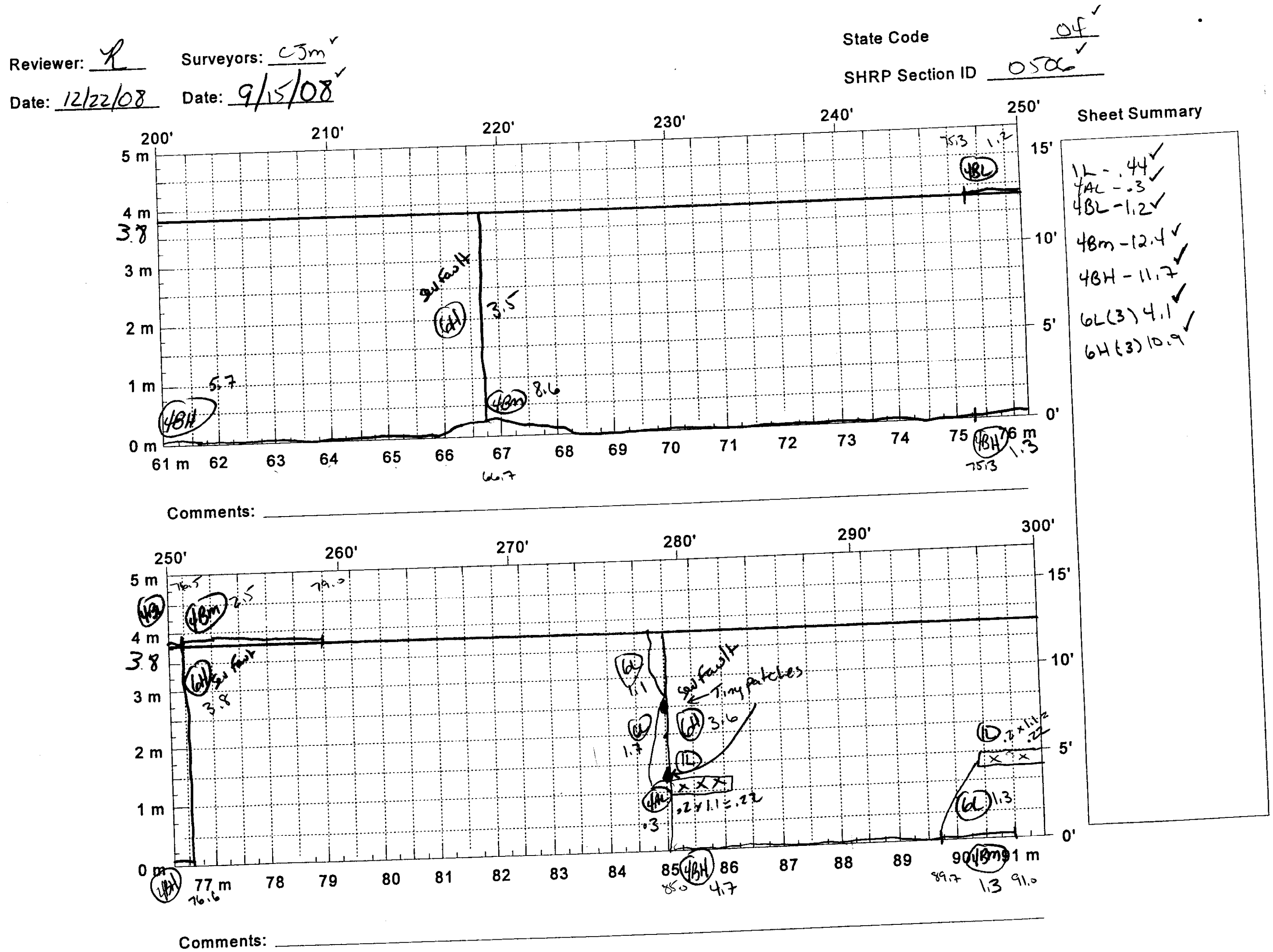

Figure D3. Pavement Distress Map; Station 2+00 to 3+00; Section 0506.

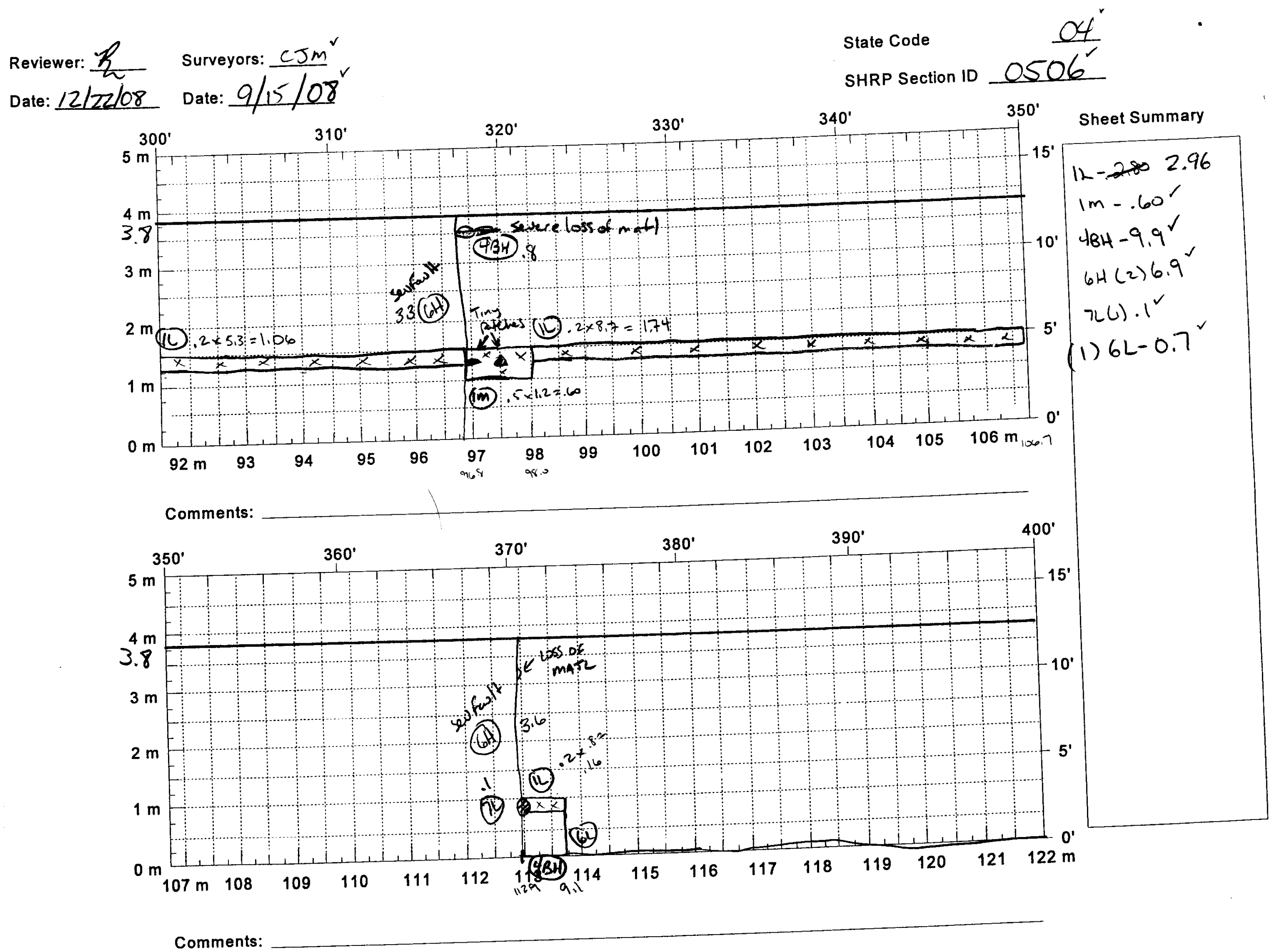

Figure D3. Pavement Distress Map; Station 3+00 to 4+00; Section 0506.

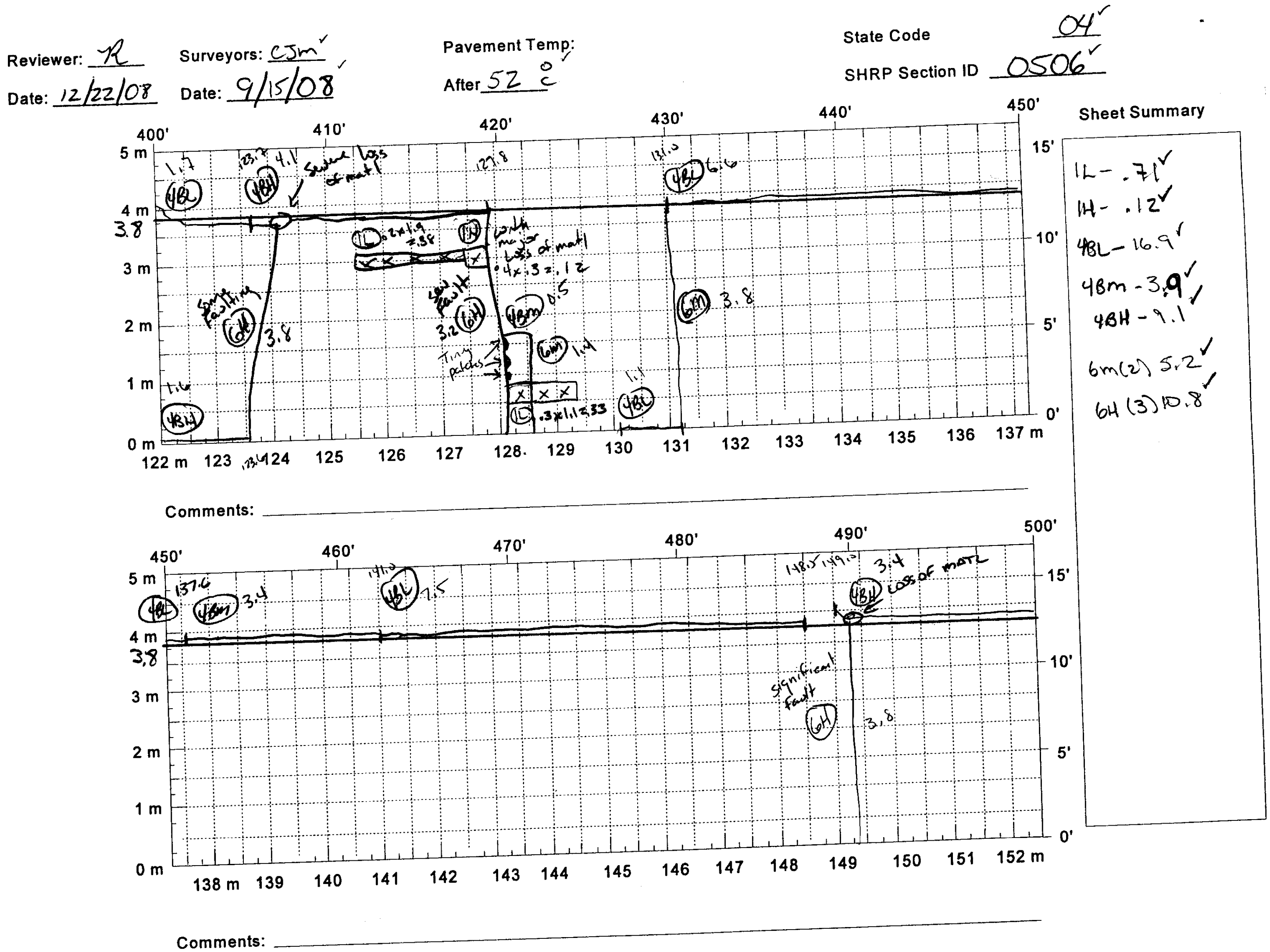

Figure D3. Pavement Distress Map; Station 4+00 to 5+00; Section 0506.

Figure D4. Pavement Distress Map; Station 0+00 to 1+00; Section 0509.

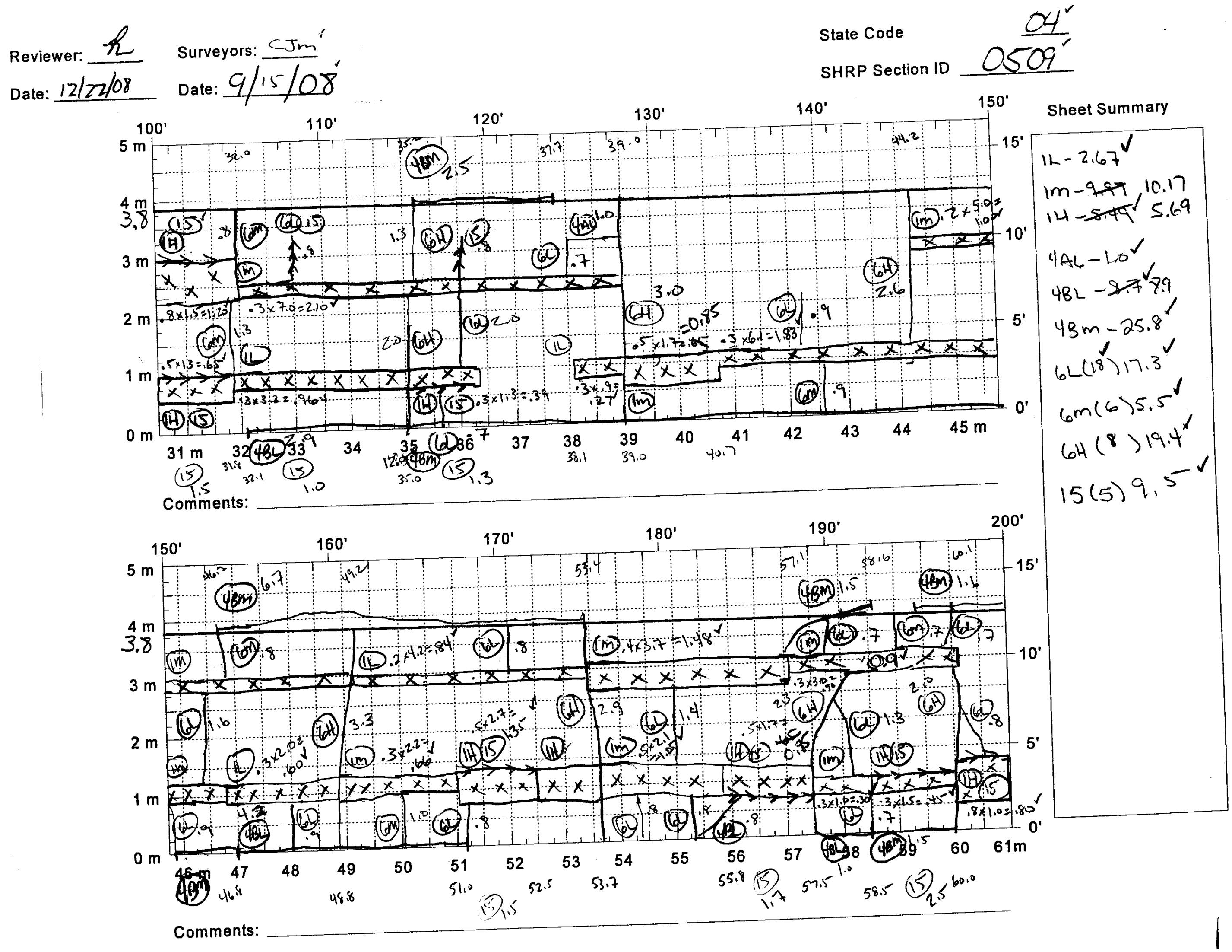

Figure D4. Pavement Distress Map; Station 1+00 to 2+00; Section 0509.

Figure D4. Pavement Distress Map; Station 2+00 to 3+00; Section 0509.

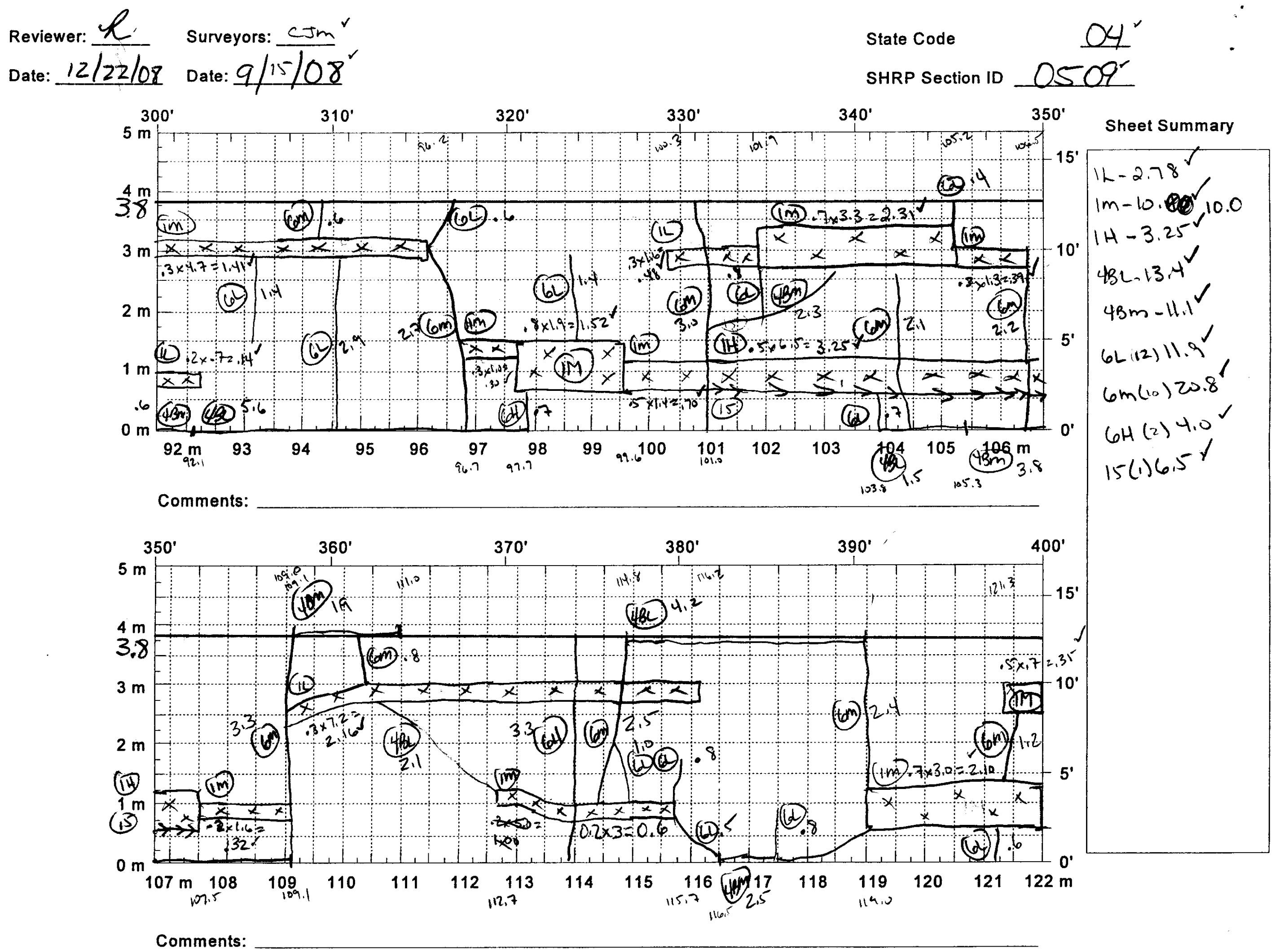

Figure D4. Pavement Distress Map; Station 3+00 to 4+00; Section 0509.

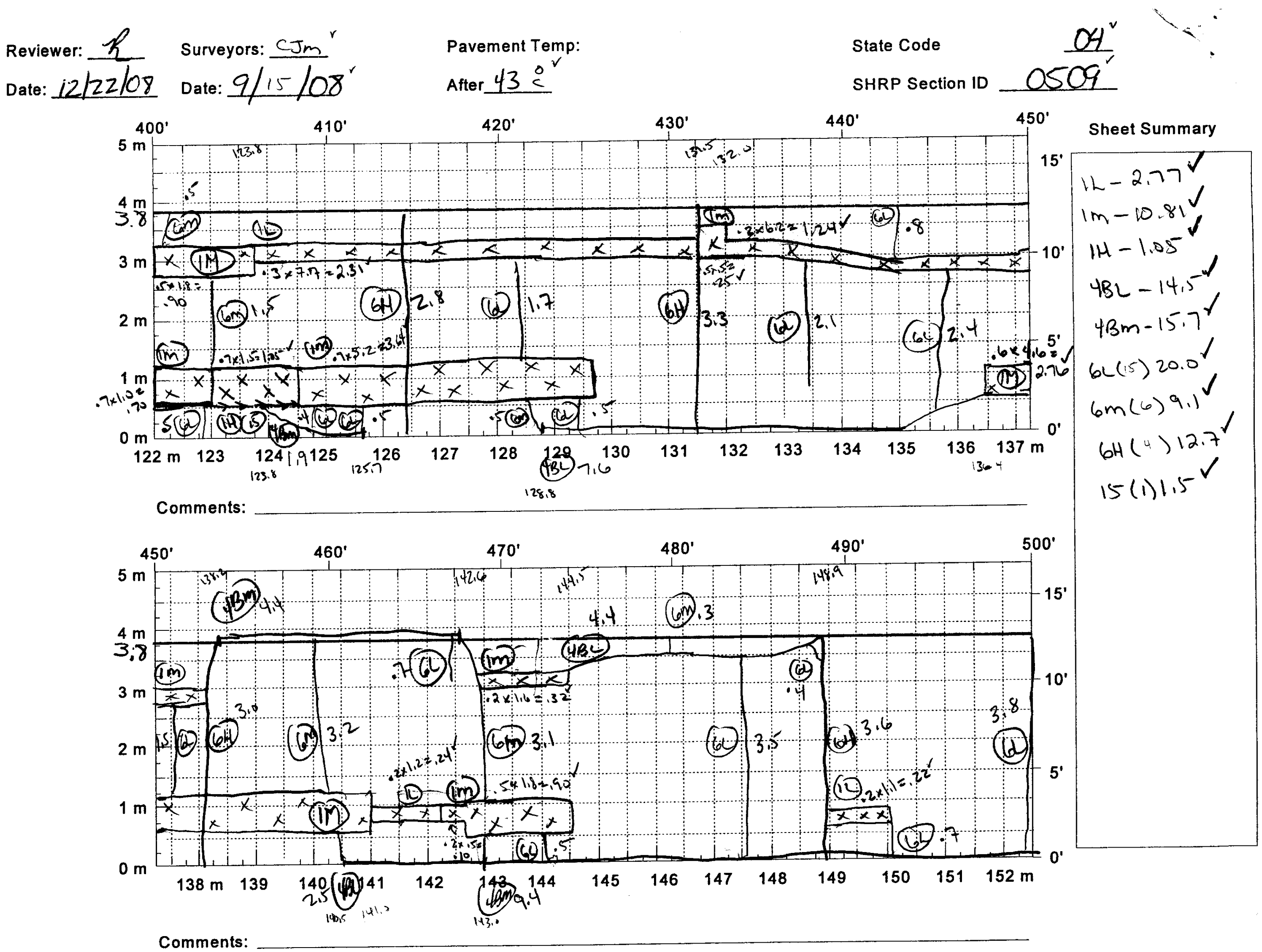

Figure D4. Pavement Distress Map; Station 4+00 to 5+00; Section 0509.